

Synthesis and investigation of triphenylene twins and dyads

Ahad Owaidh Alsahli

Submitted for the degree of Doctor of Philosophy

**School of Chemistry
University of East Anglia
March 2020**



This copy of the thesis has been supplied on condition that anyone who consults it is understood to recognise that its copyright rests with the author and that use of any information derived there from must be in accordance with current UK Copyright Law. In addition, any quotation or extract must include full attribution.

Abstract

The work set out in this thesis focuses on the synthesis and investigation of triphenylene twins and diads. Since the discovery of discotic liquid crystals by Chandrasekhar in 1977, columnar systems have been much investigated due to their practical applications. However, the nematic phase which some discotic liquid crystals exhibit have been less thoroughly investigated, despite their importance in liquid crystal displays as optical compensating films. Our group has been particularly interested in such systems which have triphenylene at their cores. These are synthetically versatile and have molecular robustness, a useful attribute when they are used within devices. Numerous triphenylene twins have previously been synthesised by Cammidge et al. The current research therefore consists of three main phases: firstly, the synthesis of a series of diads linking two triphenylene units via alkyne bridges and an investigation of their liquid crystal properties, secondly, the synthesis of triphenylene-BODIPY hybrids and thirdly, the synthesis of a compound using diaminoisindolene in a triphenylene core.

For the first phase of the work, twins were prepared through links at the 1,2-, 1,3- and 1,4-benzene sites plus through a 2,5-thiophene. Diiodobenzene and diiodothiophene were used as precursors to link between triphenylene units with Sonogashira coupling reactions used in the key steps. The difficulty in this series which arose was that the monoacetylene triphenylene starting material is reactive and tended to form a homo-coupling product, so purification proved challenging. However, the full characterisations have been obtained and liquid crystal investigation showed both columnar and nematic behaviour in 1,3-ditriphenylene benzene and 2,5-ditriphenylene thiophene. However, the linear diad 1,4-ditriphenylene benzene shows only columnar mesophase, and we rationalise this observation by noting that the separation between triphenylene units is appropriate for supporting columnar organisation. The diad 1,2-ditriphenylene benzene shows no liquid crystal behaviour, likely because the geometry and triphenylene spacing in the system prevents any efficient cofacial organisation.

The second phase of our work turned to explore the possibility of using (aza)BODIPY to synthesise symmetrical and unsymmetrical triphenylene-BODIPY hybrids. Precursor aminoisindolenes were prepared again from monoacetylene triphenylene by reaction with *ortho* bromobenzamidine. The synthesis of a further diad series was undertaken by using a variety of aminoisindolenes to produce aza-dipyrrromethene product. The new twinned structures were characterised and none were found to display liquid crystal

phases. Closer examination of their ^1H NMR spectra, alongside molecular modelling, showed that the preferred arrangement in such structures was helical. This is an interesting and unusual arrangement but is unlikely to support liquid crystal behaviour.

The final phase sought to prepare a twinned, co-planar structure incorporating both triphenylene and azaBODIPY. Initially the aim was to couple diacetylene triphenylene with bromo benzamidine by the same strategy had been used earlier but it proved unsuccessful. The strategy was changed and the diacetylene triphenylene reacted to produce dibenzonitrile triphenylene, but further reaction was not attempted due to lack of time. However, the new material was found to show mesophase behaviour.

Access Condition and Agreement

Each deposit in UEA Digital Repository is protected by copyright and other intellectual property rights, and duplication or sale of all or part of any of the Data Collections is not permitted, except that material may be duplicated by you for your research use or for educational purposes in electronic or print form. You must obtain permission from the copyright holder, usually the author, for any other use. Exceptions only apply where a deposit may be explicitly provided under a stated licence, such as a Creative Commons licence or Open Government licence.

Electronic or print copies may not be offered, whether for sale or otherwise to anyone, unless explicitly stated under a Creative Commons or Open Government license. Unauthorised reproduction, editing or reformatting for resale purposes is explicitly prohibited (except where approved by the copyright holder themselves) and UEA reserves the right to take immediate 'take down' action on behalf of the copyright and/or rights holder if this Access condition of the UEA Digital Repository is breached. Any material in this database has been supplied on the understanding that it is copyright material and that no quotation from the material may be published without proper acknowledgement.

This thesis is dedicated to my beloved parents

Owaidh A. Alsahli and Mona H. Alsahli

Acknowledgements

First of all, I would like to give thanks to the almighty God for giving me life and strength to complete this thesis. I would also like to express my sincere gratitude to my supervisor, Prof. Andrew N. Cammidge for giving me this opportunity to work under him and for all his support. Without his encouragement, help, and confidence in me, this project would not have been possible. I am grateful to him for the advice, patience and attentiveness that he has given me and the impact he has had on my life. I would also like to express my appreciation to my second supervisor Dr. Chris Richard for his commitment and Dr. Maria Paz for her support. I would also like to extend my gratitude to the teaching, technical and administrative staff of the School of Chemistry at UEA. I would also like to thank my father Owaidh Alsahli for funding my studentship and I wish to express my greatest gratitude and thanks to my parents, without them, I would not have had the strength or means to complete my PhD. Their encouragement, love and support are without bounds and I only hope my achievement in writing this thesis will go some way to repaying this debt.

My special thanks to Dr. Isabelle for her helpful advice and suggestions in general. She has been helpful in providing advice many times during my lab work. I also have to thank Faeza, Jacob, and Abdulaziz for their guidance, assistance and support. I thank all the previous and current members of the Andy group: Rhoda, Shazia, Lucas, Nora, and Bodur. I am very grateful for this opportunity to work with them in the same lab. Furthermore, I am grateful to all members of ANC group whom I have worked and shared lab 3.17 with them during my studies at UEA for their help in various ways. Also, I would like to thank my friends with whom I have shared lab 3.17 and worked with throughout my time at UEA.

I am very thankful to my husband, Adel, for his support and endless encouragement and for doing everything possible to help every step of the way, along with my wonderful brothers and sisters who encouraged me with their prayers, moral support and never-ending love. Without my family, this research would not have survived. My acknowledgements go to my sponsors, My father and the Ministry of Education in Saudi Arabia, represented in the Saudi Cultural Bureau and the Royal Embassy in the UK, for the scholarship which was given to me. To anyone else who has contributed to my success as a student, scientist or person: thank you for many others who helped along the way, thank you.

Contents

Chapter 1 Introduction	1
1.1 Liquid Crystals	2
1.1.1 Brief history of liquid crystals	2
1.1.2 Classification of Liquid Crystals	3
1.2 Discotic Liquid Crystals	4
1.2.1 Discotic Mesophases	6
1.2.2 Characterisation of DLC phases	10
1.2.3 Applications of discotic Liquid Crystals	12
1.3 Triphenylene as DLC	17
1.3.1 Synthesis of triphenylene	17
1.3.2 Mesophase formation in Triphenylene Derivatives	27
1.3.3 Triphenylene Dimers	29
Chapter 2 Results & Discussion	37
2.1. Synthesis of triphenylene diads	38
2.1.1. Previous Work from our Group	38
2.1.2. Synthesis of mono-acetylene triphenylene 97	39
2.1.3. Synthesis of triphenylene diads	48
2.2. Attempted synthesis of the triad of triphenylenes	66
2.3. Introduction to BODIPY Compounds	68
2.3.1. Previous Work	70
2.3.2. Synthesis of Aminoisoindolene	72
2.3.3. Synthesis aza-BODIPY product	79
2.4. Attempted synthesis of aza(ditriphenylene) dipyrromethene	88
2.4.1. Synthesis of Diacetylene-Triphenylene 139	89
2.4.2. Attempted synthesis of Diaminoisoindolene triphenylene	90
2.4.3. Synthesis of 6, 7-bis (hexyloxy)-2, 11-bis (2-benzonitrile) triphenylene	93
2.4.4. Synthesis of tetra (alkoxy)-diacetylene triphenylene	94
2.4.5. Synthesis of 3, 6, 7, 10-tetrakis (alkoxy)-2, 11-ethynyl-(bis (2-benzonitrile)) triphenylene	95
2.4.6. Characterisation of liquid crystal properties	97
2.4.7. Synthesis of compound 158	97
2.5. Furure work	99

2.6.	Conclusion.....	100
Chapter 3	Experimental	102
3.1.	General Information	103
3.2.	Synthetic procedures and characterization data:	104
3.2.1.	1,2-Dihexyloxybenzene 55	104
3.2.2.	Synthesis of 2-hydroxy- 3, 6, 7, 10, 11- penta-hexyloxy-triphenylene 94	105
3.2.3.	Synthesis of 2-hydroxy- 3, 6, 7, 10, 11- penta-hexyloxy-triphenylene 94	106
3.2.4.	Synthesis of 2-trifluoromethylsulfonyl - 3, 6, 7, 10, 11- penta-hexyloxy- triphenylene 95	107
3.2.5.	Synthesis of 2- (3-methyl-3-hydroxybutynyl)- 3, 6, 7, 10, 11- penta- hexyloxy-triphenylene 96	108
3.2.6.	Synthesis of 2- ethynyl- 3, 6, 7, 10, 11- penta-hexyloxy-triphenylene ^[96] 97	109
3.2.7.	1, 3-phenylene bridged triphenylene 93.....	110
3.2.8.	2- (3-iodophenyl) ethynyl-3, 6, 7, 10, 11-Penta-hexyloxy-triphenylene 101	111
3.2.9.	1, 4-phenylene bridged diad 103.....	112
3.2.10.	1, 2- Phenylene bridged diad 108.....	113
3.2.11.	(2-iodophenyl) ethynyl-3, 6, 7, 10, 11-Penta-hexyloxy-triphenylene 109	114
3.2.12.	2, 5-thiophene bridged diad 113.....	115
3.2.13.	<i>O</i> -Bromobenzamidine Hydrochloride 123.....	116
3.2.14.	1-Bromo-4-hexyloxybenzene	116
3.2.15.	4-(p-hexyloxyphenyl)-2-methyl-3-butyn-2-ol	117
3.2.16.	1-ethynyl-4-hexyloxybenzene	117
3.3.	Synthesis of Aminoisindolene.....	118
3.3.1.	General procedure A	118
3.3.2.	Azadipyrromethene compound 134.....	121
3.3.3.	Azadipyrromethene compound 137.....	122
3.3.4.	Azadipyrromethene compound 138.....	123
3.3.5.	Azadipyrromethene compound 136.....	124
3.3.6.	Aza-(ditriphenylene) dipyrromethenes (Self-Condensation of triphenylene-Aminoisindoline) compound 125.....	125
3.3.7.	Compound 143	126
3.3.8.	2,3-Bis(hexyloxy)triphenylene 144	127

3.3.9.	2,11-Dibromo-6,7-bis(hexyloxy)triphenylene	145	128
3.3.10.	4, 4'-(6, 7-Bis (hexyloxy) triphenylene-2, 11-diyl) bis(2-methylbut-3-yn-2-ol)	146	129
3.3.11.	Synthesis of 2, 11-Diethynyl-6, 7-bis (hexyloxy) triphenylene	139	130	
3.3.12.	Synthesis of 6, 7-bis (hexyloxy)-2, 11-bis yn-bis (2-benzonitrile) triphenylene	147	131
3.3.13.	4,4'-(3, 6, 7, 10-tetrakis(hexyloxy)triphenylene-2,11-diyl)bis(2-methylbut-3-yn-2-ol)	154	132
3.3.14.	2,11-Diethynyl-3,6,7,10-tetrakis (hexyloxy)triphenylene	155	133
3.3.15.	Synthesis of 3, 6, 7, 10-tetrakis (hexyloxy)-2, 11-diethynyl –(bis (2-benzonitrile)) triphenylene	156B	134
3.3.16.	bisBenzonitrile substituted diad	157B	135
3.3.17.	Synthesis of 3, 6, 7, 10-tetrakis (decyloxy)-2, 11-diethynyl (bis (2-benzonitrile)) triphenylene	156A	136
3.3.18.	Bis-benzonitrile substituted diad	157A	137
3.3.19.	Synthesis of 3, 6, 7, 10, 11-pentakis (hexyloxy)-2- ethynyl - (2-benzonitrile) triphenylene	158	138
4.	References		140

List of figures

Figure 1.1: Ordering in a liquid crystal between a crystal and liquid phase. -----	2
Figure 1.2: Historically important LC molecules.-----	3
Figure 1.3: Classification of liquid crystals. -----	4
Figure 1.4: Cores that exhibit DLC mesophases.-----	5
Figure 1.5: Self-assembly of triphenylene as DLCs into columnar phase. -----	5
Figure 1.6: Some Columnar DLC phases.-----	6
Figure 1.7: Recent example of ordered hexagonal columnar mesophase. -----	7
Figure 1.8: Structure of 2, 3, 6, 7, 10, 11-hexakis (4-n-alkoxybenzoate) triphenylene. -	7
Figure 1.9: Nematic phases observed in discotic liquid crystals. -----	9
Figure 1.10: Arrangement of molecules in the smectic phase. -----	9
Figure 1.11: Representation of polarized optical microscopy. -----	10
Figure 1.12: Polarized optical micrograph for a) Columnar phase, b) Nematic phase and c) isotropic liquid. -----	11
Figure 1.13: Representative DSC analysis showing transitions from solid to liquid crystal and liquid crystal to isotropic liquid. -----	12
Figure 1.14: TP based DLC patented by Fuji Photo Film Company. -----	14
Figure 1.15: Structure of disulfide-triphenylene ligand, structure of ZnO nanoparticle modified with triphenylene ligands. -----	15
Figure 1.16: Triphenylene derivatives utilised in OLED devices. -----	15
Figure 1.17: Molecular structures of thiophene based π -extended triphenylene. -----	16
Figure 1.18: Structure of triphenylene 17.-----	17
Figure 1.19: Range of unsymmetrically substituted functionalised triphenylenes. -----	26
Figure 1.20: Selected example triphenylenes demonstrating the effect of substitution. 28	
Figure 1.21: Other mesophase behaviour of unsymmetrical triphenylenes.-----	28
Figure 1.22: Some structures of the unsymmetrical polar triphenylene derivatives. ---	29
Figure 1.23: Structures to show meaning of terms 'diad' and 'twin'. -----	29
Figure 1.24: Structures of Diad and Triad synthesised by Boden et al. -----	30
Figure 1.25: Triphenylene spiro twins. -----	30
Figure 1.26: Transition data for triphenylene diad above. -----	31
Figure 1.27: Triphenylene diad linked by a phenylene dicarbamate unit. -----	31
Figure 1.28: Acetylene linked triphenylene diads. -----	32
Figure 1.29: Crown-ether linked triphenylene twin and triad. -----	32
Figure 1.30: Antiaromatic triphenylene twin linked by acetylene bridges. -----	33
Figure 1.31: Structure of compound 87 that showed discotic nematic mesophase. ----	34
Figure 1.32: Structure of the diads 88 synthesised by Bala et al. -----	35
Figure 2.1: The target structure -----	39
Figure 2.2: An expansion aromatics region of compound 94.-----	41
Figure 2.3: aromatic region in compound 95.-----	43
Figure 2.4: $^1\text{H-NMR}$ aromatic regions of compound 96. -----	47
Figure 2.5: $^1\text{H-NMR}$ aromatic regions of compound 97. -----	48
Figure 2.6: $^1\text{H NMR}$ spectra of aromatic region for compounds 93 and 101.-----	50
Figure 2.7: Maldi-TOF spectrum of the compound 93. -----	50
Figure 2.8: Compound 93 showing columnar (left) at 87°C and nematic (right) mesophases at 142°C.-----	51
Figure 2.9: DSC thermograph of compounds 93 and 101 on heating and cooling (scan rate 10°C min ⁻¹) -----	51

Figure 2.10: Schematic representation of the Kumar's diad. -----	52
Figure 2.11: Schematic representation of the diad 93, twin 92 and their monomers 91, 101. -----	53
Figure 2.12: Aromatic region of ¹ H-NMR spectra of compound 103. -----	55
Figure 2.13: DSC thermograph of 1,4-phenylbridged diad 103, and Col _h phase texture at 212°C. -----	55
Figure 2.14: Schematic representation of the compound 103 and the monomer HAT6. -----	56
Figure 2.15: Aromatic region of ¹ H-NMR spectra of compounds 108 and 109. -----	58
Figure 2.16: DSC thermograph of compounds 101 and 109. -----	59
Figure 2.17 Schematic representation of the compound 108. -----	59
Figure 2.18 : The effect of length of the spacer on diad mesophase. -----	60
Figure 2.19 : Crude MALDI-MS showing the crude of the reaction. -----	62
Figure 2.20: An expansion of the aromatic region for compound 113. -----	63
Figure 2.21 Compound 113 during a) columnar phase, b) nematic phase. -----	63
Figure 2.22: Comparison between the twin and the diad structures and mesophases. -	64
Figure 2.23: -----	65
Figure 2.24: UV/Vis spectra of 1 st series of triphenylene compounds. -----	66
Figure 2.25: Crude MALDI-MS showing presence of compounds 97 and 102. -----	67
Figure 2.26: Boron dipyrromethene (BODIPY) (left) the aza-BODIPY core (right). -	68
Figure 2.27: BODIPY–Hexaoxatriphenylene structure. -----	69
Figure 2.28: Triphenylene-Bodipy diad. -----	70
Figure 2.29: Dipyrromethane-triphenylene. -----	71
Figure 2.30: Possible mechanisms for the copper-free Sonogashira reaction. -----	73
Figure 2.31: MALDI-TOF spectrum showing the mass for the target compound 124. 77	77
Figure 2.32: Pyrenyl-aminoisoindolene. -----	77
Figure 2.33: Aromatic region of ¹ H-NMR spectrum of compound 133. -----	79
Figure 2.34: MALDI-MS spectra of aza-dipyrromethene triphenylene 125. -----	81
Figure 2.35: The expansion of the aromatic region for compound 134. -----	82
Figure 2.36: COSY experiment showing cross peaks in compound 134 at 263K. -----	83
Figure 2.37: Modelling of compound 134. -----	84
Figure 2.38: Aromatic region of ¹ H-NMR spectra of compound 136. -----	85
Figure 2.39: aromatic region of the compound 137. -----	86
Figure 2.40: COSY experiment showing cross peaks in compound 137 at 263K. -----	87
Figure 2.41: UV-Vis spectra of compounds 2 nd series in dichloromethane. -----	88
Figure 2.42: The precursor structure. -----	89
Figure 2.43: The target compound. -----	90
Figure 2.44: Maldi-TOF spectrum of the crude. -----	91
Figure 2.45: ¹ H-NMR aromatic regions of compound 147. -----	94
Figure 2.46: Comparison of the aromatic region of ¹ H-NMR of compounds 156A and 157A respectively. -----	96
Figure 2.47: DSC thermograph of compounds 156A, 156B. -----	97
Figure 2.48: ¹ H-NMR spectra for aromatic regions of compound 158. -----	98
Figure 2.49: MALDI-TOF desired structure 158 with isotopes pattern. -----	98
Figure 2.50: The structure of compounds 157 and 158. -----	99

List of schemes

Scheme 1.1: Synthesis of triphenylene dimer showing nematic mesophases. -----	8
Scheme 1.2: Synthesis of hexa(hexyloxy) triphenylene 21 using terphenyl cyclisation as final step. -----	18
Scheme 1.3: Synthesis of 2, 3-Bis (hexyloxy) triphenylene 23. -----	18
Scheme 1.4: Synthesis of 2, 7-Bis(hexyloxy) triphenylene 27. -----	19
Scheme 1.5: Palladium-catalysed synthesis of triphenylene. -----	20
Scheme 1.6: Synthesis of substituted triphenylene from heterocyclic dienes. -----	20
Scheme 1.7: Synthesis of substituted triphenylene from biaryl 35.-----	21
Scheme 1.8: Synthesis of triphenylene 17 via Diels-Alder reaction. -----	21
Scheme 1.9: Synthesis of triphenylene 17 via Friedel-Crafts reaction. -----	22
Scheme 1.10: Synthesis of 1, 4-dimethyl triphenylene. -----	22
Scheme 1.11: Synthesis of benzotriphenylenes 45 -----	23
Scheme 1.12: Oxidative trimerisation of dimethoxy benzene 46 to yield 47. -----	24
Scheme 1.13: Synthesis triphenylene 17 from cyclohexanone. -----	24
Scheme 1.14: Synthesis substituted hexa-aza-triphenylenes 51. -----	25
Scheme 1.15: Acid catalysed cyclisation of 52 to yield 54. -----	25
Scheme 1.16: Synthesis of triphenylenes 57 from biphenyl. -----	26
Scheme 1.17: Synthesis of asymmetrical triphenylene derivatives. -----	26
Scheme 1.18: Synthesis of asymmetrical triphenylene. -----	27
Scheme 2.1: acetylene-benzene twin 92 -----	38
Scheme 2.2: The full synthetic route towards mono-acetylene triphenylene 97. -----	40
Scheme 2.3: alternative method of synthesise MHT. -----	42
Scheme 2.4: the synthesis of compound 95. -----	43
Scheme 2.5: Basic representation of Sonogashira cross-coupling reaction.-----	44
Scheme 2.6: Mechanism of Sonogashira cross-coupling reaction. -----	45
Scheme 2.7: The synthesis of compound 96. -----	46
Scheme 2.8: Synthesis of mono-acetylene triphenylene.-----	47
Scheme 2.9: Synthesis of m-triphenylene diad -----	49
Scheme 2.10: Attempted synthesis of 1, 4-Phenylene-bridged triphenylene twin. -----	54
Scheme 2.11: Synthesis of triphenylene diad 103-----	54
Scheme 2.12: Synthesis of the 1, 2-ditriphenylene benzene 108.-----	57
Scheme 2.13 Synthesis of 2, 5-thiophene-bridged twin -----	61
Scheme 2.14 Synthesis of ditriphenylene-thiophene diad.-----	61
Scheme 2.15: attempted synthesis of 1, 3, 5-tri-triphenylene benzene. -----	67
Scheme 2.16: Synthesis of BODIPY-triphenylene 119.-----	71
Scheme 2.17: outline plan in this series.-----	72
Scheme 2.18: Synthesis of amidine 123. -----	72
Scheme 2.19: The formation of 2-bromobenzamidine 123. -----	73
Scheme 2.20: Proposed mechanism for the aminoisoindolene. -----	74
Scheme 2.21: Synthesis of aminoisoindolene 126. -----	74
Scheme 2.22: Synthesis of compound 124. -----	76
Scheme 2.23: Preparation of 4-hexyloxyphenyl ethylene. -----	78
Scheme 2.24: Proposed mechanism for the formation of aza-dipyrrromethene. -----	79
Scheme 2.25: Synthesis of aza-dipyrrromethene triphenylene. -----	80

Scheme 2.26: Synthesis of the compound 134.-----	81
Scheme 2.27: Synthesis of the compound 136.-----	85
Scheme 2.28: Synthesis of compound 137. -----	86
Scheme 2.29: Plan to synthesise aza(ditriphenylene)dipyrromethene. -----	89
Scheme 2.30: Full synthetic route to compound 139. -----	90
Scheme 2.31: Attempted synthesis of diaminoisindolene triphenylene. -----	92
Scheme 2.32: Synthesis bis benzonitrile triphenylene 147.-----	93
Scheme 2.33: Synthesis of diacetylene-triphenylene 155. -----	95
Scheme 2.34: Synthesis of 3, 6, 7, 10-tetrakis (alkoxy)-2, 11-bis (2-benzonitrile) triphenylene.-----	96
Scheme 2.35: Synthesis of compound 158. -----	98
Scheme 2.36: Proposed synthesis of compound 140 -----	99

List of tables

Table 1.1: Effect of methyl position on mesophase behaviour. -----	8
Table 1.2: The composition of the technologically important nematic liquid crystal preparation E7. -----	13
Table 1.3: Thermal behaviour of the pure 88 compounds.-----	35
Table 2.1: Comparison of the yield of the two methods. -----	42
Table 2.2: Phase transfer temperature (°C) of compounds and enthalpy changes (KJ/mol in brackets). -----	70
Table 2.3: Reaction of amidine with acetylenic precursors to produce aminoisindolene compounds.-----	75
Table 2.4: Solvent effect in aza-dipyrromethene reaction.-----	80

Chapter 1

Introduction

1.1 Liquid Crystals

Liquid crystals (LCs) are materials that share the properties of the two states: liquids and solid crystals. The molecules of conventional liquids can translate and rotate freely, which means that they do not have either positional or orientational ordering.^[1] Crystalline solids, meanwhile, have both orientational and positional ordering because molecules are positioned at specific places within a three-dimensional lattice. Liquid crystals have phases which lack long-range positional ordering. However, they do possess long-range orientational order, which occurs when they are in their mesomorphic state within specific ranges of temperature, pressure or concentration.

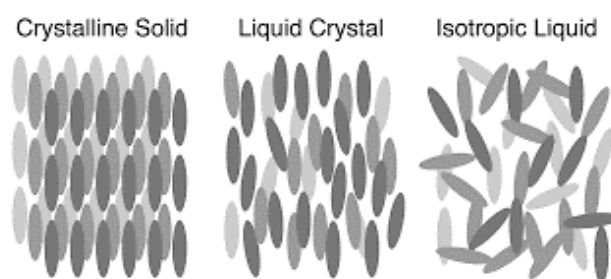


Figure 1.1: Ordering in a liquid crystal between a crystal and liquid phase.

1.1.1 Brief history of liquid crystals

In 1888, Freidrich Reinitzer observed that cholesteryl benzoate **1** exhibited an interesting melting behaviour.^[2] When the compound melts at 145.5°C, it forms a cloudy liquid. A further transition is observable at 178.5°C, when a clear liquid forms.^[2] This was explained by the German physicist, Otto Lehmann, as a “double melting”.^[3] Lehmann initially termed these compounds “soft crystals”, but later changed this to “crystalline fluid”, then to “liquid crystals” once he was certain of the uniqueness of the opaque phase and that it shared properties of liquids and solids. Prior to this, chemists had studied liquid crystals, but without fully understanding the phenomenon.^[4]

Disc-shaped compounds exhibiting mesomorphic properties were first reported in 1977 by Chandrasekhar.^[5] He observed that hexa-esters of benzene **2** were able to form structures with columnar mesophases. Since Chandrasekhar's discovery, over three thousand different compounds have been found to exhibit this mesomorphic behaviour. Fifty different core units for these compounds have been reported. Research into this phenomenon has continued, in particular due to the usefulness of discotic compensation films^[6] and opto-electronic devices. Discotic liquid crystals have great potential for use in new technologies, for example organic solar cells^[7] and organic semi-conductors.^[8]

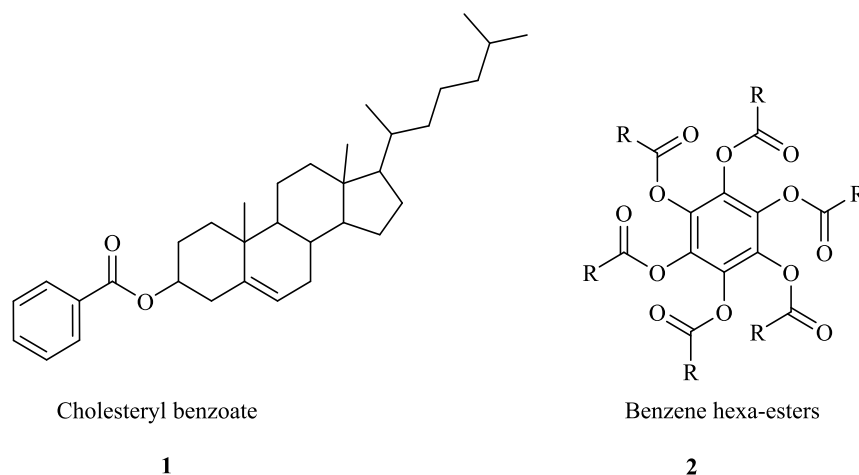


Figure 1.2: Historically important LC molecules.

1.1.2 Classification of Liquid Crystals

The widest used classification of LCs is into two basic types: lyotropic and thermotropic. Lyotropic liquid crystals are derived from amphiphilic materials^[9], as a result of which their mesophases can be formed in the presence of solvents.^[10] Thermotropic liquid crystals rely on temperature to produce their mesophases, which can be achieved when the crystalline solid is heated or when the isotropic liquid is cooled. These are subdivided into calamitic (rod like), bent-core (banana-like) and discotic (disk-like). These classifications depend on the shape of the mesogenic molecules. There are various kinds of liquid crystal phases, depending on their molecular ordering properties, such as smectic, nematic and columnar. The main focus of the current research is on discotic liquid crystals.

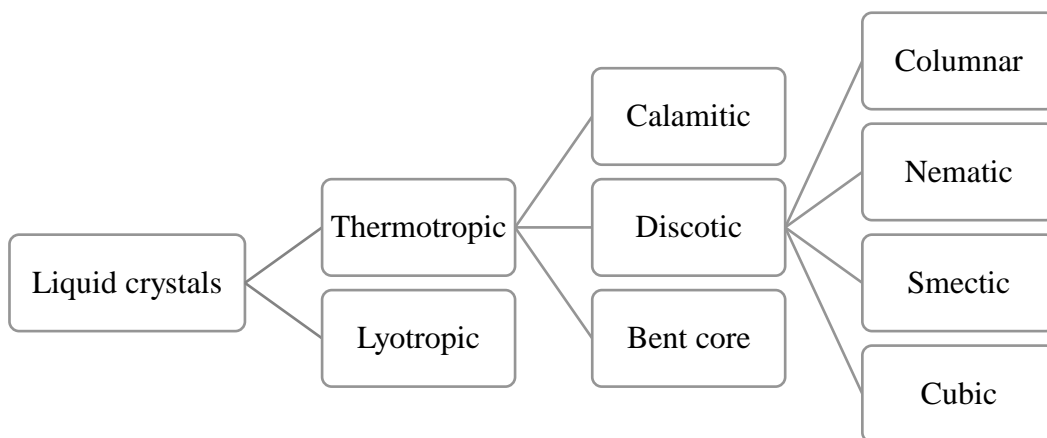


Figure 1.3: Classification of liquid crystals.

1.2 Discotic Liquid Crystals

Discotic liquid crystal molecules are usually comprised of a disc-like central core around which there are between three and twelve substituents, in the form of chains containing at least three carbon atoms. Much research has been conducted into the central core unit and also into the nature of the side chains, their size and number. Rotational symmetry has often been noted as one of the properties of discotic materials. Thermotropic discotic liquid crystals have a number of unique properties. They are usually π -conjugated structures, are relatively fluid, processible and self-organising. These characteristics, in addition to the liquid crystals' orientational ordering, mean that they are anisotropically conductive and have optical anisotropic features. Amongst the numerous different cores which have been observed to form discotic liquid crystals are phthalocyanine, naphthalene, perylene, anthracene, porphyrin and triphenylene. The use of a triphenylene core to produce discotic mesogens has been the focus of much recent research and is the main area of interest for the current project.

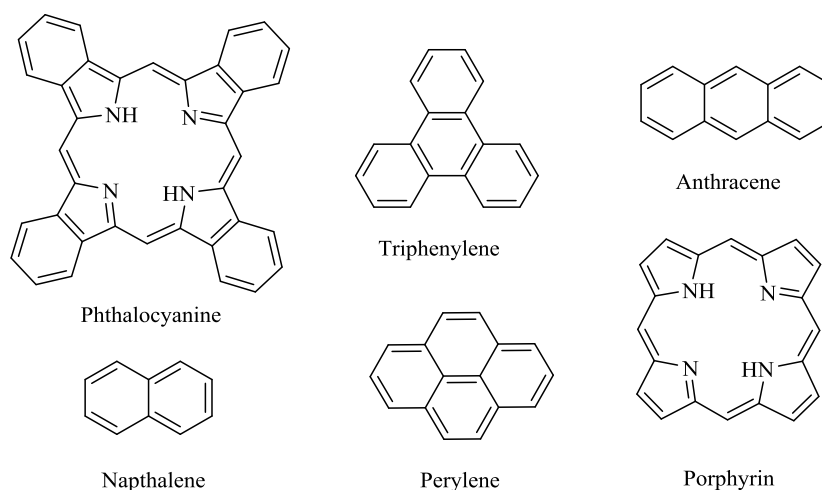


Figure 1.4: Cores that exhibit DLC mesophases.

Of all the DLCs which have been investigated, triphenylene has been more frequently synthesized and studied than any other DLCs. Triphenylene (TP) was introduced as a DLC core in 1978, by Billard et al.^[11] Triphenylene derivatives have a number of practical advantages, such as their thermal and chemical stability, their relative accessibility, their variety of mesophases and their interesting electronic properties.^[12] They therefore have considerable potential for use in a wide range of practical applications. For this reason, much research effort has been put into synthesising DLC-based TPs, with more than 500 having been reported so far in the literature. The most common type of mesophases seen in triphenylene-derived compounds are columnar, with nematic discotic phases being much less common.

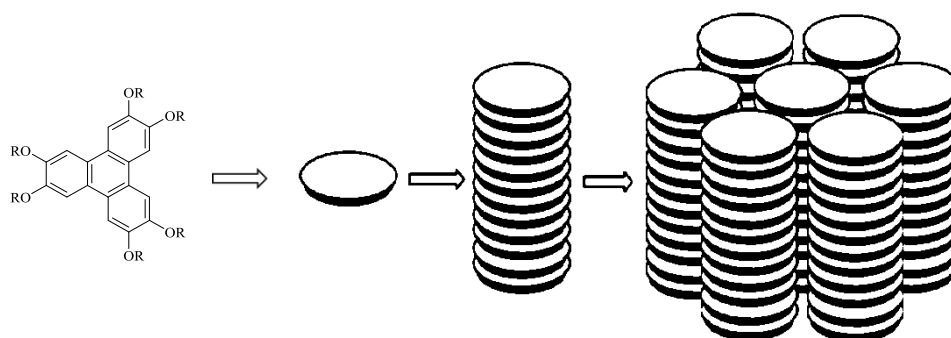


Figure 1.5: Self-assembly of triphenylene as DLCs into columnar phase.

1.2.1 Discotic Mesophases

There are four major types of discotic liquid crystal mesophase, which depend on the molecules' shape and symmetry:

1. Columnar
2. Nematic
3. Smectic
4. Cubic

Most discotic molecules exhibit only one of these mesophases, the most common of which is columnar. However, there are some which can have more than one, a phenomenon known as polymorphism.^[13] Researchers have been aware of columnar mesophases ever since Chandrashekar first demonstrated that disk-like molecules could have liquid crystal phases. Columnar phases are the most common because the π - π interactions between the aromatic cores cause the mesogens to form stacks, one on top of the other. These columns become part of a bigger 2D lattice. Various different symmetries have been reported and the patterns within the columns of mesogens can be regular and ordered or disordered. Seven different classes of columnar mesophases have so far been identified, and these depend on the packing arrangements of the molecules and the type of lattice they form. The three most commonly observed arrangements within the columnar mesophase are hexagonal columnar (Col_h), rectangular columnar (Col_r), and oblique columnar (Col_{ob}) as shown in figure 1.6. The rectangular packing of the columns of discotic mesogens is characterised as the rectangular columnar phase. In terms of a distinct an oblique mesophase, the molecules stacking of into the column with tilted orientation.^{[14],[15]}

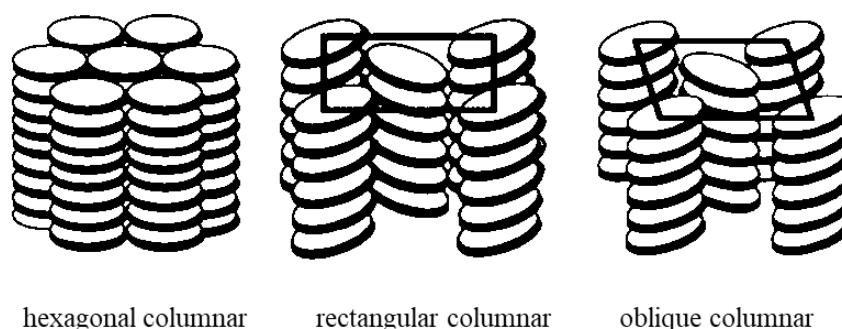


Figure 1.6: Some Columnar DLC phases.

In hexagonal phases, the columns self-assemble into a hexagonal packing arrangement. The cores in the columns can be relatively either ordered or disordered. Triphenylene derivatives shown various columnar mesophases. A recent paper published by Yang et al. (2018) reported novel liquid crystals with bowl-shape structure built on cyclotrimeratrylene CTV derivative with ordered hexagonal columnar mesophase.^[16]

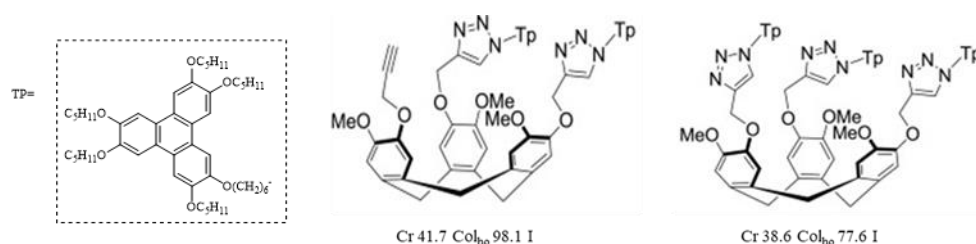


Figure 1.7: Recent example of ordered hexagonal columnar mesophase.

Nematic discotic liquid crystals lack order although there is a parallel arrangement of mesogens and orientational order. However, these mesogens do not have long-range positional order. The molecules have a short axis, and this defines the director. There are three subdivisions of nematic mesophases: discotic nematic N_D , columnar nematic N_c and chiral nematic N_D^* . Nematic mesophases have been reported 2, 3, 6, 7, 10, 11-hexakis(4-n-alkoxybenzoates) triphenylene as shown in figure 1.8.^[17]

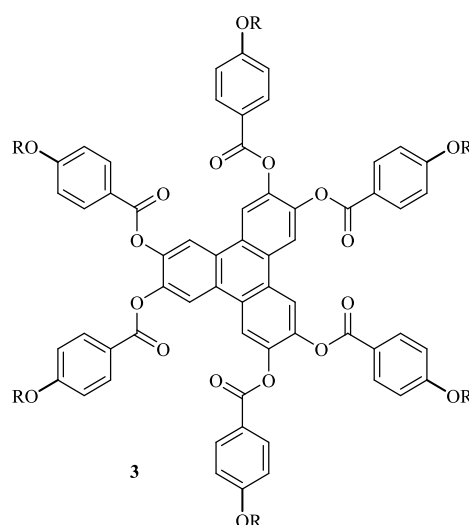


Figure 1.8: Structure of 2, 3, 6, 7, 10, 11-hexakis (4-n-alkoxybenzoate) triphenylene.

Research into triphenylene-hexabenzoate compounds has demonstrated that it is possible to prevent columnar mesophase formation by introducing methyl groups *ortho* to the ester linkage.^[18] This leads to the formation of N_D mesophases. It is also possible to suppress the columnar phase by introducing substituents *meta* to the ester link group. However, a hexagonal disordered columnar mesophase is then observed.

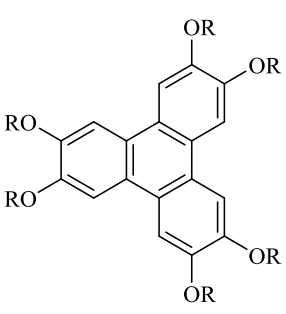
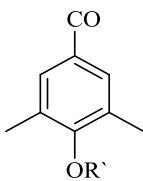
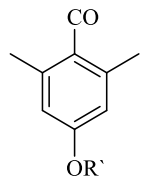
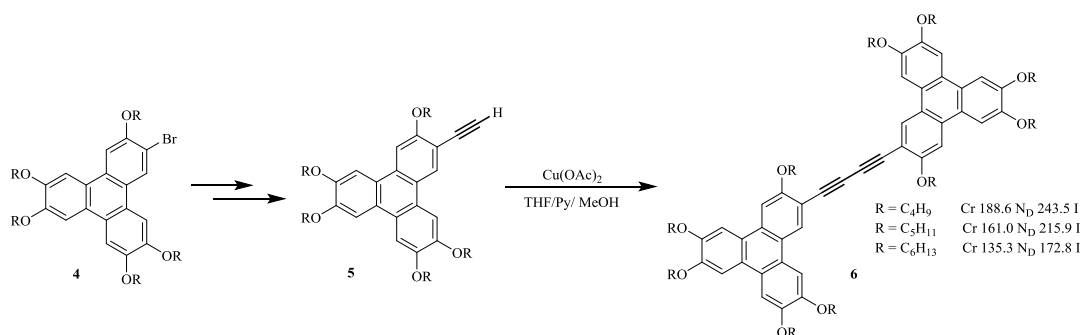
Structure	R	R'	mesophase
		C ₆ H ₁₃	Cr 150 Col _{hd} 210 N _D 243 I
		C ₈ H ₁₇	Cr 170 Col _{hd} 195 N _D 215 I
		C ₁₀ H ₂₁	Cr 157 Col _{hd} 167 N _D 182 I
		C ₁₂ H ₂₅	Cr - Col _{hd} 143 N _D 151 I
		C ₆ H ₃ CH(CH ₃)	Cr 125 Col _{hd} 156 N _D 183 I
		C ₆ H ₁₃	Cr 170 N _D 196 I
		C ₈ H ₁₇	Cr 155 N _D 170 I
		C ₁₀ H ₂₁	Cr 108 N _D 134 I
		C ₁₂ H ₂₅	Cr 88 N _D 99 I
		C ₆ H ₃ CH(CH ₃)	Cr 161 I

Table 1.1: Effect of methyl position on mesophase behaviour.^[18]

Few discotic mesogens which display nematic discotic phases have been observed due to the problems in designing them. Research efforts have focused on the synthesis of triphenylene dimers, which builds on the work conducted on the triphenylene hexabenzoate series. If nematic phases are to form, it is necessary to decrease the π - π interactions. If two triphenylene units are linked using a rigid conjugated spacer, nematic material can be produced (Kumar, 2002).^[19] A diacetylene bridge was used to join the dimers **6** and nematic mesophases were observed across a wide range of temperatures. However, the monomers **5** only exhibited ordered columnar mesophases.



Scheme 1.1: Synthesis of triphenylene dimer showing nematic mesophases.

It is possible to produce a nematic columnar mesophase by means of charge-transfer interactions. These occur between donor and an acceptor molecule. The resulting stacks of molecules are columnar and have short-range orientational order. However, these columns do not assemble into a 2D lattice because the side chains differ in length. The same symmetry is seen in N_{Col} , N_D and N phases. These can be characterised through the observation of Schlieren optical microscopy textures.

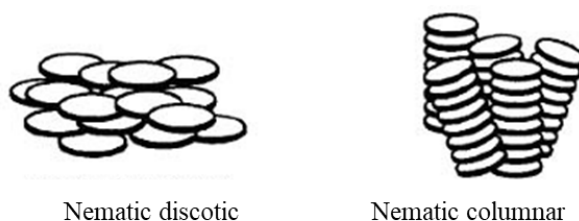


Figure 1.9: Nematic phases observed in discotic liquid crystals.

Smectic mesophases are very unusual in discotic mesogens. They do, however, occur when the number of peripheral chains is reduced or if the distribution of the side chains is unequal. The discs are organised in a layered manner. Sub-layers of peripheral alkyl chains separate these layers.^[20] Ortho-terphenyl crown ether **7** is an example of a discotic mesogen showing a smectic phase, as illustrated in figure **1.10** below.

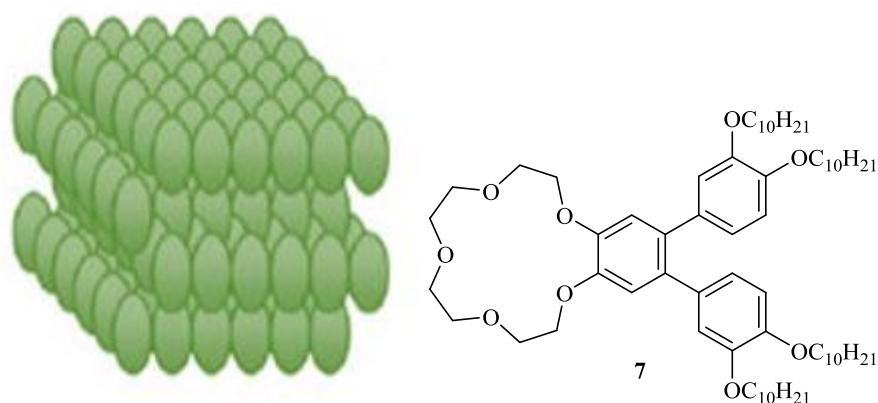


Figure 1.10: Arrangement of molecules in the smectic phase.

Cubic phases are very uncommon in discotic mesogens, although they are often observed in lyotropic liquid crystals. However, in some discotic phthalocyanine derivatives, a bicontinuous cubic phase has been observed.^[21] This displays columns which are branching and linked in a cubic lattice form.^[22]

1.2.2 Characterisation of DLC phases

There are several techniques that are utilized to identify and characterize liquid crystal phases. The characterization of thermotropic phase behaviour of liquid crystals is usually done by using Polarized Optical Microscopy and Differential Scanning Calorimetry. A discussion of the basic theory behind these techniques and how they are used will be presented.

1.2.2.1 Polarized Optical Microscopy

Initial characterization of a liquid crystal requires polarized optical microscopy (POM). Different ordered phases in LCs material such as crystalline solids and liquid crystals can be identified. Different characteristic textures for each of the mesophase types are observed.^[23] LCs compounds are optically anisotropic, their optical properties depend on orientation. This unique property describes the materials as having a different refractive index depending on the orientation of the sample, which is known as birefringence. The liquid crystal material is placed between two linear polarizing filters which are perpendicular to each other. In this technique, the plane polarized light will only be transmitted if anisotropy occurs, where refraction and interference leads to the texture to confirm LCs phases after a transition temperature.^[24]

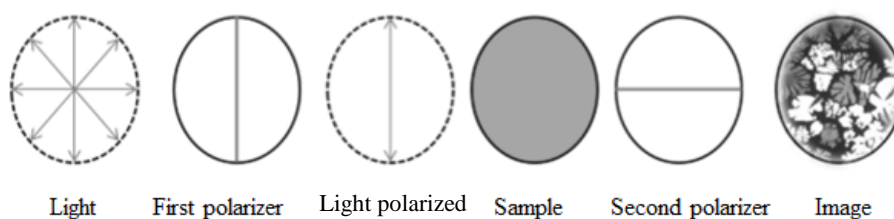


Figure 1.11: Representation of polarized optical microscopy.

Furthermore, many polarized optical microscopes are equipped with a heating stage which is used to heat and cool the sample that allows the phases of a liquid crystal to be observed to detect the transition temperatures of the liquid crystal, (figure1.12). Therefore, a polarized optical micrograph can also be used to classify the varied texture for empirical assignment of the phases, while further characterization is required to fully identify the mesophase.

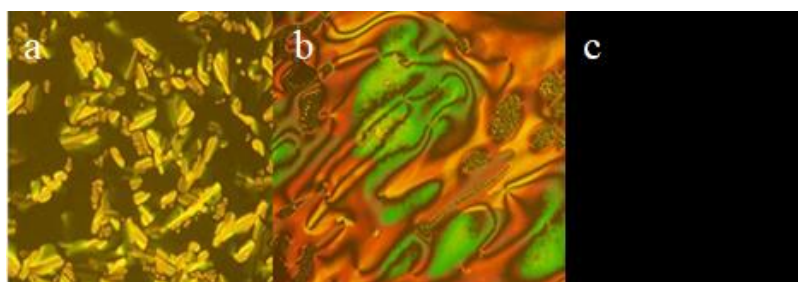


Figure 1.12: Polarized optical micrograph for a) Columnar phase, b) Nematic phase and c) isotropic liquid.

1.2.2.2 Differential Scanning Calorimetry

Differential scanning calorimetry (DSC) is another effective tool that can be used for analysis of liquid crystals by detecting the phase transition with enthalpy change for each phase. DSC is a thermoanalytical technique that is used for the precise measurements of the temperatures of transition of a liquid crystal and the enthalpy of transitions but it can't identify mesophase.^[25] A DSC instrument can detect different phase transitions by measuring the energy absorbed or released. The desired sample is cyclically heated and cooled. It will be required to maintain a constant temperature-change rate alongside the reference cell. A transition into a liquid crystal from a solid, which is an endothermic process, and will require more energy for the transition.^[23] The transitions when the sample crystallises in a cooling cycle is an exothermic process, it will release the energy. A classic DSC can be seen in figure 1.13, where the peaks relate to the phase transition temperatures and the enthalpies of these transitions can be obtained by integration of the area under the peak. In liquid crystalline compounds data, a DSC analysis typically indicate number of transitions: a solid to liquid crystal transition and a liquid crystal to liquid transition.

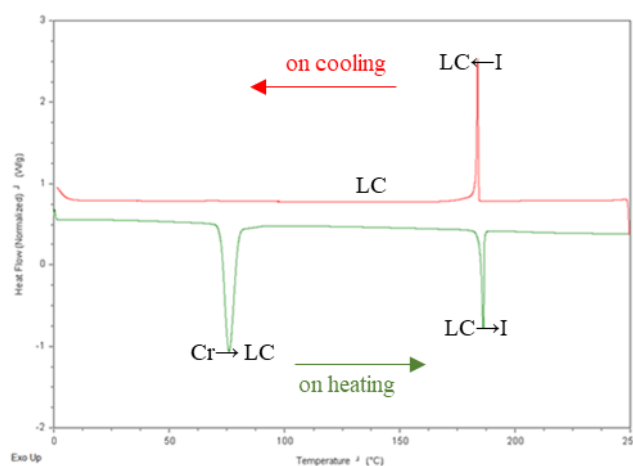


Figure 1.13: Representative DSC analysis showing transitions from solid to liquid crystal and liquid crystal to isotropic liquid.

Thus, this data can be used to support the results from POM to determine those mesophases.^[26] However, there are some transitions that may or may not be visible by microscopy or by calorimetry such as transitions from one distinct columnar phase to another distinct columnar phase or from a liquid crystal to a glassy phase.

1.2.3 Applications of discotic Liquid Crystals

DLCs have been used for some years for many practical applications, for example as functional parts in electronic devices. In this field of organic electronics, DLCs have been found useful in organic semiconductors, liquid crystal displays (LCD), discotic solar cells, organic light emitting diodes (OLED) with one-dimensional energy migration and field effect transistors.^{[27], [28]} DLCs have been used in, and they have the potential to be important materials, for innovative organic electronic purposes in future. It is this practical usefulness that has led to intensive and detailed research into the relationship between the structure and the properties of these organic molecules which results from their chemical and physical characteristics.

Certain properties of DLCs give them the potential to be used in organic semiconductors. They can form ordered, two-dimensional structures and have the capacity to heal their own structural defects. In addition, using discotic liquid crystals in organic semiconductors because they have band gap. Organic semiconductors have been the

focus of recent research due to their possible application in photovoltaic cells, for which they are attractive because they are relatively inexpensive and easy to process.^[29]

The materials which are in use at the present time are inorganic material, such as silicon, which have an acceptable level of efficiency but are challenging to prepare and extremely costly. DLCs enable faultless chemical structure to be synthesised. Their low molecular weight means that they are easier to synthesise, easier to purify and are better conductors than conducting polymers.^{[30], [31], [13]}

The best-known application of all liquid crystals is in LCDs, which are important in such devices as TVs, laptops and mobile phones. In the 1960s, the concept of LCDs was first developed. It was only in the 1970s that they became commercially viable, thanks to the work of Gray at the University of Hull.^[32] Currently used types of LCD technology include ferroelectric, in plane switching and twisted nematic, which is the most straightforward and most commonly used in LCDs.

It was challenging for researchers to synthesise materials with a nematic phase at a temperature range of -9°C to $+50^{\circ}\text{C}$, which also had a suitable dielectric anisotropy to allow the molecules' orientation to be altered by an electric field. It was also necessary for the molecules to be long-lasting and not to have a tendency to decompose. As it was unlikely to find just one compound which could meet all these requirements, particularly that of the temperature range, it became usual to select a mixture of compounds. Gray et al. used compounds 8, 9, 10 and 11 to produce the desired characteristics in their E7 mixture which was used in TN devices.^[33]

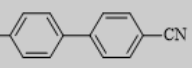
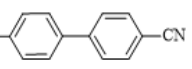
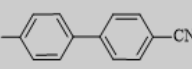
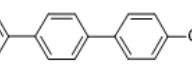
Compounds	Mesophase	Mixture composition
C_7H_{11}  8	Cr 24 N 35 I	51%
C_7H_{15}  9	Cr 30 N 43 I	25%
$\text{C}_8\text{H}_{17}\text{O}$  10	Cr 54.5 SmA 67 N 80 I	16%
C_9H_{11}  11	Cr 130 N 239 I	8%

Table 1.2: The composition of the technologically important nematic liquid crystal preparation E7.

A combination of twisted nematic and super twisted nematic displays has been used, but these types of displays have had limited applications due to two major flaws: narrow viewing angle and slow response time. Fuji Photo Film Company filed a patent in 1996 for a thin film made of a triphenylene-based discotic liquid crystal with groups of diacetylene in the side chain. The compensation film is made of discotic liquid crystals, polymerized by a photoreaction.^[34] A negative optical compensation film with birefringence was used to solving these problems was that would expand the viewing angle to improve the contrast ratio reduce the cost of LCDs.^[6, 35]

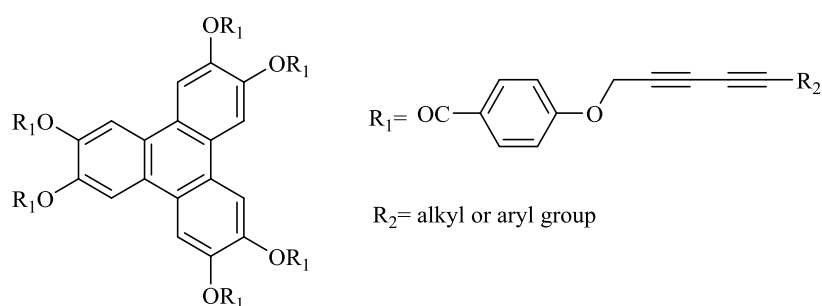


Figure 1.14: TP based DLC patented by Fuji Photo Film Company.

Triphenylene units have been applied in photovoltaic solar cells. Zinc oxide nanoparticles have been modified by Chen et al (figure 1.15) for the purpose of introducing disulfide functionalised triphenylene ligands. They discovered an improved transfer efficiency and charge separation in those nanoparticles which had been modified. Following such adaptation of the nanoparticles, there was a 0.55% increase in the solar cells' power conversion efficiency.^[7] Although this efficiency level remains low, in terms of practical applications, it still represents an improvement, and research is seeking to enhance efficiency yet further.

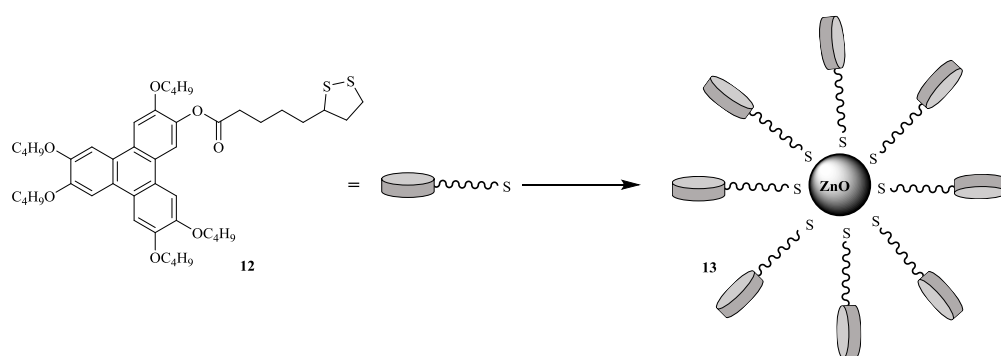


Figure 1.15: Structure of disulfide-triphenylene ligand, structure of ZnO nanoparticle modified with triphenylene ligands.

In 1997, Wendorff et al. demonstrated that it was possible to use triphenylene derivatives **14** in a single layer^[36] organic light-emitting diode (OLEDs). OLEDs are devices with two electrodes, one of which is a transparent anode, the other being a metallic cathode^[37]. In between these, there is a layer of organic material. Materials which can be used within this organic, emissive layer need electroluminescent properties. Hanack et al., in 2001 discovered bridged triphenylene derivatives **15** demonstrating just such properties^[38], which could be utilised in either double- or single-layer displays. OLEDs could be superior to liquid crystal displays in that they are thinner and lighter and do not need a backlight. Furthermore, it is possible to see them from different angles.

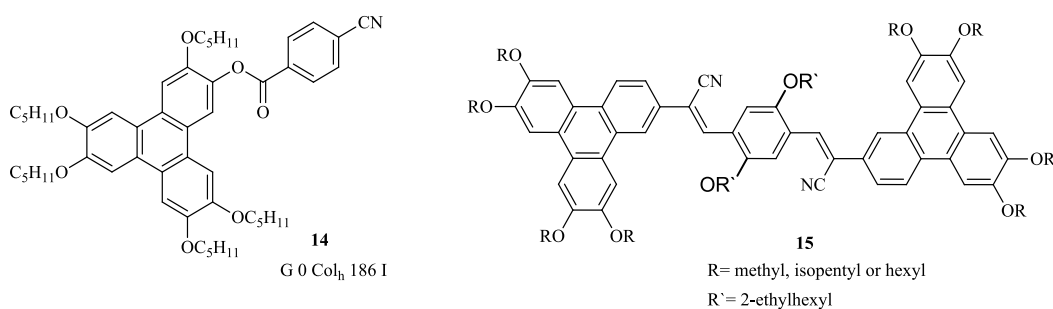


Figure 1.16: Triphenylene derivatives utilised in OLED devices.

Since 1987, it has been known that columnar liquid crystals can be used as one dimensional systems for electronic transport.^[39] The molecules within the columnar stacks are so close together that the orbitals of the neighbouring molecules overlap. This permits the occurrence of charge transport along the columnar axis. This axis therefore

functions as a molecular wire.^[40] The rigid aromatic cores are surrounded by alkyl chains, and these peripheral chains insulate the columns. This characteristic is useful for opto-electronic applications.

Lilienfeld first developed the concept of a field-effect transistor (FET) in 1930^[41], but it was a further thirty years before the first metal oxide semiconductor FET was made. The first organic field-effect transistor (OFET) to be produced used polythiophene as its active semiconducting material.^[42] There were two main benefits to this OFET. Firstly, it was less expensive, in terms of both materials and manufacture. Secondly, it meant that the product was less damaging to the environment. Triphenylene derivatives have high bandgap energy which led to poor semi-conducting properties, and for this reason, they were not initially used in the field of OFETs.

However, the design and synthesis of new semi-conducting materials, using a triphenylene core, were reported in 2009 by Hoang et al. These materials were suitable for use in OFETs^[28]. Figure 1.17 shows a thiophene-based π -extended triphenylene compound **16**. Such materials were found to possess good film forming features; their level of crystallinity is high.

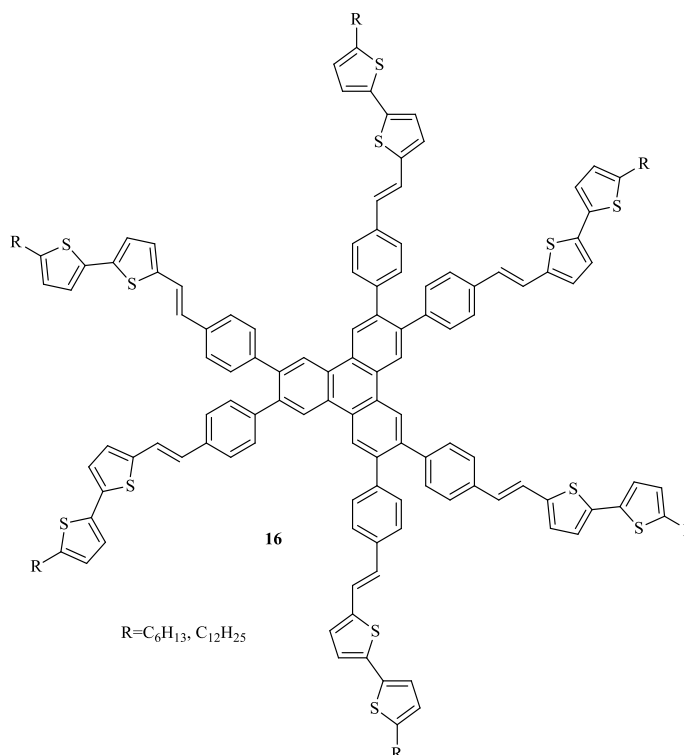


Figure 1.17: Molecular structures of thiophene based π -extended triphenylene.

1.3 Triphenylene as DLC

Triphenylene (TP) **17** was initially isolated from benzene's pyrolytic^[43] products that were discovered by Schultz. It is a symmetrical, planar, aromatic hydrocarbon consisting of four fused benzene rings and has the molecular formula of C₁₈H₁₂ (Figure **1.18**). It is possible to draw the three benzenes as the three outer rings which are interconnected by single carbon-carbon bonds. TP, as an aromatic hydrocarbon, has a delocalized 18- π electron system. Since it is a trimer of benzene, more TP derivatives can also be generated and prepared synthetically. It has been widely studied in the literature for over a century in terms of its properties. In the TP structure there are twelve potential positions for substitution, however, the most common, are those in peripheral sites 2, 3, 6, 7, 10 and 11.

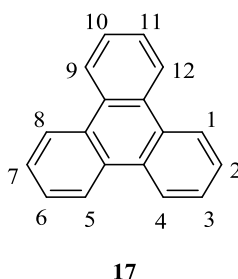


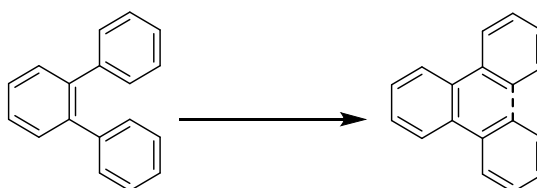
Figure 1.18: Structure of triphenylene **17**.

1.3.1 Synthesis of triphenylene

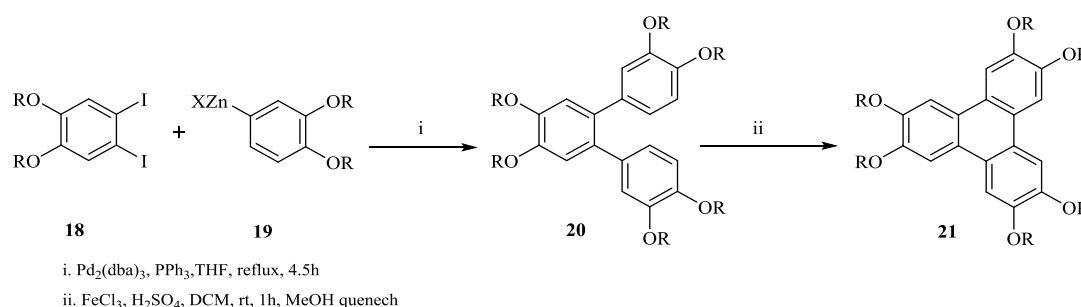
Numerous methods of triphenylene synthesis have been developed since it was first discovered. Initially, the emphasis of work was on the synthesis of triphenylene itself. In recent years, there has been a greater focus of attention on synthesising substituted triphenylene. Symmetrical hexaethers were the early types of substituted triphenylene investigated. ^[44]

1.3.1.1 Synthetic route to build triphenylene core

1.3.1.1.1 Synthesis using terphenyl compounds

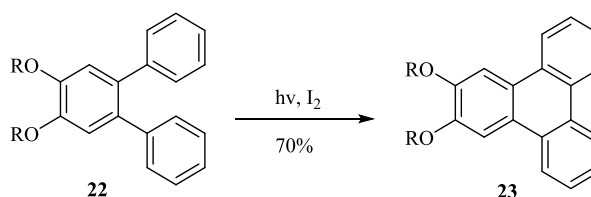


In this method the synthesis is the cyclisation of an ortho-terphenyl as the key intermediate compound. There are two procedures applied to the synthesis of triphenylenes from terphenyls. Initially, oxidative cyclisation was designed for phenol synthesis, and is now a classic reaction to form biaryl bonds which can produce both symmetrically and unsymmetrically substituted triphenylenes. There are various oxidising agents used in this coupling reaction, such as VOCl_3 , MoCl_5 , VOF_3 , $\text{K}_3\text{Fe}(\text{CN})_6$ and FeCl_3 .



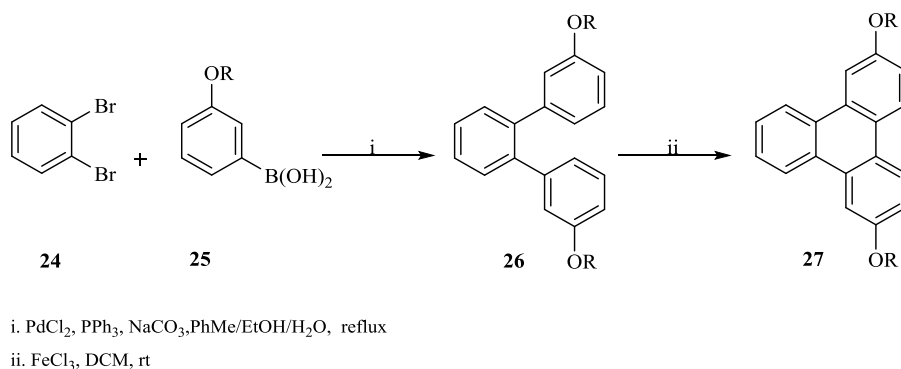
Scheme 1.2: Synthesis of hexa(hexyloxy) triphenylene **21** using terphenyl cyclisation as final step.

The other procedure photocyclization strategy is used for producing symmetrically and unsymmetrically substituted TP. Also, using iodine as oxidant in irradiation of the terphenyl **22** can improve the yield to obtain the desired triphenylene.^[45]



Scheme 1.3: Synthesis of 2,3-bis(hexyloxy) triphenylene **23**.

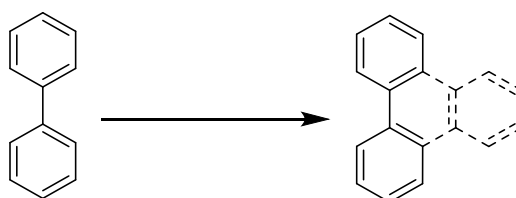
Following the example shown in Scheme 1.2, it is noteworthy that palladium-catalysed coupling has been frequently used to synthesise terphenyls, followed by oxidative cyclisation. The desired terphenyls were obtained by using the catalyst tris(dibenzylideneacetone) dipalladium [Pd₂(dba)₃] and triphenylphosphine PPh₃. With iron chloride and a trace of sulfuric acid the previous precursor was treated in dichloromethane to give the required triphenylene derivatives.^[46]



Scheme 1.4: Synthesis of 2, 7-Bis(hexyloxy) triphenylene **27**.

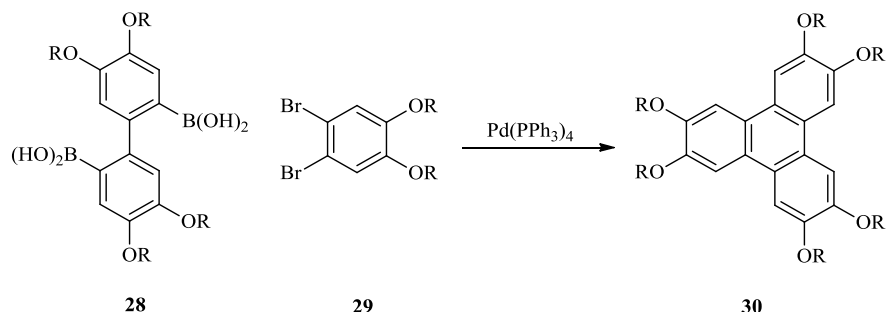
Similarly, Suzuki coupling reaction (scheme 1.4) has been used to prepare other terphenyl from boronic acids **25** to couple with *o*-dihalobenzene **24** to synthesise symmetrically^[47] and unsymmetrically substituted triphenylene.

1.3.1.1.2 Synthesis via phenyl-biphenyl oxidative coupling route



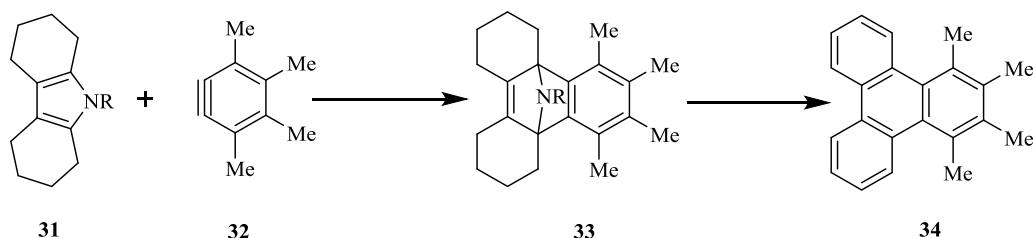
In this method of synthesis of TP, biphenyl is an important precursor. There are three methods which can be used to obtain the target compound: palladium-catalysed coupling, Diels-Alder cycloaddition and oxidative coupling. A Suzuki coupling is the reaction where a palladium-catalysed coupling procedure was used. Biphenyl can be

produced by using a coupling reaction with boronic acid which is usually used to form a C-C bond with the substituted aryl group. Generating substituted triphenylene depends on the different R-groups which were substituted on both reactants. This interesting approach has been reported to work with TP synthesis.^[44]



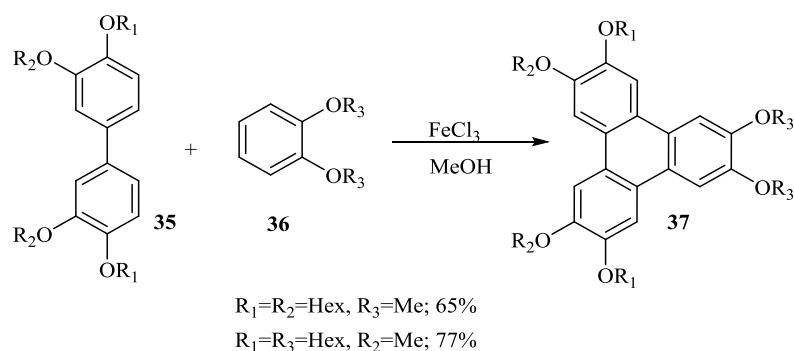
Scheme 1.5: Palladium-catalysed synthesis of triphenylene.

Another strategy uses biphenyl as a diene reacting with aryne **32** to form the target. This reaction is a Diels-Alder cycloaddition reaction. It is a remarkable synthesis of triphenylene. Shown in scheme **1.6** is an example starting from heterocyclic dienes with benzyne leading to adduct **33**, which can be transformed into triphenylene **34** by heating followed by oxidation with 2,3-Dichloro-5,6-dicyano-1,4-benzoquinone DDQ.^[48]



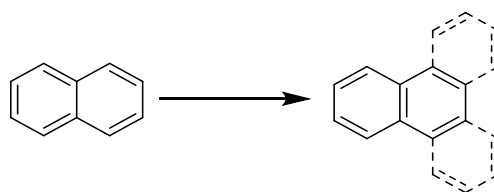
Scheme 1.6: Synthesis of substituted triphenylene from heterocyclic dienes.

Oxidative cyclisation is a method which is applied to biphenyl as in the previous example, in terms of the number of oxidants which can be utilised. To produce triphenylene derivatives in a reasonable yield as illustrated in the scheme **1.7**^[49] a substituted biaryl **35** was reacted with dialkoxybenzene **36** in presence of FeCl₃. Boden et al. have showed that this method allows substituents to occur in the α -position, which had been difficult to achieve previously because it is sterically hindered.^[50]

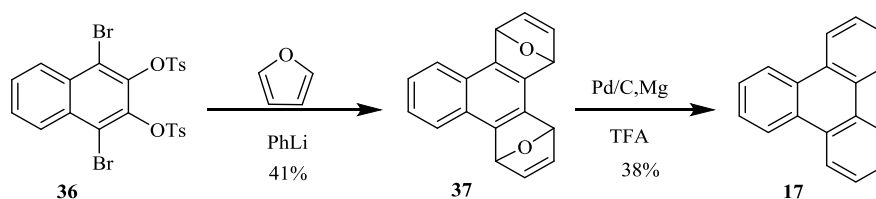


Scheme 1.7: Synthesis of substituted triphenylene from biaryl **35**.

1.3.1.1.3 Synthesis via a naphthalene core

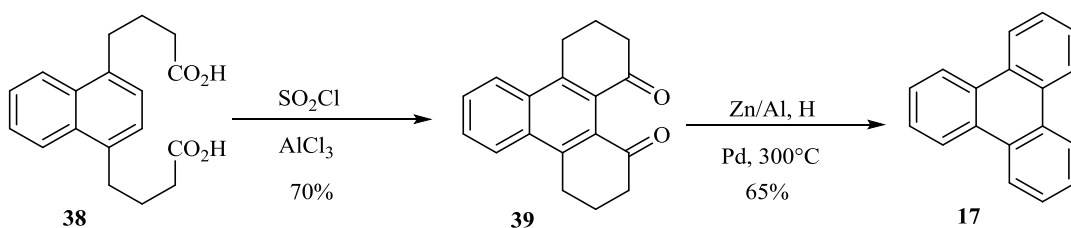


This method uses naphthalene as peripheral rings for the synthesis of triphenylene. There are two routes using naphthalene and its derivatives as starting material to produce the triphenylene. The common procedure is the Diels–Alder cycloaddition as shown in the scheme below. When Naphthalene or its derivatives are eliminated after the metal–halogen exchange, they generate aryne, then the next step is to react with furan as diene. The further step to obtain triphenylene **17**, is when compound **37** is treated with Pd/C and Mg followed by TFA for deoxygenation.^[51]



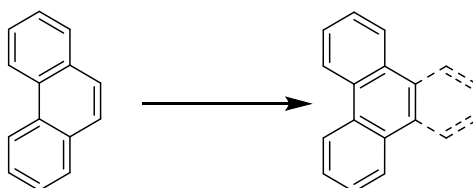
Scheme 1.8: Synthesis of triphenylene **17** via Diels-Alder reaction.

A similar method to the above scheme for producing triphenylene is by a Friedel-Crafts reaction. Cyclisation of the substituted naphthalene **38** yields a diketone ^{[52],[53]} **39**. Using a palladium catalyst for reduction and dehydrogenation can then yield a triphenylene (scheme **1.9**).

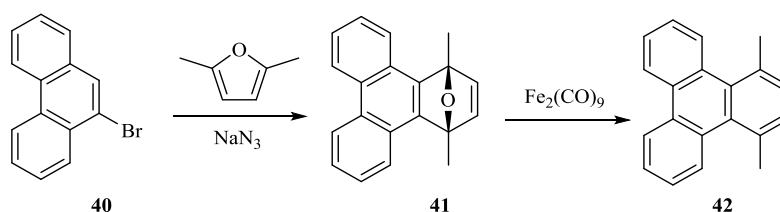


Scheme 1.9: Synthesis of triphenylene **17** via Friedel-Crafts reaction.

1.3.1.1.4 Synthesis using a phenanthrene moiety

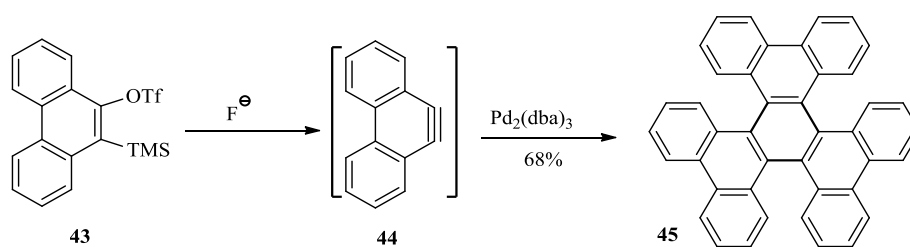


In this method the triphenylene is produced by the Diels-Alder reaction, photocyclisation, and palladium-catalysis, using a phenanthrene derivative as an important precursor to prepare the triphenylene. Diels-Alder reactions are again a usual route for these types of reactions with deoxygenation step, to give the triphenylene. In the example shown below in scheme, the phenanthrene derivative **40** reacts with furan in presence of sodium amide, followed by deoxygenated step to produce compound **42**.



Scheme 1.10: Synthesis of 1, 4-dimethyl triphenylene.^[54]

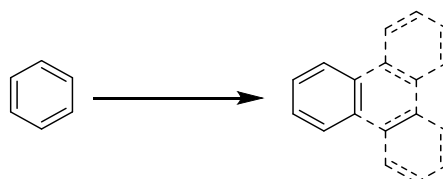
Formation of the benzotriphenylenes by photocyclisation has also been achieved from phenanthrene derivatives. Also, palladium-catalysed trimerization is another strategy towards the synthesis of triphenylene derivatives which should be mentioned under this classification because it uses phenanthrene as starting material.^[44]



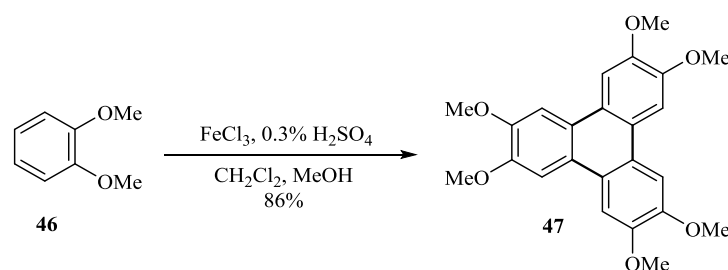
Scheme 1.11: Synthesis of benzotriphenylenes **45**

This procedure is suitable to prepare TP with substituents other than alkoxy, which are difficult to prepare in other ways, and benzoannulated triphenylene is an example of this route.^[55] There are other routes to use for the preparation of functionalized triphenylenes such as Friedel–Crafts cyclization, Cationic cyclizations, Classical carbanion and in some cases by Wittig reaction.^[44]

1.3.1.1.5 Synthesis via a cyclotrimerization step

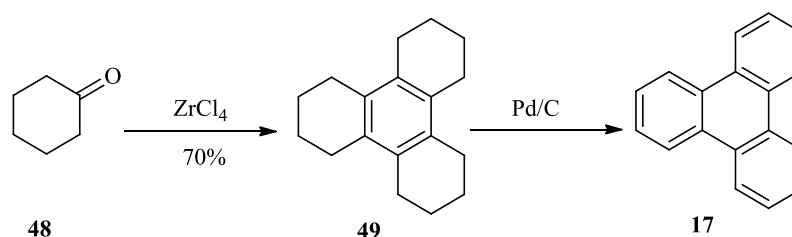


This method for the synthesis of triphenylene proceeds by formal trimerization of 6-membered rings. The main route is oxidative trimerization as one of the classic syntheses of triphenylene, shown in the scheme below which gives an example that followed this strategy. Most of the focus has been on the synthesis of hexaalkoxytriphenylenes since the discovery of their liquid crystal nature and properties. This procedure is widely used in the formation of symmetrically substituted alkoxytriphenylenes. In 1960, Mannich successfully conducted oxidative trimerization of catechol derivatives **46** by using oxidants agent as FeCl_3 in sulphuric acid. Later the experiment was improved by Bushby and co-workers^[49] and they optimised the conditions to obtain a higher yield. The modification of the experiment involved decreasing concentrations of sulfuric acid H_2SO_4 to 0.3% and to stop the reaction by using methanol as reducing agent for work-up^[56].



Scheme 1.12: Oxidative trimerisation of dimethoxy benzene **46** to yield **47**.

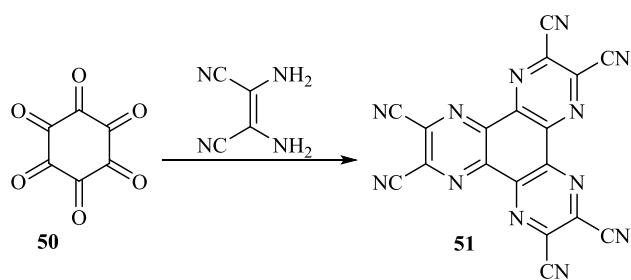
There are a number of oxidizing agents such as MoCl_5 and VOCl_3 which can be used for this reaction, under the same conditions to produce many substituents ranging from hydroxyl, crown ether to chiral moieties. Mannich's original procedure, H_2SO_4 -catalysed trimerization of cyclohexanone, has hardly been used since 1960, but alternative procedures that use catalysts such as HfCl_4 , ZrCl_4 , and Cp_2ZrCl_2 have been developed.^[57] In these cases the reactions are aldol/dehydration reactions rather than oxidative cyclisations. Triphenylene formation then requires dehydrogenation of the intermediate.



Scheme 1.13: Synthesis triphenylene **17** from cyclohexanone.

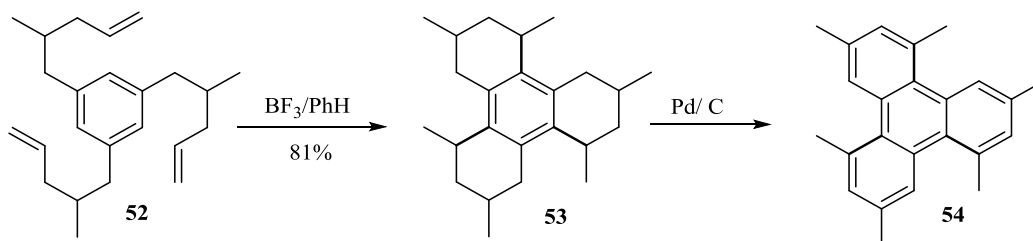
1.3.1.1.6 Synthesis via the addition of peripheral rings in one step

The previous methods of synthesising TP and its derivatives depended on the different precursors. In spite of that there have been only a few preparations of TP by one-pot synthesise, this is a method often used to synthesise compounds which are not easily synthesised using the standard techniques. In recent years there has been growing interest in the synthesis and properties of aza-triphenylenes. Some examples of this type in the literature are shown below in Scheme **1.14**.^[58] Most heterocyclic analogues similar to compound **51** have been prepared using a condensation strategy for hexaketocyclohexane **50** with 1, 2-diaminoethylene derivatives.



Scheme 1.14: Synthesis substituted hexa-aza-triphenylenes **51**.

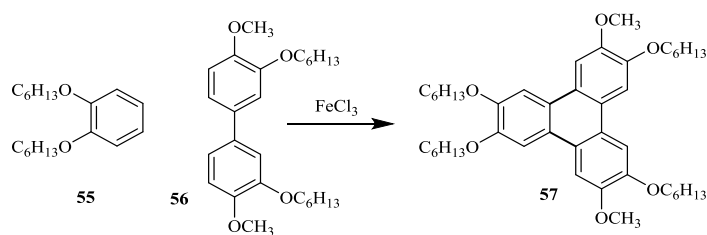
The literature also contains examples of acid cyclisation methods with benzene derivatives to synthesise the TP derivative, as presented in the scheme showing the cyclisation of **52** using an acid catalyst. This produces **53** which can be further changed to **54** via dehydrogenation with palladium on carbon to yield the compound (Scheme 1.15).^[59] These reactions are also Friedel-Crafts cyclisations and can be compared directly to those previously described (Scheme 1.9)



Scheme 1.15: Acid catalysed cyclisation of **52** to yield **54**.

1.3.1.2 Synthetic routes to build unsymmetrical triphenylene cores

Structures with unsymmetrically substituted triphenylenes have attracted much research interest because they have the potential for the introduction of functional groups. For a long time, the most frequently used route to produce these compounds is oxidative coupling of benzene derivative and biphenyl derivative using iron (III) chloride. This requires a reductive workup step using methanol. Scheme 1.16 illustrates an oxidative coupling of 1, 2-disubstituted benzene **55** with biphenyl derivative **56**. The process uses ferric chloride and produces unsymmetrically substituted triphenylene **57**.



Scheme 1.16: Synthesis of triphenylenes **57** from biphenyl.

Some of the functional groups which can be introduced to the triphenylene using this successful procedure^[60] include electron donating methoxy groups, electron withdrawing aldehyde and nitrile groups, also electron deficient pyridines and electron rich thiophenes and furans.^[61]

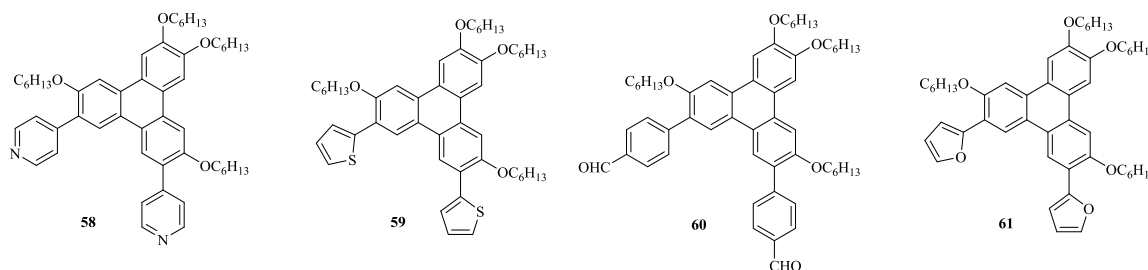
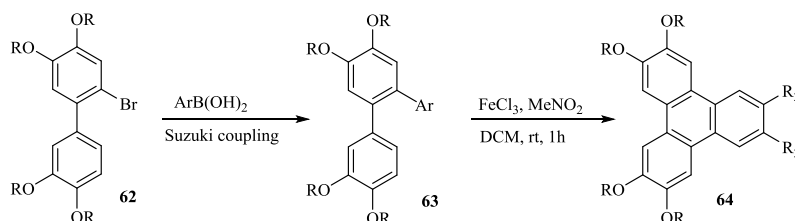


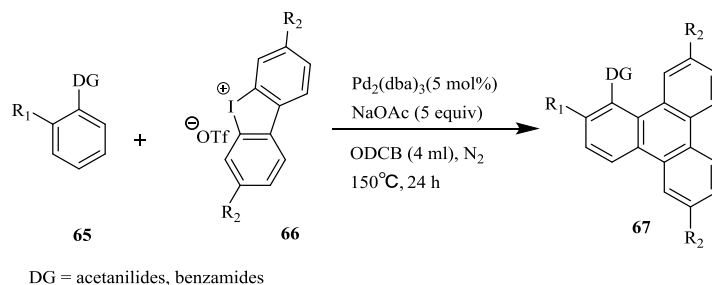
Figure 1.19: Range of unsymmetrically substituted functionalised triphenylenes.

Zhoa et al. (2017)^[8] described the synthesis of new triphenylene derivatives based on the triphenylene core. A Suzuki cross-coupling reaction between biphenylenes derivatives and different boronic acid produced the intermediate terphenyl **63**. Tetra (alkyloxy) triphenylene **64** can be achieved by oxidative coupling using ferric chloride.



Scheme 1.17: Synthesis of asymmetrical triphenylene derivatives.^[8]

Mathew et al. described one of the recent strategies to afford asymmetrical substitution in triphenylene derivatives by Palladium-catalysed C–H activation reported in 2017. One such example is shown in Scheme 1.18, reaction of **65** with diaryliodonium salt **66** in presence of catalyst was used to obtain unsymmetrically substituted triphenylene **67**.^[62]



Scheme 1.18: Synthesis of asymmetrical triphenylene.

1.3.2 Mesophase formation in Triphenylene Derivatives

Symmetrical hexaalkoxy triphenylenes **68** are typical of DLCs exhibiting columnar hexagonal mesophases covering a wide range of temperatures.^[63] Unsymmetrical TP structures can also be identified and since their character and properties are different from the symmetrical TPs, they have different mesophase behaviours. Our group is of the opinion that various factors in combination determine the formation and stability of mesophases in triphenylene discotics. One essential factor for synthesising triphenylene with conjugating groups substitution to extend the core and determine mesophase formation and stability. It is also the case that investigation is needed in non-conjugating systems. For steric reasons these also have a tendency to destabilise the formation of columnar mesophases. The best way to improve the stability of the mesophase is by attaching electron withdrawing substituents to the alkoxytriphenylene core which is rich in π -electrons. This is most likely because this polarises and strengthens the π - π interactions between the aromatic cores.^[64] It is already well-known that combining discotic materials which are rich in electrons with such electron-accepting aromatics such as TNF has the effect of stabilising columnar mesophases.^[65]

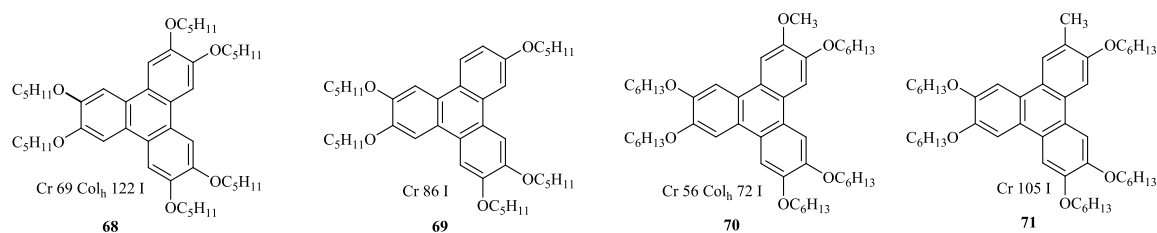


Figure 1.20: Selected example triphenylenes demonstrating the effect of substitution.

The formation of the mesophase can be destroyed if one of the alkoxy chains is removed **69**.^[66] Methoxy substitution **70** tends to enhance mesophase formation^[67] while using methyl as a non-conjugating substitution **71** prevents mesophase behaviour.^[65c] If a conjugating substituent is incorporated, however, the mesophase formation can be reinstated.^[8, 68]

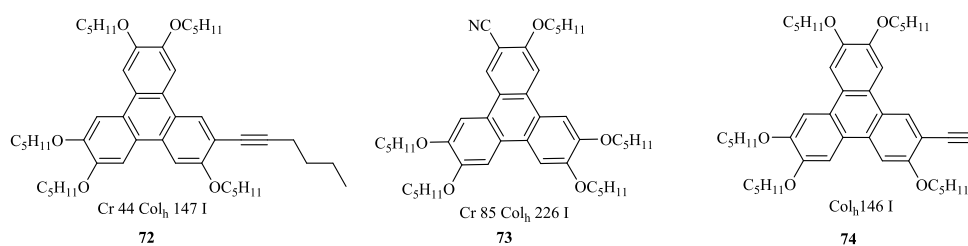


Figure 1.21: Other mesophase behaviour of unsymmetrical triphenylenes.

If one compares substituents with similar chain lengths, it is possible to appreciate the extent to which this depends on extending the core π -system **72**. The best stabilisation of the mesophase occurs with cyanide **73** substitution.^[69] However, a notable improvement in mesophase formation is found in a non-polar acetylene **74**.

Zhao and his group have reported a series of various unsymmetrical triphenylenes with electron-withdrawing substituents.^[8] They prepared the desired compounds in two steps. Initially 2-bromobiphenylenes react with variety of arylboronic acids by using Suzuki cross-coupling reaction to produce the intermediate *o*-terphenylenes. Unsymmetrical, novel polar triphenylenes has been obtained by Intramolecular oxidative cyclodehydrogenation by $\text{FeCl}_3/\text{MeNO}_2$. Analysis has showed that some of the synthesized molecules exhibit a hexagonal columnar mesophase (figure 1.22) by common methods to characterise LC compounds.

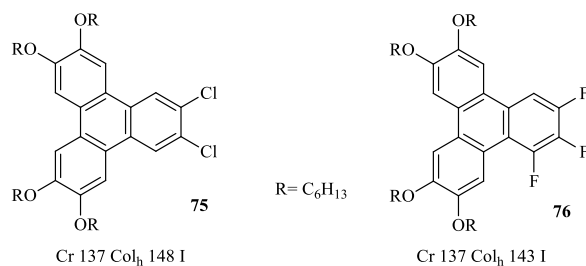


Figure 1.22: Some structures of the unsymmetrical polar triphenylene derivatives.

1.3.3 Triphenylene Dimers

Dimer is a general term used for liquid crystals which are comprised of two mesogenic groups. These may be identical or not and joined by either a rigid or a flexible spacer.^[70] These compounds have become an important focus for research. Two triphenylene units joined by a single spacer will be referred to as a “diad”,^[71] while two triphenylene moieties linked by two spacers will be termed a “twin”^[72]. The literature contains reports of numerous diads but only a small number of triphenylene twins have so far been reported.

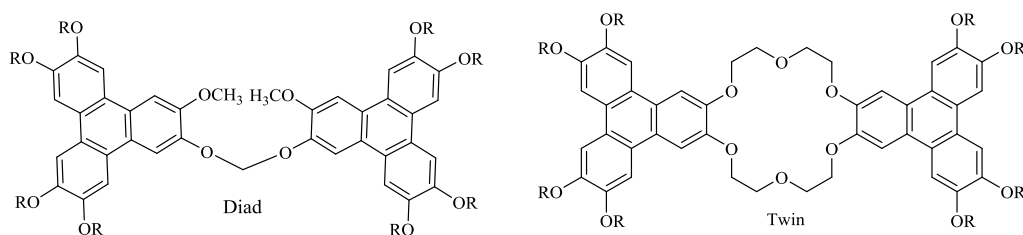
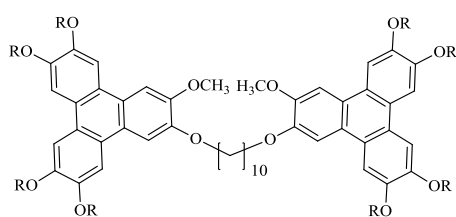


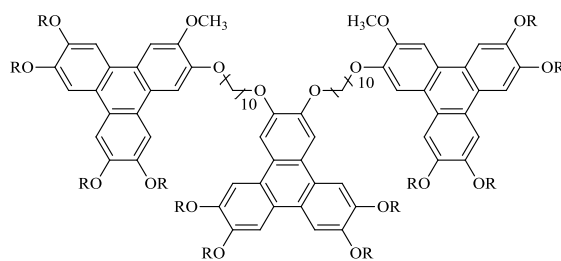
Figure 1.23: Structures to show meaning of terms ‘diad’ and ‘twin’.

In figure 1.24 both the diad and triad structure, first reported in 1995 by Boden et al. are illustrated. Both compounds crystallised slowly at room temperature and formed glassy mesophases. This demonstrates that triphenylene diads share some properties with polymers.



1 98 Col_h 33 Glassy Col_h (hours) Cr

77



Cr 60 Col_l 92 Col_h 109 I

1 105 Col_h 32 Glassy Col_l (months) Cr

78

Figure 1.24: Structures of Diad and Triad synthesised by Boden et al.

Spiro twins **79** were first synthesised in 1998.^[73] Although the researchers originally thought that the central, spiro twist might prevent columnar mesophases from forming, in fact, they did form, making these compounds potentially useful for photo conductivity.

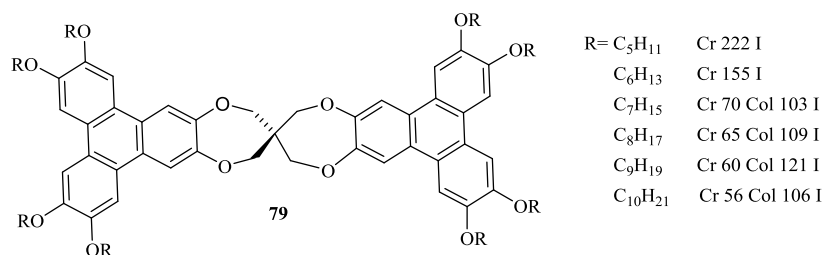
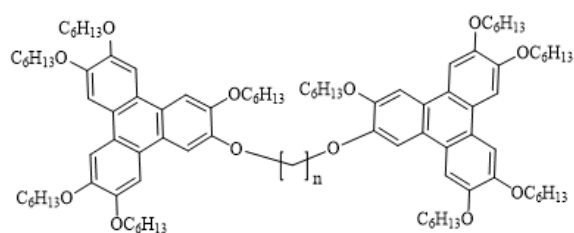


Figure 1.25: Triphenylene spiro twins.^[73]

During further work on diads, Boden et al. (1999) revealed more characteristics of the liquid crystal properties of triphenylene diads.^[74] They discovered that the length of the spacer has a considerable effect on how the diad behaves. If the spacer is not long enough, the diad will not have a liquid crystal phase. There is a negative correlation between the length of the spacer and the lifetime of the glassy phase.



n=3	Cr 81 I
5	Cr 98 I
7	Cr 69 I
8	Cr 58 Col _h 91 I
9	Cr 72 Col _h 92 I
10	Cr 50 Col _h 104 I
12	Cr 68 Col _h 107 I
16	Cr 41 Col _h 84 I

Figure 1.26: Transition data for triphenylene diad above. ^[74]

Another possible triphenylene diad uses a phenylene dicarbamate unit as its link **80** (figure 1.27) and its film forming properties were better than those of its monomer. This might be a result of its flexible spacer and the formation hydrogen bonds between the diads. This compound has good charge carrier mobility and hole transporting characteristics, which made it suitable for use in OLEDs. ^[75]

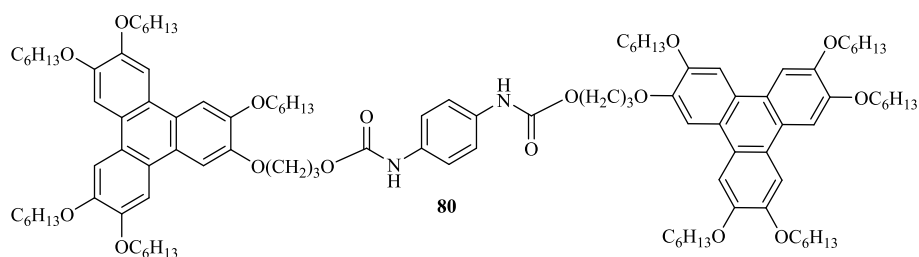


Figure 1.27: Triphenylene diad linked by a phenylene dicarbamate unit.

Acetylene units were used a linker in a number of diads synthesised in 2009. ^[76] These diads were shown to be stable and to have a columnar mesophase, which improved their semi-conductive properties.

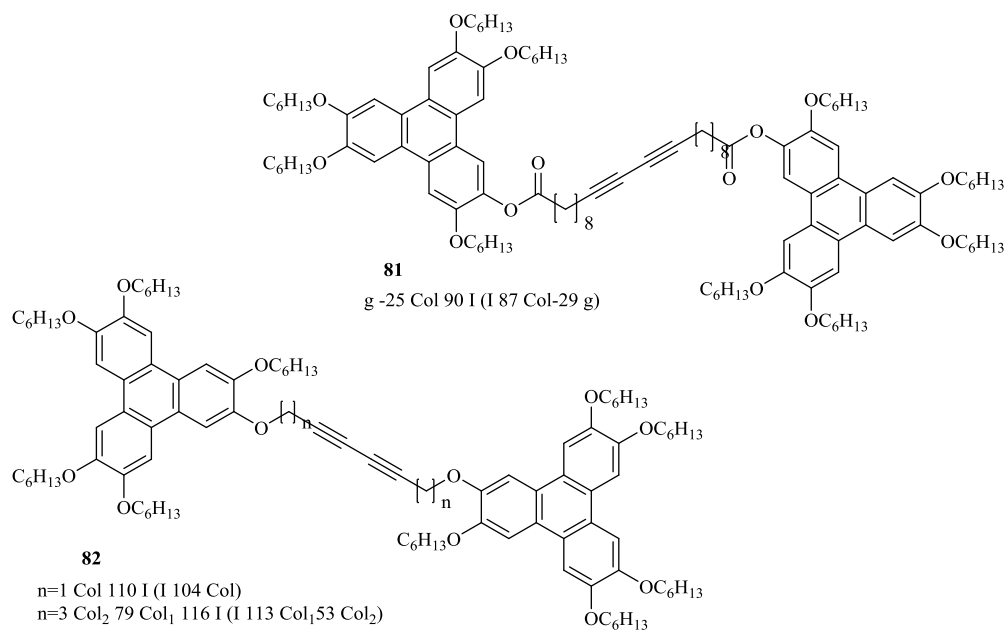


Figure 1.28: Acetylene linked triphenylene diads.

In 2010, the Cammidge group synthesised triphenylene twins and triads linked by crown-ether.^[72] No mesophase behaviour was found for the twin **83**, but the triad **84** had a columnar phase which made it potentially applicable in optoelectronic devices.

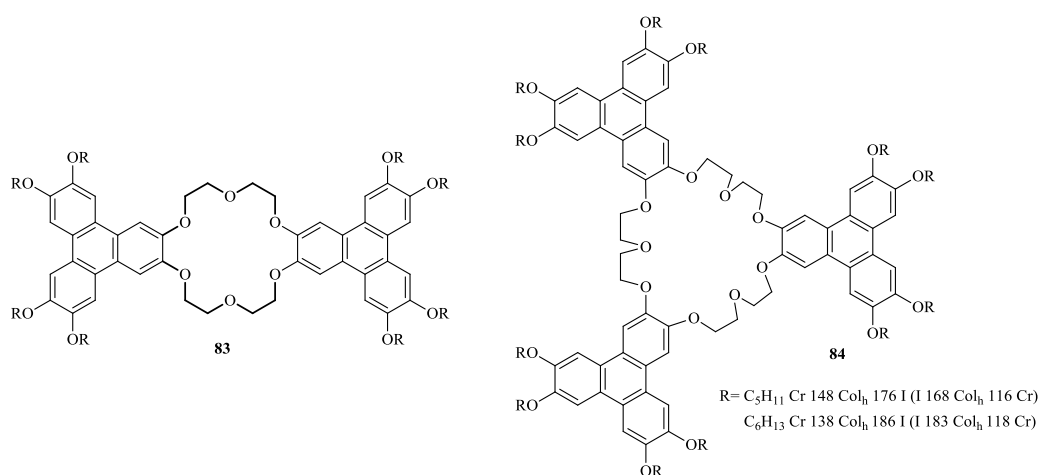


Figure 1.29: Crown-ether linked triphenylene twin and triad.

A similar structure to the crown ether was also used by the Cambridge group, in the same year, to synthesise antiaromatic triphenylene twins with diacetylenes as the bridge. The problem was that, when the triphenylenes were linked at the ortho positions **85**, they decomposed through pericyclic reactions. This problem was solved by separating the acetylene units, creating a void. Thus, the 3, 6 position was chosen as the sites for the acetylene coupling **86**. This retained the antiaromatic core but prevented the issue of decomposition.^[77]

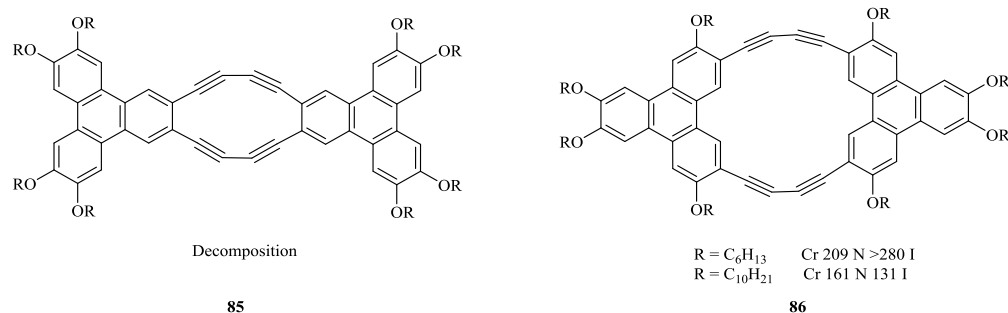


Figure 1.30: Antiaromatic triphenylene twin linked by acetylene bridges.

It was observed that this twin formed a stable, board-like, planar molecule. On heating, it showed the rare nematic mesophase. The packing of the molecules in the crystal was of particular interest. The twins were overlapping in their stacks, because column formation was impossible due to the free space this would leave because of the void in the twin. This is the reason for the occurrence of the nematic mesophase and makes communication possible both along the rows and through the columns.^[78] The observation of nematic phase in discotic molecules was unusual.

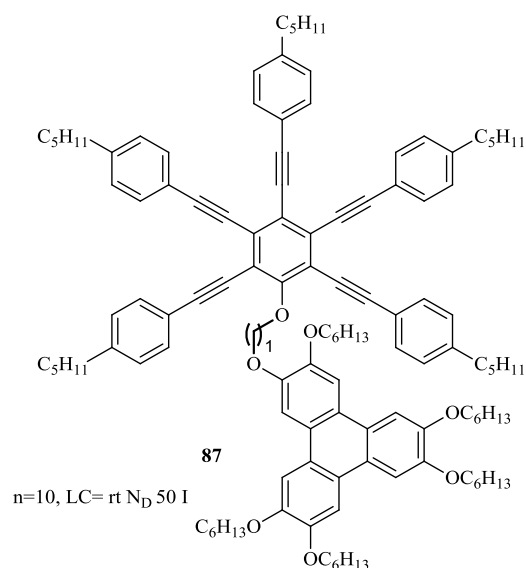


Figure 1.31: Structure of compound **87** that showed discotic nematic mesophase.

However, joining two different mesogenic moieties into a single compound could enhance the existence of N_D phase. In 2017, Gupta et al. published a method for synthesis of discotic diads **87** which are stable liquid crystal at room temperature after cooling from isotropization. The target diads containing of triphenylene and pentaalkynylbenzene (PA) connected by alkyl chain as flexible spacers demonstrated the N_D phase at ambient temperature. It can result from the folding of two discs between π - π interactions and prevent stacking between triphenylene units.

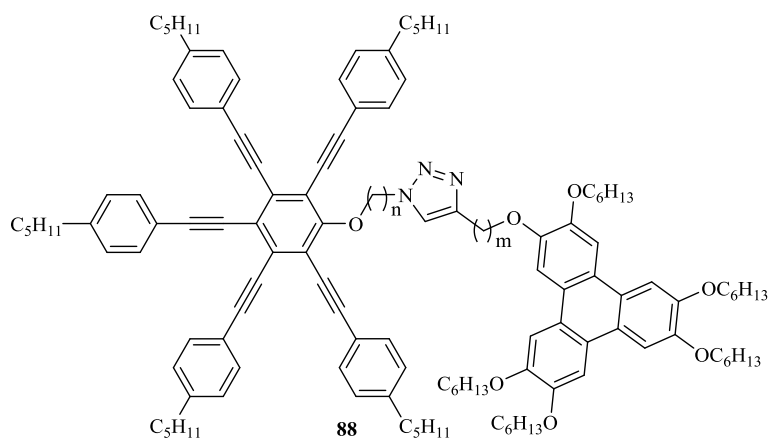


Figure 1.32: Structure of the diads **88** synthesised by Bala et al. ^[79]

<i>m</i>	<i>n</i>	<i>Phase transition temperatures in heating/ cooling cycle</i>
1	6	Col _r 46.1 Iso/ Iso13.2 N _c
	8	Col _r 62.5 Iso/ Iso11.5 N _c
	10	Sm 51.8 Iso/ Iso11 Sm
3	6	Col _r 53 Iso/ Iso12.8 N _c
	8	Col _r 68.8 Iso/ Iso 3 N _c
	10	Sm 76.5 Iso/ Iso14.5 Sm

Table 1.3: Thermal behaviour of the pure **88** compounds.

In 2019, a number of related unsymmetric diads **88** have been synthesized successfully. They are composed two discotic components as shown in figure 1.32. ^[79] The structures have linked TP to PA moieties by a triazole as rigid spacer. These compounds have exhibited columnar rectangular behaviour and weak smectic phase when the chain was longer (Table 1.3).

1.4 The Aim of the thesis

The synthesis of triphenylene twins have been the topic of common research recently with the aims to improve the liquid crystals properties. As presented, many triphenylene compounds are discotic liquid crystals which shows characteristic of the hexagonal columnar mesophase. Our group has been focused on synthesising twining triphenylenes that exhibit the formation of nematic mesophase. The aim of this project is initially to synthesis triphenylene diads and investigate the syntheses and characterisation of these compounds that are comparable to previous twin studies and their precursor mesophases. To achieve this aim, Cammidge's earlier work was made us of regarding the synthesis of triphenylene twins together with their liquid crystals behaviours to synthesis a new series of triphenylene diads which have nematic behaviour as the target feature. In the first set of experiments, Bridges was chosen as the earlier twin molecules. With some considerations to the structural modifications to study the effect of structural geometry that the positions of spacers substitution have on the diads properties. However, diiminoisoindoline has been selected as the second series bridge for new triphenylene diads and study the potential of their properties. Result of this research, will hopefully provide a contribution to display nematic mesophase in discotic systems.

Our aims for the project included:

- To prepare triphenylene diads, triads linked by aromatics bridge.
- Investigate their nematic behaviour or other liquid crystals properties
- Employ Bodipy moiety as a linker between triphenylene units and follow the same techniques that used in the recent work.

Chapter 2

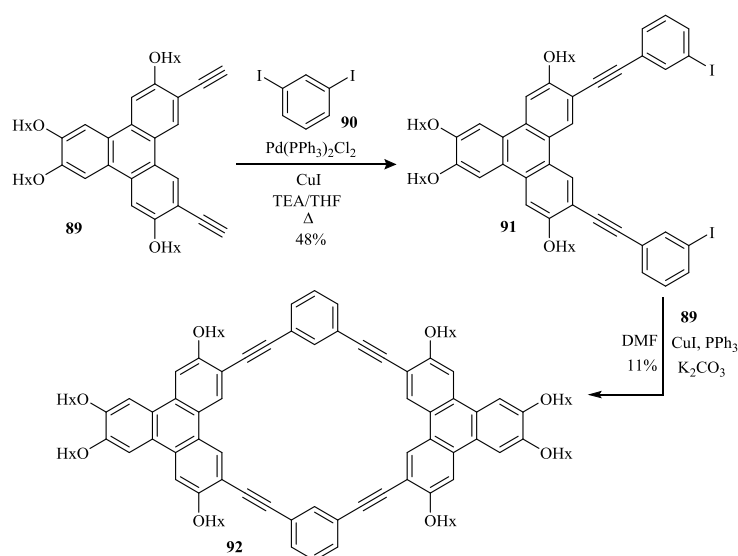
Results &

Discussion

2.1. Synthesis of triphenylene diads

2.1.1. Previous Work from our Group

Since the discovery of discotic liquid crystals by Chandrasekhar in 1977,^[3] there has been a considerable research effort directed at understanding the structure of these molecules and the factors controlling the way in which the columnar mesophase forms in these discotic systems. This is of practical significance because of the applications for which columnar systems can be used, such as photovoltaic systems and light-emitting diodes. Discotic liquid crystals can, like conventional, rod-shaped or calamitic liquid crystals, form nematic phases which are less ordered than the columnar phases. To date, the factors which drive the formation of nematic phases have not been well elucidated. However, they are important because they can be used in liquid crystal displays as optical compensating films. One particularly important area of interest for our group has been those systems which have triphenylene at their cores. These have the advantage of being synthetically versatile and having molecular robustness, which is a useful when they are used within devices. Previous work by Cammidge et al. successfully reported the synthesis of numerous triphenylene twins.^[77] The 1, 3-phenylene-bridged twin **92** showed nematic behaviour and proved to be an interesting structure. It was followed by the synthesis and investigation of more complex twins, such as those with heterocyclic links and those which include aromatic units.



Scheme 2.1: acetylene-benzene twin **92**

The synthesis of acetylene-benzene twin **92** is shown in Scheme **2.1**. The benzene bridge allowed the creation of the void between the triphenylene moieties. Furthermore, it minimised the strain in the structure because of the angles of the matched bonds. The synthesis proceeded in a stepwise fashion, starting by introducing the benzene moiety via Sonogashira coupling between triphenylene diacetylene **89** and excess 1, 3-diiobenzene. The twin structure was formed by a further coupling between **91** and its precursor **89**. Given the interest in and importance of the nematic behaviour of the twin **92**, the starting point for this project, was to focus on the preparation of novel triphenylene diads and to investigate the nematic behaviour and other liquid crystal properties. The target structure was *m*-di-triphenylene benzene **93**, as shown in figure **2.1**. With the synthesis of 1,3-bridge twin **92** developed, the plane has been expanded to obtain series of diads have the same linker as the twin which already mentioned and investigate the impact on mesophase behaviour.

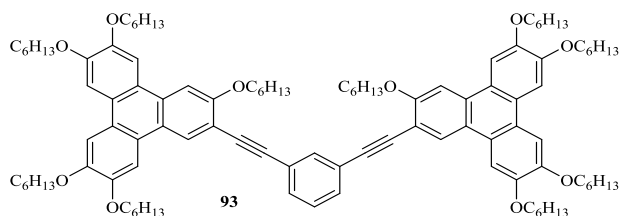
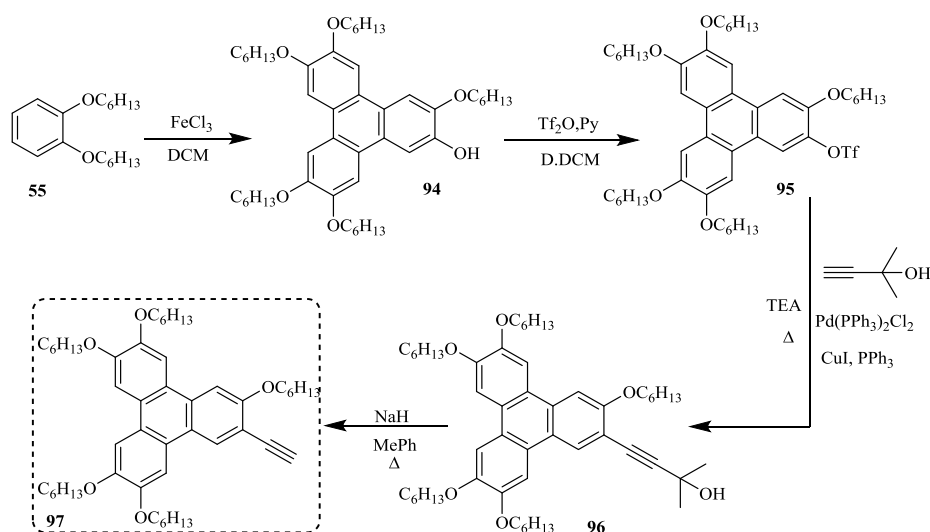


Figure 2.1: The target structure

2.1.2. Synthesis of mono-acetylene triphenylene **97**

Synthesis of the intermediate (mono acetylene triphenylene) was prepared and used in further syntheses to prepare triphenylene diads linked through a rigid spacer. Mono acetylene triphenylene is a key precursor for building number of triphenylene derivatives, which had been successfully reported by our group.^[80] The full synthetic route toward intermediate compound is shown in scheme **2.2** below. It is therefore important for the synthesis of the target triad and diad triphenylenes.



Scheme 2.2: The full synthetic route towards mono-acetylene triphenylene **97**.

The initial step towards achieving the target compound (mono-acetylene-triphenylene) was to prepare 1, 2- Di-Hexyloxy-Benzene (DHB) **55**. Catechol, 1-bromohexane and potassium carbonate were stirred in ethanol under reflux to form DHB in 60% yield with mono-substituted phenol as a side product. The production of DHB was increased by 15% when using excess equivalents of the 1-bromohexane, in the presence of potassium iodide as the catalyst for this reaction. Distillation was the purification method used to obtain the pure compound. The pure compound **55** was used to obtain the next compound in the synthetic route, Mono-Hydroxy-Triphenylene (MHT) **94**. The active hydroxyl group is a useful point of attachment to introduce different functional groups to form new triphenylene derivatives. There are a number of methods to produce this compound, but the routes which have been chosen for use in these experiments are those which have been refined and improved by our group and were further optimised in this work.^[81] The first method was to treat the DHB with anhydrous ferric chloride (FeCl_3) in two portions in dichloromethane at 0°C . After two hours, the reaction was stopped using methanol and water. The desired structure was formed as a side product while the symmetrical structure 2, 3, 6, 7, 10, 11-Hexakis (hexyloxy) triphenylene (HAT) was the major product. There were some difficulties with the purification of the product because firstly, the yield of MHT was low and secondly, the crude included a number of different compounds. On the TLC plate, these could be identified but the distance between them was very small. Applying the column was more of a problem because all the compounds were mixed and had a tar-like nature. The entire column was dark, and it was difficult to identify the different compounds.

To overcome this problem, a slower, non-polar purification system has been used to try to isolate the HAT as a pure fraction, thus avoiding it becoming mixed with the MHT. However, the compounds were still produced as a mixture. All these difficulties meant the process proved very time-consuming and inefficient. Furthermore, the crystallisation also took a long time and had to be conducted in the dark under re-fridgeration because MHT was found to be a light-sensitive compound. After the filtration of the solid MHT, the yield was too low and there was not an adequate amount of product for use in all the future steps required to reach the target. The reason behind the low yield was that the reaction formed the symmetrical structure first and after the second portion of FeCl_3 was added, one of the hexyloxy chain was deprotected and the MHT was produced. The reaction has been stopped to avoid more hydrolysis for alkoxy chain. The NMR spectrum confirmed the formation of the target as a single peak at 5.9 ppm that corresponded to hydroxyl group and the integration of 6 protons in the aromatic were matched with triphenylene interior protons. This was consistent with the existing reference values. However, the purple colour was surprising because both MHT and HAT are colourless, according to previous reference material.^[82]

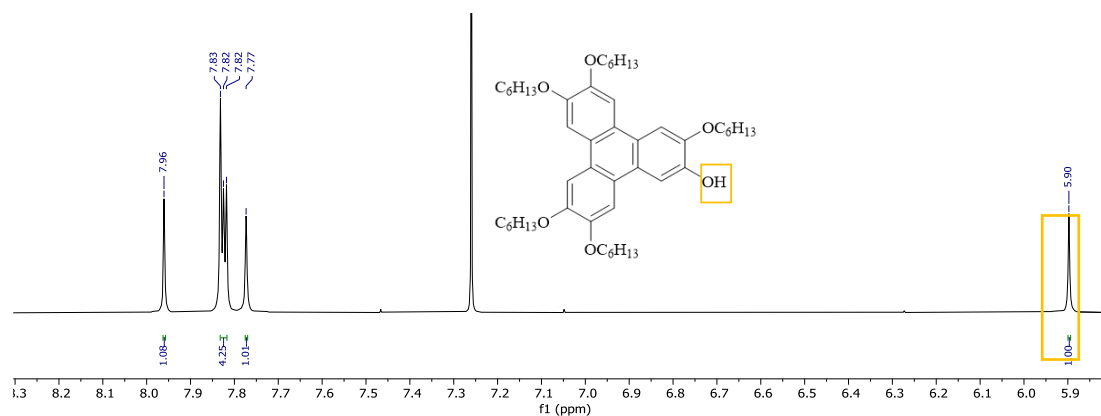
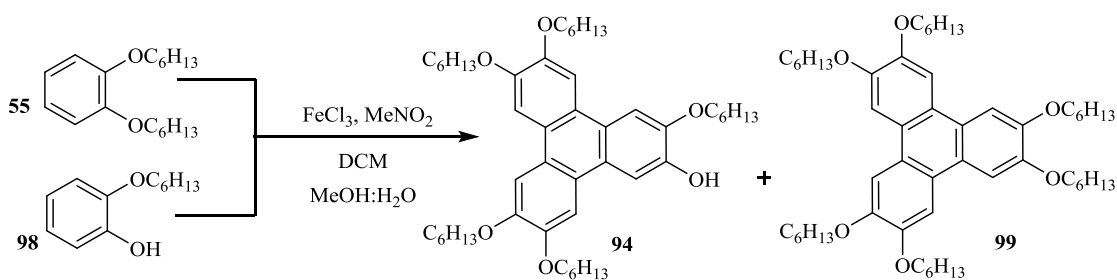


Figure 2.2: An expansion aromatics region of compound 94.

Another method which was used to synthesise MHT was carried out by using a mixture of 2:1 equivalent of DHB and mono-hexyloxy-phenol, which were reacted with 3 equivalents of FeCl_3 in ice bath in DCM. Nitromethane (MeNO_2) was also added to the reaction mixture to improve the yield because it worked to increase the solubility of FeCl_3 . The reaction was allowed to proceed for 1h. After that 2 more equivalents of FeCl_3 was added then left in room temperature.



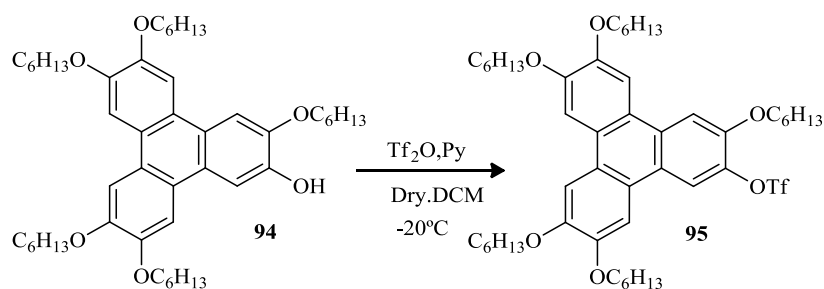
Scheme 2.3: alternative method of synthesise MHT.

The reaction was monitored by TLC and quenched as described in previous reaction. The product was easier to separate in column chromatography because it showed the coloured bands of the different components of the crude. Although MHT and HAT are both colourless compounds, the presence of coloured bands made it easier for us to ascertain which band corresponded to the target, MHT. The correct compounds had produced and matched the ^1H NMR references. In terms of comparing the yield in both reactions the one using the mixture and MeNO_2 was increased by 15%.

Starting material	Reagent	Time	MHT Y%
DHB	FeCl_3 (3eq), FeCl_3 (2eq)	2.5h	20%
DHB (2eq)	FeCl_3 (3eq), Mono-substituted phenol (1 eq)	2.5h	35%
	FeCl_3 (2eq), CH_3NO_2		

Table 2.1: Comparison of the yield of the two methods.

Once sufficient quantities of MHT had been obtained, it was necessary to convert the hydroxyl group to another functional group because MHT does not remain stable for a long period of time. The required compound is compound **95** in which the hydroxyl group in the triphenylene is converted to triphenylene triflate (TP-OTf).



Scheme 2.4: The synthesis of compound **95**.

This would provide a useful functional group to couple with the alkyne terminal in the next reaction. The starting material was the MHT already collected, treated under nitrogen with trifluoromethanesulfonic anhydride with pyridine dissolved in dry DCM at -20 °C. After the workup, the crude was purified by column chromatography to collect the product as the first fraction. An off-white solid was obtained (70%) after crystallisation from (2:1) ethanol: DCM. The ¹H NMR spectrum of the TP-OTf showed a peak at 8.2 ppm for the proton close to OTf group because it is more deshielded than those of triphenylene aromatics peaks. Also, to confirm the starting material was totally consumed the hydroxyl proton peak disappeared from 5.9 ppm. The data is consistent with the value in the reference.^[82]

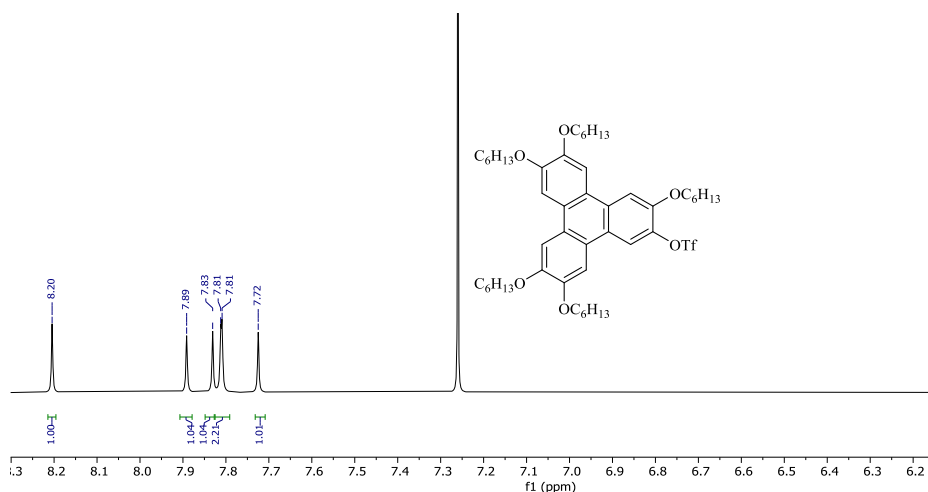


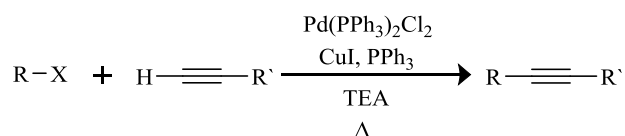
Figure 2.3: aromatic region in compound **95**.

It is worth noting that prior to improving the process by purifying the tar-like column, by using the nitromethane, the whole crude product was used in a triflate reaction to save time and solvent, without purifying the MHT because the distance between the triflate and the HAT on the TLC plate was good, compared to the poor separation between the MHT and the HAT.

However, the problem with this method is that it is not possible to know exactly how much MHT is present. It is therefore difficult to calculate the amount of reagent required for the reaction. While this did not improve the yield, the process was much quicker and more efficient. Once the triflate had been produced in sufficient quantities, it was then necessary to introduce the aromatic bridge or rigid spacer to the triphenylene moieties, which require acetylene to create the link between the aromatic units and the triphenylene. To achieve this the formation of carbon-carbon bonds is essential for linking the building blocks. This is an important tool for the synthesis of complex compounds by the substitution of different functional groups. Therefore, such cross-coupling reactions have been extensively used by our group to build triphenylene twins.^[80]

Sonogashira coupling

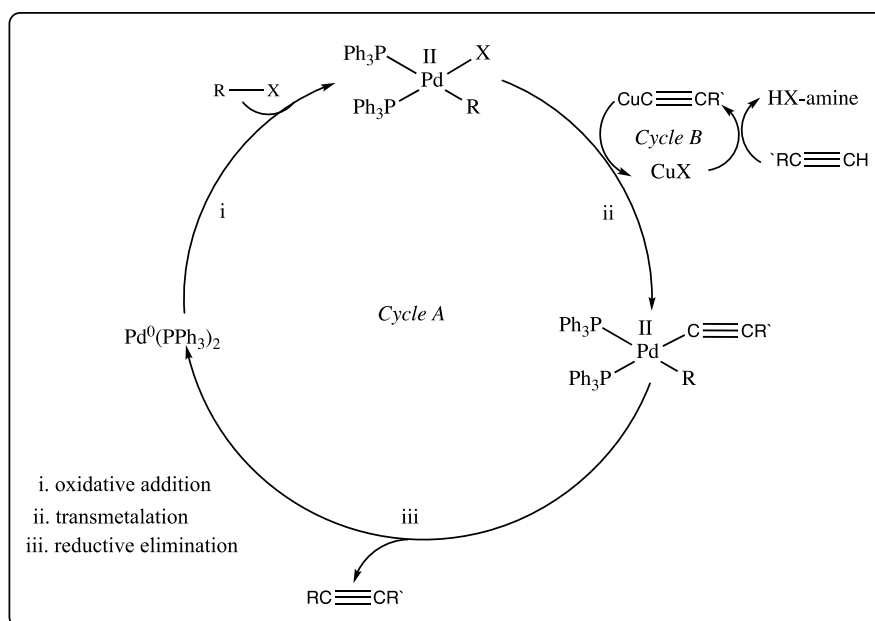
One of the most common sp –sp carbon-carbon bond formation reactions used in the synthesis of complex organic compounds, including triphenylene twins, is the so-called Sonogashira cross-coupling reaction, which couples terminal sp hybridized carbon from acetylenes with sp² carbon of an aryl halides (or triflate) using a palladium catalyst or some other transition metals. The reaction is often used to synthesise natural products and biologically active molecules.



Scheme 2.5: Basic representation of Sonogashira cross-coupling reaction.

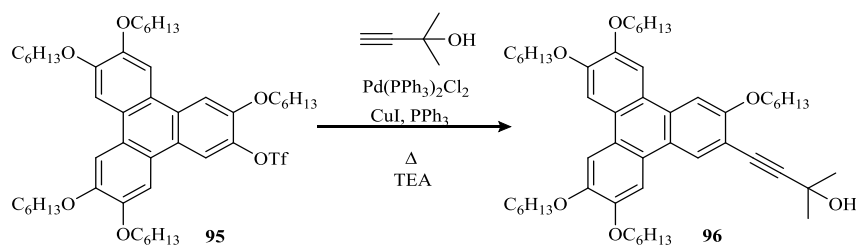
The reaction name dates back to 1975 when Sonogashira, Tohda, and Hagihara discovered that this coupling could be performed, using a palladium catalyst, but without the high temperatures used by Cassar and Dieck and Heck.^[83] The Sonogashira reaction can easily be conducted at room temperature, due to the combination of copper-mediated transmetalation of the alkynes. This is advantageous when using thermally sensitive compounds. The absence of oxygen in the reaction is important to prevent the homo-coupling compound from the terminal alkyne. However, in the current research, the Sonogashira reaction was used, with a high temperature because triphenylene derivatives are thermally stable but, the addition rate of the acetylenic is the crucial point at refluxing temperature.

This would lead to homo-coupling formation because the triphenylene is quite reactive with itself. Also, it is better to use a stable and soluble Pd^[57] derivative than a Pd (0) species. Bis(triphenylphosphine)palladium^[57] chloride, is a good example and allows the active palladium (0) catalyst to be generated following a transmetalation step with the copper acetylide.



Scheme 2.6: Mechanism of Sonogashira cross-coupling reaction.

Scheme 2.6 shows the general coupling mechanism of the reaction. The oxidative addition step starts when the Pd (0) reacts with the organic halide producing a palladium^[57] intermediate which is transmetalated with the alkynyl copper (generated in Cycle B). The next step of the cycle is reductive elimination with coupling of the two organic components which gives the desired product and regenerates the palladium (0) catalyst. The Sonogashira coupling reaction, as outlined above, was used in the current research in order to introduce the acetylene group to the triphenylene. This was the most suitable method for an acetylene function group to couple to TP-OTf to give the required structure **96**.



Scheme 2.7: The synthesis of compound **96**.

3, 6, 7, 10, 11-Penta-hexyloxy-2-triflate triphenylene **95** was dissolved in freshly distilled triethylamine and a palladium catalyst. A copper iodide co-catalyst was added. The mixture was heated for 30 minutes to ensure the reactants had dissolved. Once the mixture had cooled down, a syringe pump had been used, to add a solution of 2-methylbut-3-yn-2-ol in 10ml freshly distilled triethylamine. All these processes were conducted under a nitrogen atmosphere, in the absence of oxygen to prevent the homo-coupling formation of compounds from the acetylene terminal (presumably due to competing homo-coupling of the acetylene). The syringe pump was used to ensure that the reaction was slow, which also helped to avoid the previously mentioned homo-coupling problem. After the addition was successfully completed, the mixture was then heated to reflux temperature. The formation of 2-methyl-4-(3, 6, 7, 10, 11-pentakis (hexyloxy) triphenylene-2-yl) but-3-yn-2-ol **96** was monitored by TLC analysis and the starting material was shown to have been consumed. ¹H NMR spectroscopy confirmed the formation of the target compound, and there was a singlet peak at 1.72 ppm, which corresponds to the two methyl group protons. Also, the compound mass peak was observed by MALDI-TOF MS; this gives a true representation of the product and matches earlier reference values.

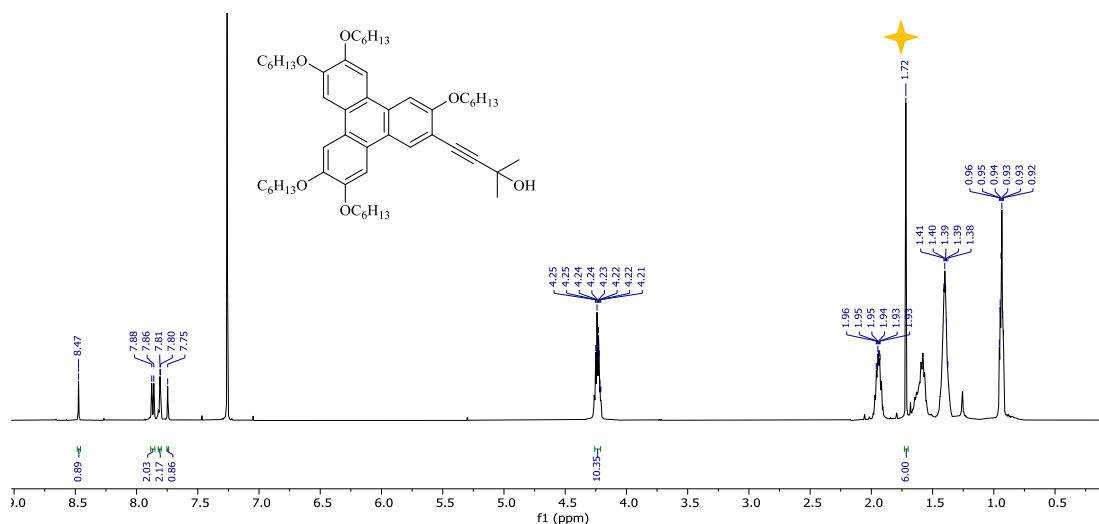
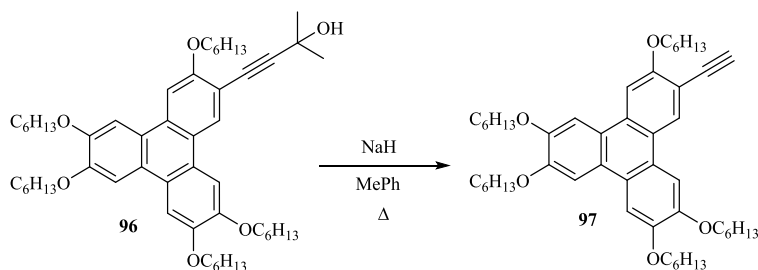


Figure 2.4: ^1H -NMR aromatic regions of compound **96**.

The preparation of the mono-acetylene triphenylene **97** was straightforward from this point onwards and required only the deprotection step of compound **96**. This process used sodium hydride (60% dispersion in oil) in dry toluene.



Scheme 2.8: Synthesis of mono-acetylene triphenylene.

After work-up was done, purification was achieved via column chromatography, producing 3, 6, 7, 10, 11-penta-hexyloxy-2- ethynyl triphenylene **97** in good yield. As shown in figure 2.5 the peak at 3.39 ppm is the ethyne proton in ^1H NMR spectrum of the product. Also, the singlet peak of the isopropyl protons is no longer present.

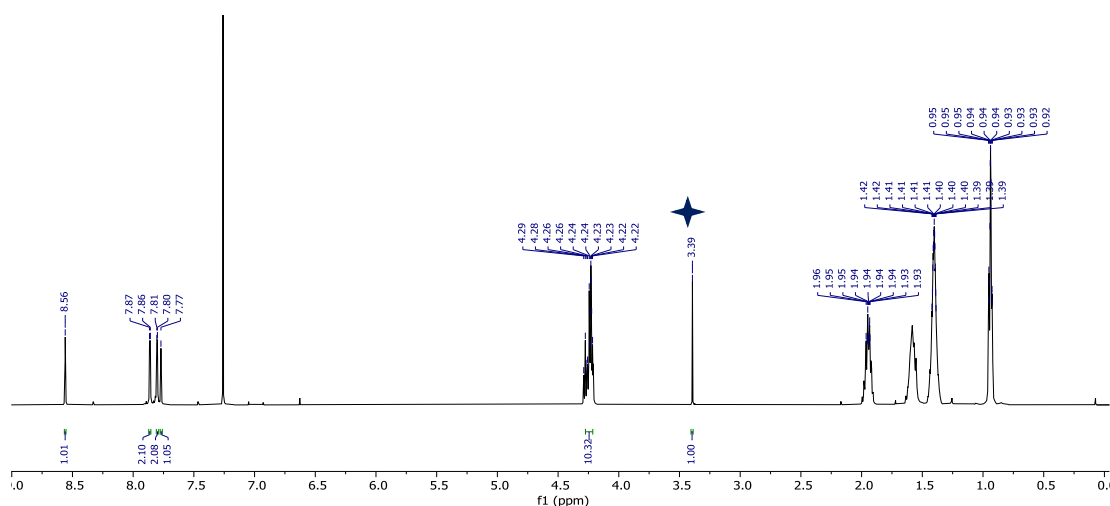


Figure 2.5: $^1\text{H-NMR}$ aromatic regions of compound **97**.

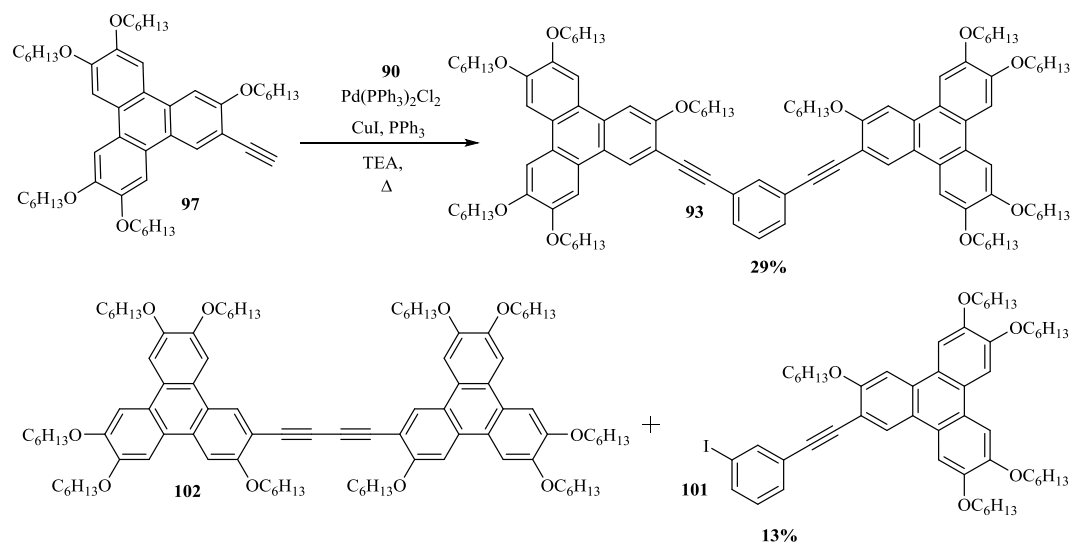
Triphenylene twins have been shown, in our group's previous work, to have liquid crystal properties. To synthesise similar structures with liquid crystal properties and investigate these further, it was decided to start with a diad structure using a benzene bridge to link to triphenylenes. The same condition was used as in our group's synthesis of twinned triphenylene.^[77]

2.1.3. Synthesis of triphenylene diads

2.1.3.1. Synthesis of 1, 3-Phenylene bridged diad **93**

The Sonogashira reaction condition was used, as discussed earlier, using 1, 3-diodobenzene **90** to draw a comparison with the synthesis of the twin, mentioned above. The reaction was heated for half an hour at 60°C to ensure that all the reagent was dissolved. The dilute acetylene was then added slowly using syringe pump for 10h. Unfortunately, the inside of the plastic syringe disintegrated overnight, with the possible loss of some of the mono-acetylene triphenylene. Nevertheless, the reaction process had been continued. The mixture was returned to the heat at 60 °C. The whole reaction was monitored by TLC and at this stage. It showed that there were three spots which corresponded to the homocoupling **102** and the starting materials. This suggested that the process did not work at 60°C, so the temperature was raised to 90°C. The amount of palladium was doubled because it was thought the initial mixture had consumed the palladium and that there were insufficient quantities to continue the experiment. The reaction TLC showed that there was none of the triphenylene starting material left, even

when three equivalents and the 1, 3-diiodobenzene has been used the spot was still apparent, even though it was just one equivalent and should have been consumed.



Scheme 2.9: Synthesis of m-triphenylene diad

To overcome the problem described above, the reaction has been continued by adding more mono-acetylene triphenylene at a slower rate for 3 hours to consume the remaining 1, 3-diiodobenzene. The reaction was left overnight. After the addition of the triphenylene, the TLC at this stage showed the starting material and a new yellow-coloured spot. The decision was taken to stop the reaction at this point and undertake the analysis to look deeply into what had occurred. The work up was done as set out in the experimental section but some difficulties with purification were experienced. The spots were very close together and the whole column was yellow. The homocoupling was one of the unwanted products shown on the TLC and was mixed with the target product. It was necessary to conduct the purification in a less polar system to isolate the pure fraction for analysis. Finally, the target compound **93** has been isolated, in the form of a light green solid, which was obtained by recrystallization in DCM / EtOH, at a yield of 29%. There was also a mono product **101** which had formed as a side product at a yield of 13%. It is interesting to compare the yields and methods in the current research with those of Cammidge et al.'s synthesis of the triphenylene twin **92**. In the case of the twin, a good yield was produced in the first step of the coupling, in which palladium was used as a catalyst. However, the palladium free step of synthesis the twin produced a low yield (under 15%), suggesting that the palladium remains important in terms of the coupling reaction. In our current research, the diad structure was produced by using the same catalyst.

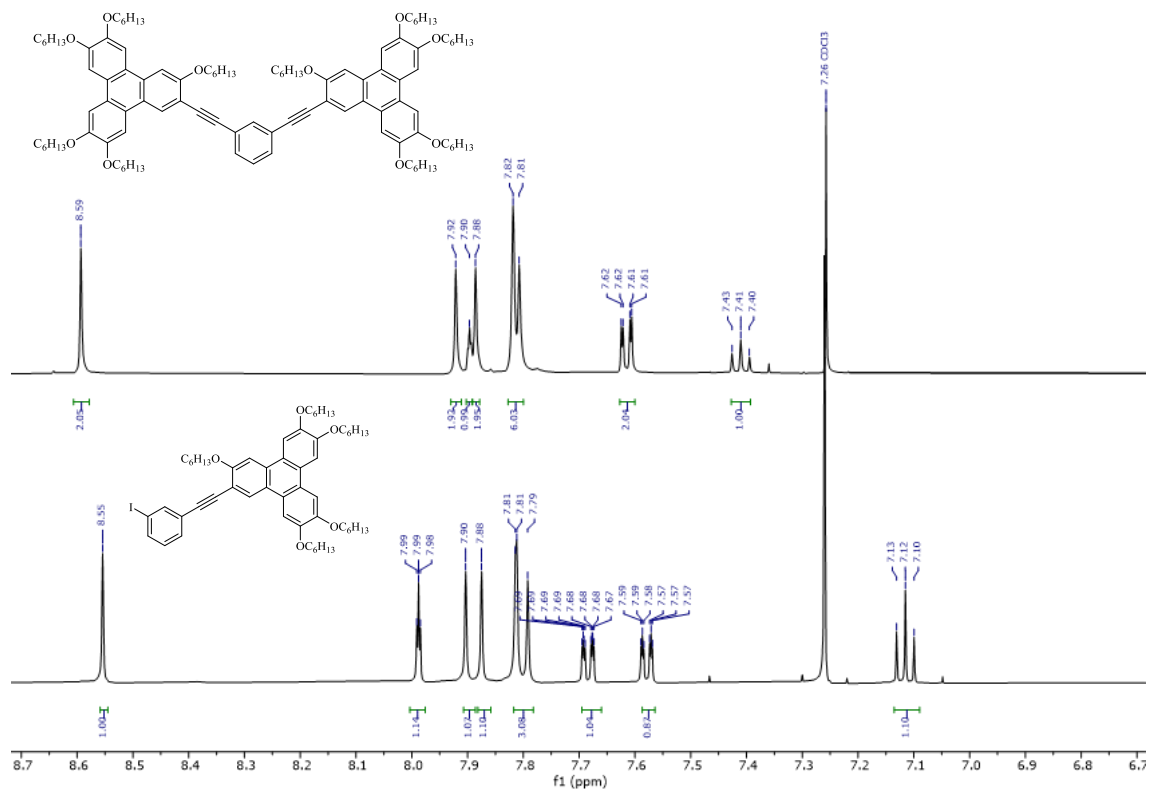


Figure 2.6: ¹H NMR spectra of aromatic region for compounds **93** and **101**.

The analyses were conducted to confirm the formation of the target structure. ¹H NMR spectroscopy data clearly matched the expectation of the disubstituted product as the main product (Figure 2.6). The resulting peak from the MALDI-TOF MS showed (M, 100%) 1582 m/z.

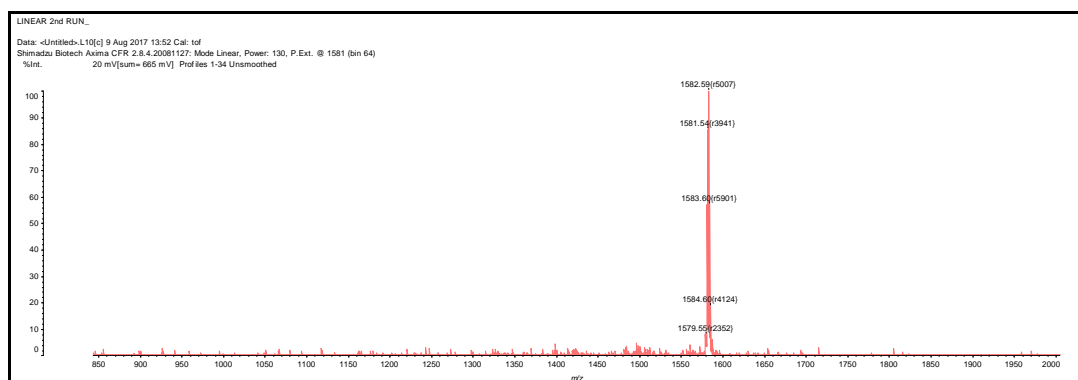


Figure 2.7: Maldi-TOF spectrum of the compound **93**.

Liquid crystal properties:

Both disubstituted and mono-substituted molecules showed they have mesophase behaviour. The structure of diad showed characteristics of columnar mesophase at 87°C. Interestingly it exhibited a nematic discotic mesophase at 142°C. The columnar phase was shown in the mono-structure at temperature 72°C. However, as compared to the twin structure behaviour which only have nematic discotic mesophase.

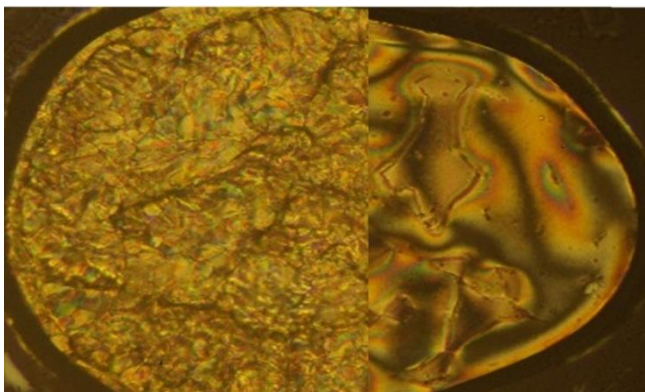


Figure 2.8: Compound **93** showing columnar (left) at 87°C and nematic (right) mesophases at 142°C.

DSC confirmed the characterisation of liquid crystal products which obtained initially from POM observations (figure 2.8). DSC thermograph of diad **93** highlights three thermal peaks for the heat effect.

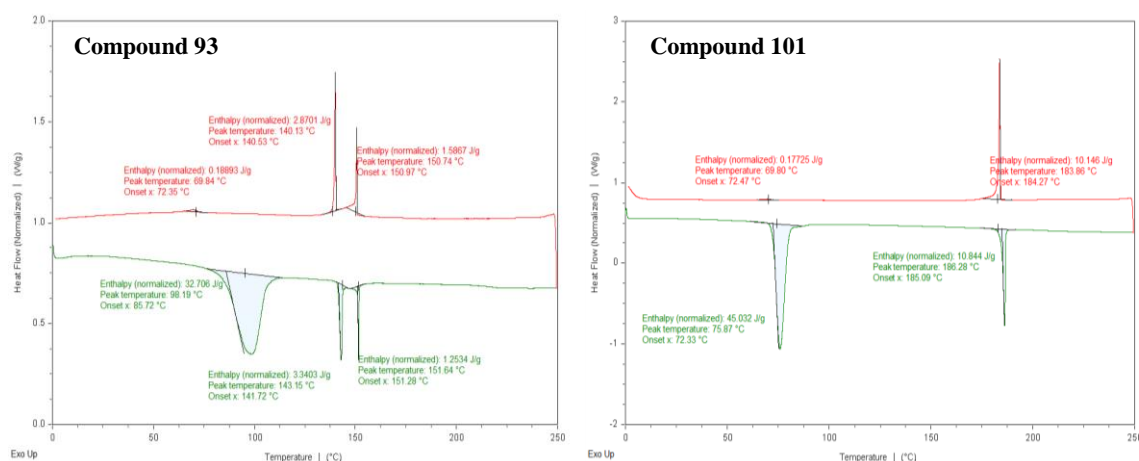


Figure 2.9: DSC thermograph of compounds **93** and **101** on heating and cooling (scan rate 10°C min⁻¹)

A comparison of compound **93** with compound **102**, which was connected by means of an acetylene unit, it is possible to observe that both compounds exhibit nematic behaviour. Compound **102** provides an example of a dimer linked by an acetylene unit, which exhibits a nematic phase, as shown in the figure. The separations of the 1,3-phenylene diad is 16.532 Å. The core-core distance in the compound **102** is 13.394 Å.

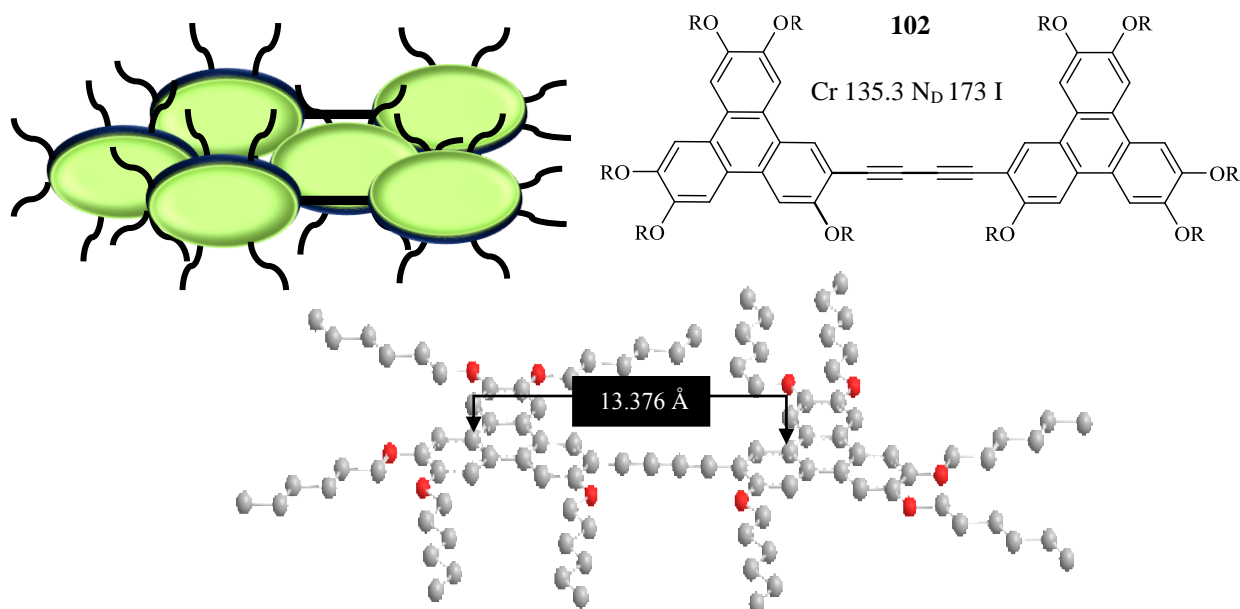


Figure 2.10: Schematic representation of the Kumar's diad.

Other comparisons can be made with the work our group on twins to determine the importance of the same spacer. The twin shows the nematic mesophase while its monomer displays columnar behaviour. Similarly, in this series the intermediate *s* of meta substituted phenylene diad exhibited a columnar phase.

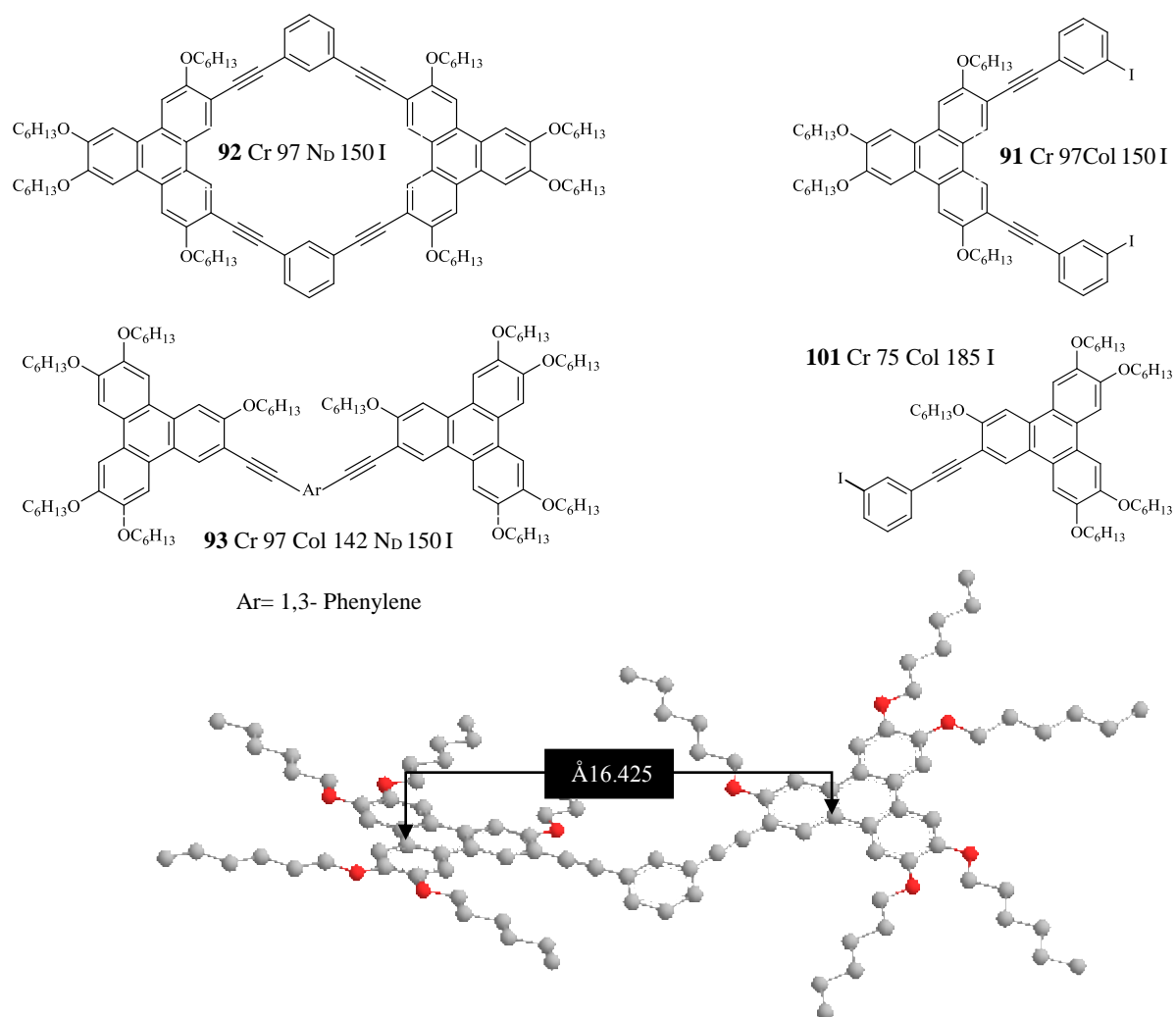
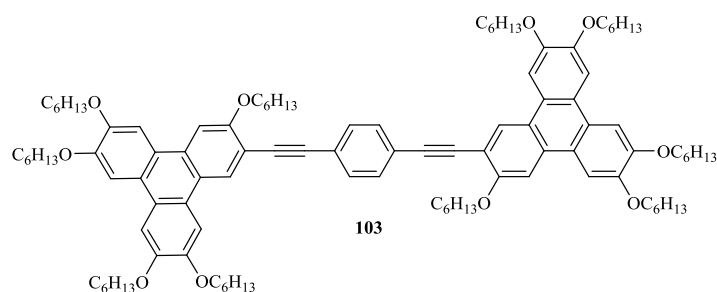


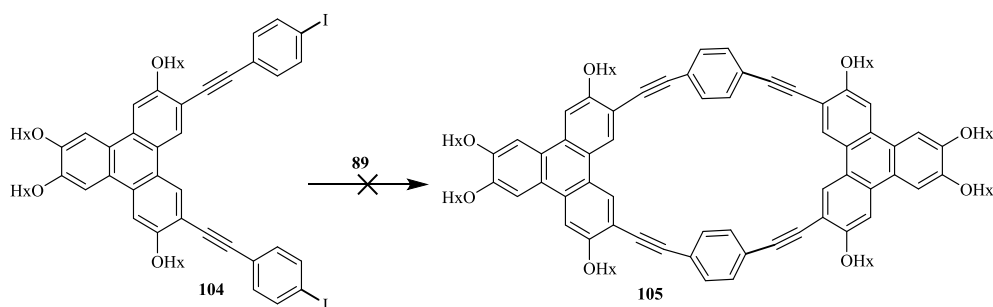
Figure 2.11: Schematic representation of the diad **93**, twin **92** and their monomers **91**, **101**.

2.1.3.2. Synthesis of 1,4-phenyl bridged diad **103**



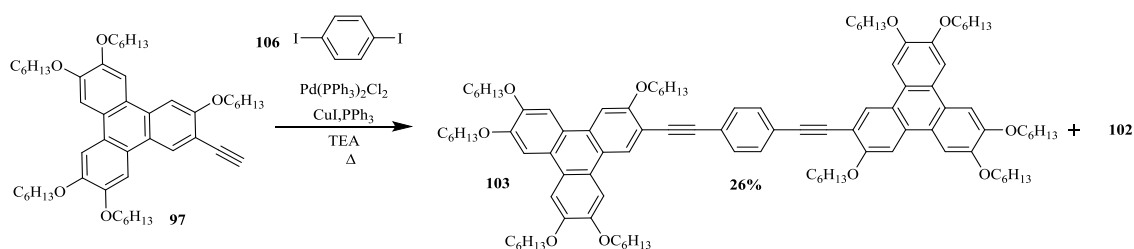
Although working with the *meta* position had been successful, it did present a number of challenges, as discussed. Previously, the Cammidge group had attempted to synthesise 1,4-Phenylene-bridged twin, using triphenylene diacetylene **89**, coupled with 1,4-diiodobenzene. They obtained the diiodo intermediate but failed to produce twin **105**.

The para linked diad **103** presents a linear geometry and allows comparison with directly linked diad **102** and non-linear diad **93**.



Scheme 2.10: Attempted synthesis of 1,4-Phenylene-bridged triphenylene twin.

This led us to consider using the link 1,4-Phenylene, between the two triphenylene moieties. To produce di-triphenylene in *para* position the decision has been taken to follow the same strategy has been applied in earlier work in the synthesis of disubstituted phenylene (scheme **2.10** above), starting the reaction from dissolving all the reagents which were to be used. The acetylene solution was added to the reaction mixture at a slower rate than earlier reaction to minimise the formation of **102**. The mixture was returned to the heat at 90°C, once the addition had been completed. The reaction was monitored by TLC to show whether the desired molecule was formed, or the reactants were consumed. The TLC revealed there was no starting material left. A very light creamy-green coloured solid was produced. However, no mono product was obtained. Only the target diad **103** and the homocoupling product **102** were isolated.



Scheme 2.11: Synthesis of triphenylene diad **103**

The $^1\text{H-NMR}$ spectrum was run in CDCl_3 , and the spectrum obtained proves the formation of the diad compound **103**, Figure **2.12**. The aromatic regions of the desired structure giving 16 aromatic peaks, 12 protons for the triphenylene units, and 4 for the benzene protons which appear as a singlet at 7.65 ppm.

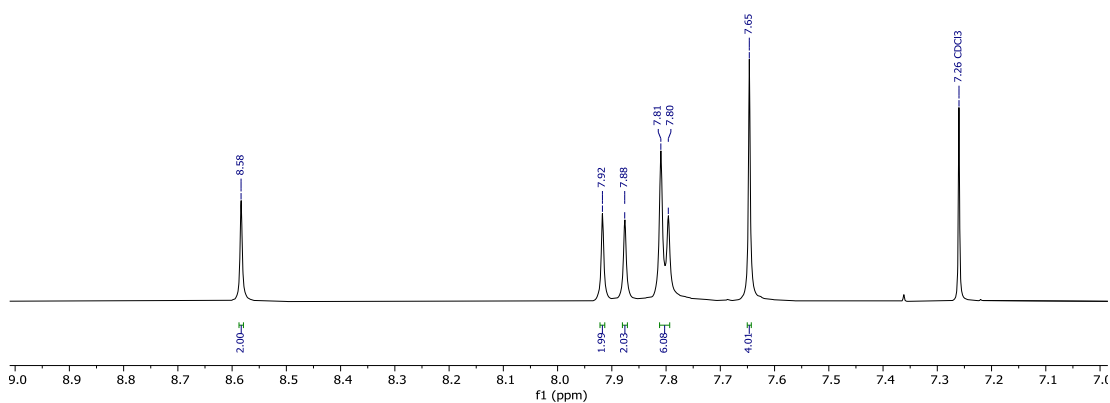


Figure 2.12: Aromatic region of $^1\text{H-NMR}$ spectra of compound **103**.

Liquid crystal properties:

The initial examination of thermal properties of the desired compound **103** exhibited mesophase behaviour through transition temperatures with a characteristic hexagonal columnar phase. Figure **2.13** shows the thermograph of the desired compound **103** and the LC behaviour at temperature at 235°C before it reached isotropic melt at 250 °C.

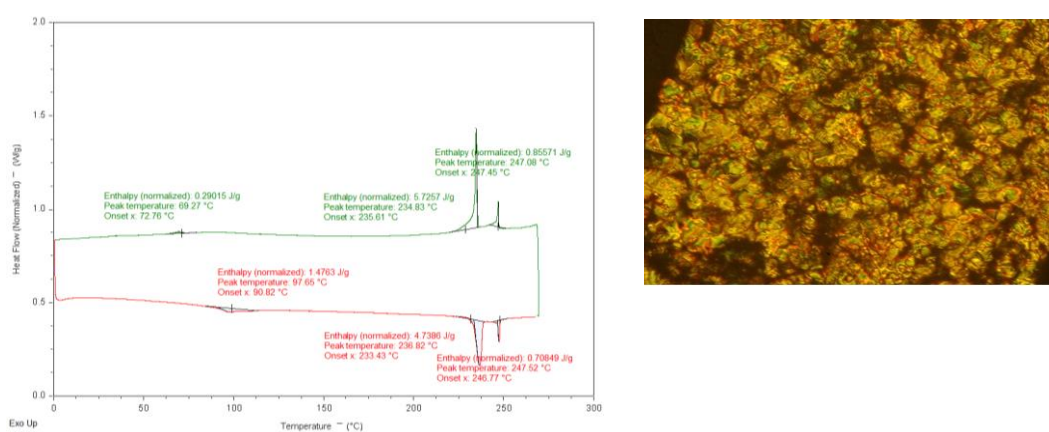


Figure 2.13: DSC thermograph of 1,4-phenylbridged diad **103**, and Col_h phase texture at 212°C.

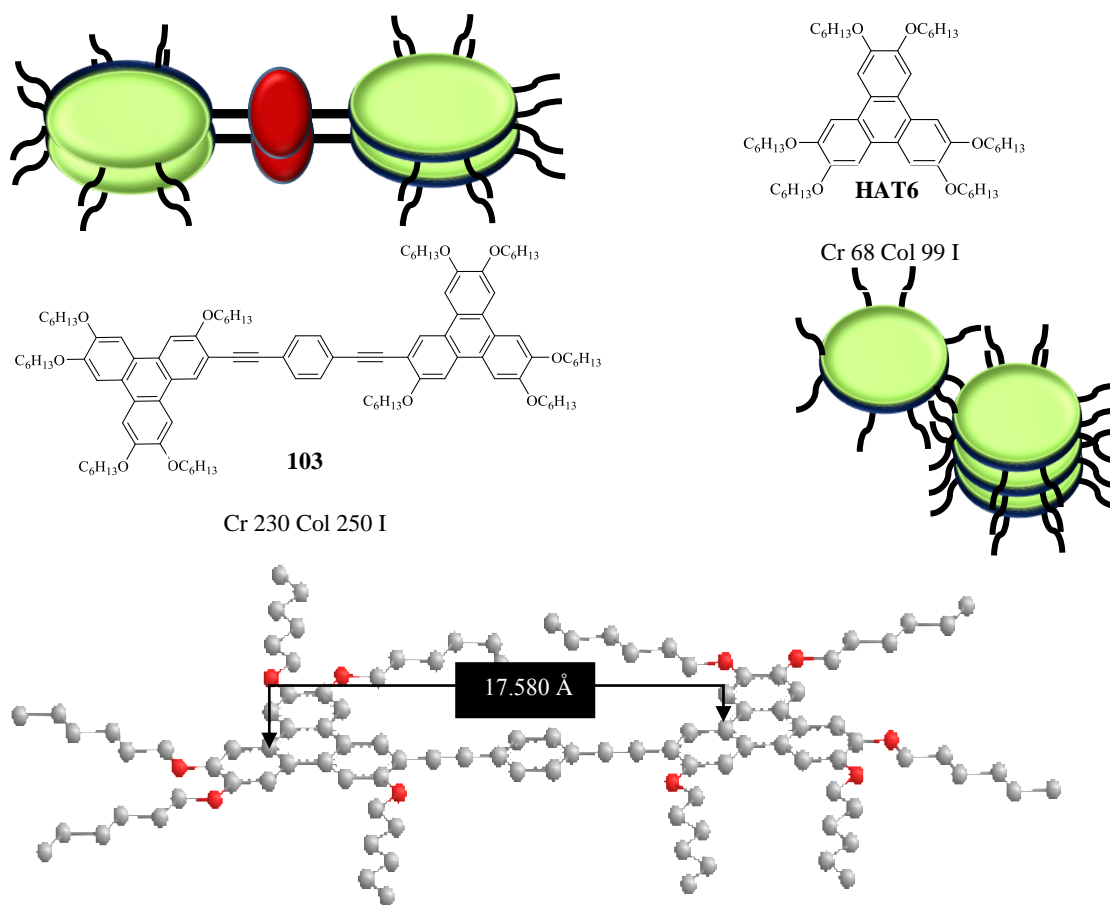
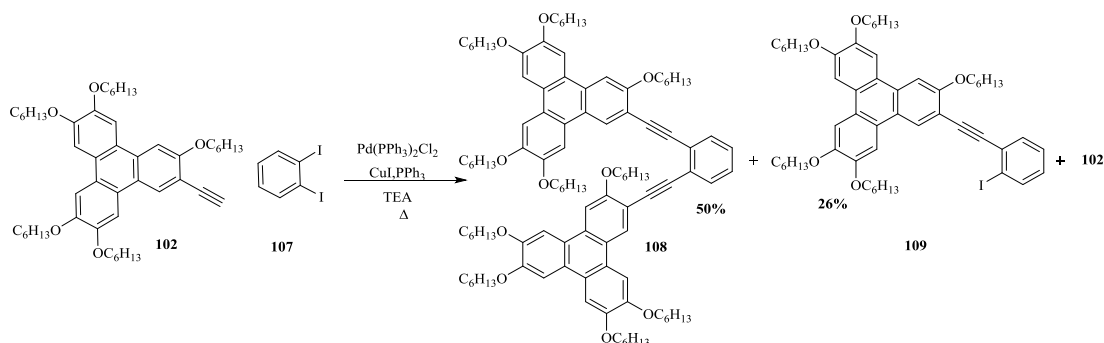


Figure 2.14: Schematic representation of the compound **103** and the monomer **HAT6**.

The linear system is more compatible with columnar mesophase formation and this is the same mesophase type that observed at HAT6. The separation of the TP-TP is approximately similar therefore the columns can arrange themselves in discs and accommodate the side chains. Another comparison to compound **103** with Kumar's dimer, which was connected by means of an acetylene unit, it is possible to observe that both compounds are linear but they both exhibit different liquid crystal properties. However, when the discs come closer together as in the meta substituted derivative, the nematic behaviour has been observed. This in line with the observations of rigidly linked dimeric structures prepared by Kumar. Compound **102** provides an example of a dimer linked by an acetylene unit, which exhibits a nematic phase, as shown in the figure. The separations of the 1,4-phenylene diad is 17.580 Å. The core-core distance in the compound **102** is 13.394 Å which shows the nematic mesophase while its monomer displays columnar behaviour. Other comparisons can be made with the work our group on twins to determine the importance of the same spacer.

2.1.3.3. Synthesis of 1, 2-phenyl bridged diad 108

Having isolated the triphenylene diad with para link, the possibilities has been considered offered by synthesising the diad with an ortho position. This reaction might be complicated and that it might not produce a liquid crystal, but it was important to carry it out to complete the sequence. The 1,2-linked diad presents an unusual architecture and it would be interesting to see if self-assembly into a mesophase (columnar or nematic) is possible.



Scheme 2.12: Synthesis of the 1, 2-ditriphenylene benzene **108**.

The same conditions were used again but the problem on this occasion was that the steric hindrance prevented the formation of a solid product, so that the di triphenylene remained in a brown, sticky, oily form. However, the mono-substituted product was perfectly crystallised and light green in colour.

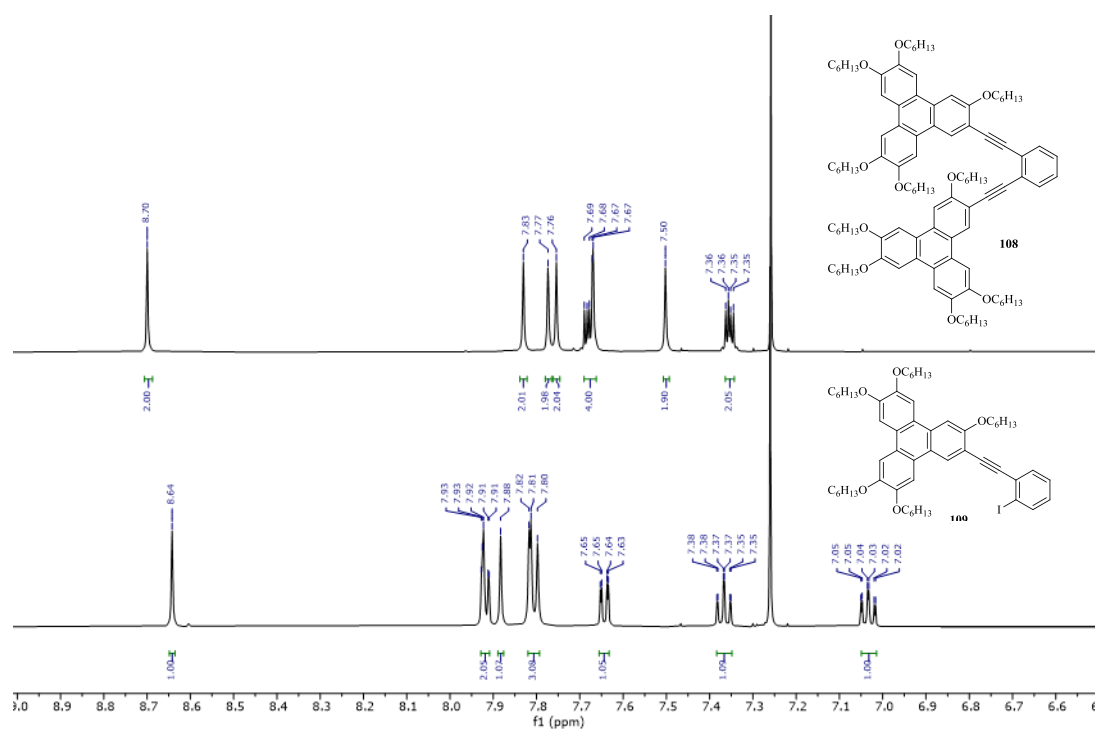


Figure 2.15: Aromatic region of $^1\text{H-NMR}$ spectra of compounds **108** and **109**.

The $^1\text{H-NMR}$ -data of both compounds **108** and **109** were relatively simple to analyse. The aromatic regions are shown in figure 2.15. The spectrum simplifies with unique triphenylenes peaks with benzene protons. However, the monosubstituted compound **109** giving slightly different set of peaks because of the effect of iodine on the benzene.

Liquid crystal properties:

The diad structure **108** exist as sticky oil which have did not display any transition temperature to suggest that product had melt to isotropic phase completely at temperature 77°C . Also, the observation when the sample was cooled it does not exhibit any liquid crystal behaviour. The mono-structure exhibited columnar phase in compound **109** as shown in figure below (figure 2.16). Similarly, the intermediates of meta substituted phenylene diad **101** exhibited a columnar phase, as did the intermediate of 1,2-phenylene substituted diad **109**.

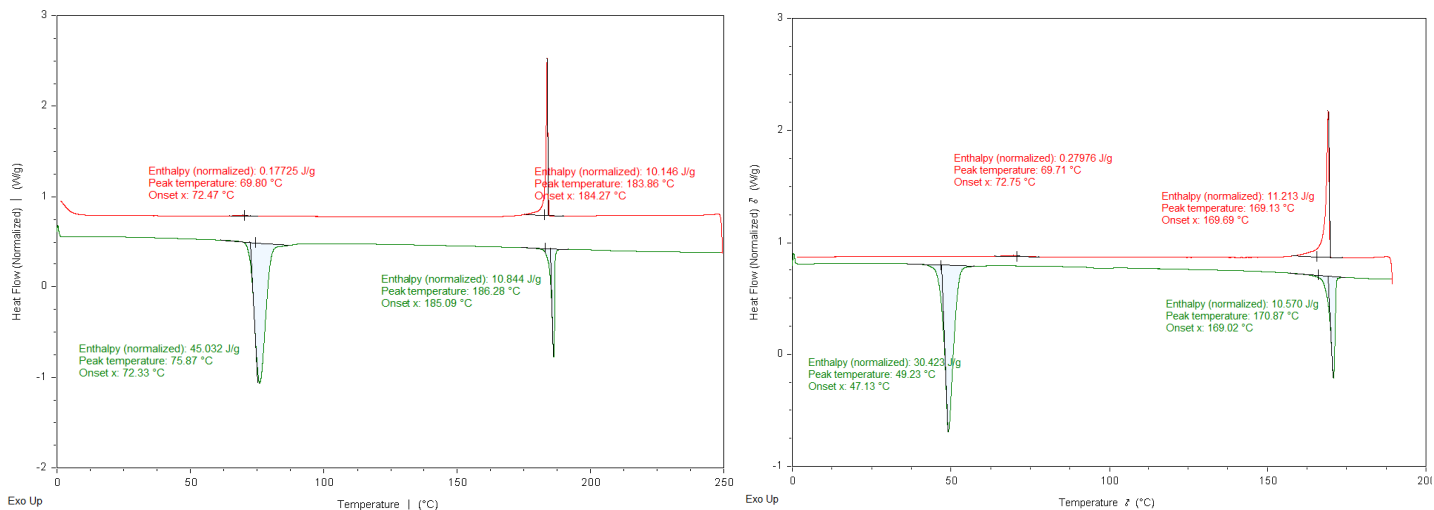


Figure 2.16: DSC thermograph of compounds **101** and **109**.

The absence of mesophase formation in 1,2-phenylene diad **108** is not surprising, since the shorter distance between the TP units destroyed the liquid crystal behaviour due to the overlapping of the two halves. The core-core distance in the compound **108** is 10.761 Å. The study of the influence of the spacer length on mesophase properties was conducted by Boden et al. (1999), and this produced more information about triphenylene diads, and the nature of their liquid crystal properties.^[78]

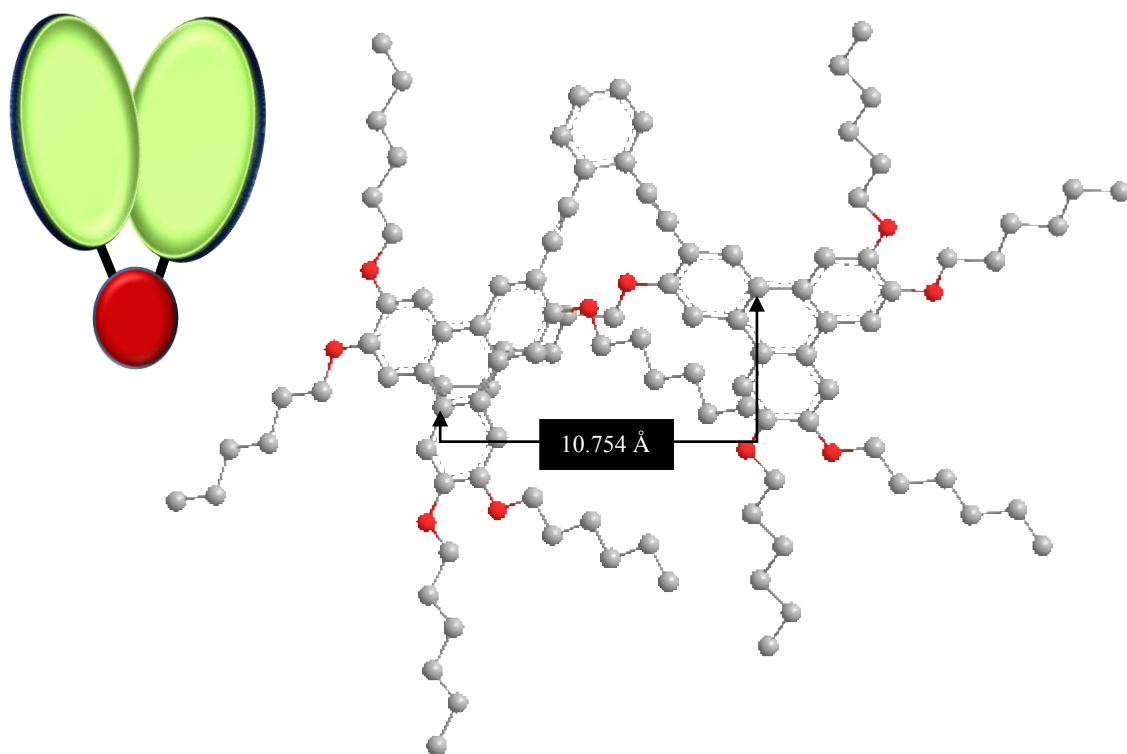
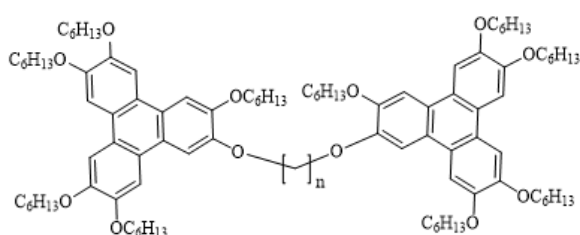


Figure 2.17: Schematic representation of the compound **108**.

One significant point among their discoveries was that the behaviour of the diad is affected by the spacer length. A spacer which is too short (where $n=3-7$) produces a diad which does not have a liquid crystal phase. The work of Hao et al., (2017), supported Boden et al. (1999)'s understanding of the significance of spacer length. They observed that the highest order of dimers in each series were those which has a spacer length which was almost double the length of the side chain. They also found that dimers with spacers which were longer or shorter than double that of the side chain were subject to steric hindrance or space filling.



$n=3$, Cr 81 I

$n=7$, Cr 69 I

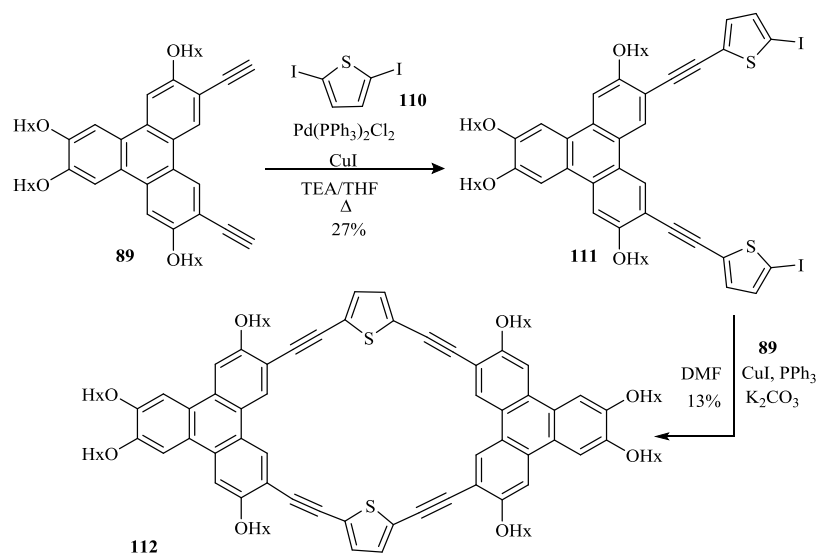
$n=8$, Cr 58 Col_h 92 I

$n=10$, Cr 50 Col_h 104 I

Figure 2.18: The effect of length of the spacer on diad mesophase.

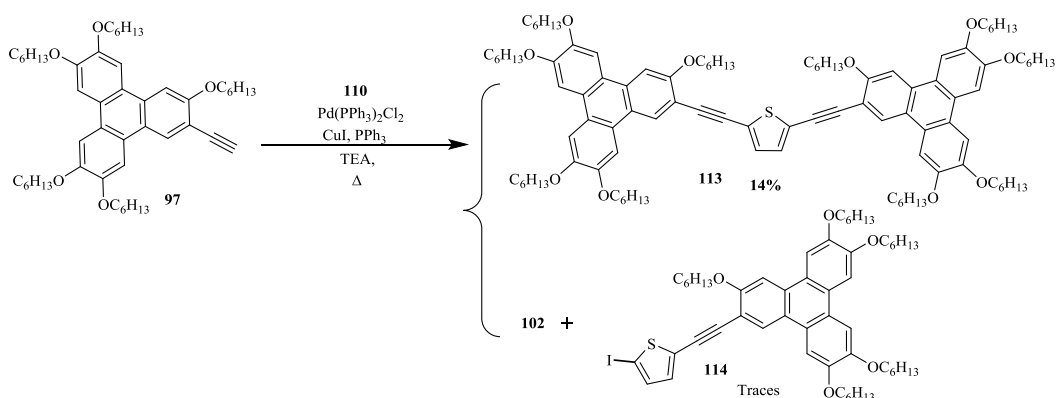
2.1.3.4. Synthesis of 2, 5- thiophene bridged triphenylene diad

The next step was to try using a different linker but using the same conditions as before to complete the set. This time thiophene was selected as the spacer because the Cammidge group had produced the twin linked with a 2, 5-thiophene bridge, and it seemed a logical conclusion to the current series to attempt to use a thiophene bridge to create a diad **113**.



Scheme 2.13: Synthesis of 2, 5-thiophene-bridged twin

Furthermore, thiophene bridges have been shown to fulfil a number of requirements, such as reducing overall strain across the molecule, producing a near perfect bonding angle and allowing communication across the entire structure, allowing molecular and self-assembly properties to be combined. The Cambridge group's twin also showed nematic behaviour, therefore the plane has been set to prepare a thiophene linked diad, this would have the same liquid crystal properties. The Sonogashira coupling was the method used to link 2, 5-diiodothiophene **110** with the mono acetylene triphenylene **97** as used earlier in the series.



Scheme 2.14: Synthesis of ditriphenylene-thiophene diad.

Various problems occurred with this reaction. The first issue was that the TLC, used to monitor the reaction, showed a yellow colour throughout, making it impossible to see if there was a spot at any point, so nothing could be identified. At this point, no more could

be done because it was not possible to identify anything from the crude NMR. The MALDI only confirmed that the target compound had formed. There was a peak indicating homo-coupling (figure 2.19). However, other peaks also appeared which were difficult to identify. Column chromatography was the method used to purify the desired product. To isolate the pure fraction was not easy because of the homo-coupling product which was mixed in with the target compound. The yellow colour of the homo coupling product was the same as that of the target compound, making it difficult to distinguish the two. The crystallisation process has been tried to separate the target compound and the homo-coupling product. Repeating the recrystallisation several times, allowed the successful removal of the homo-coupling product and the NMR showed the pure component. The mono-substituted product was present in tiny quantities but was very difficult to purify.

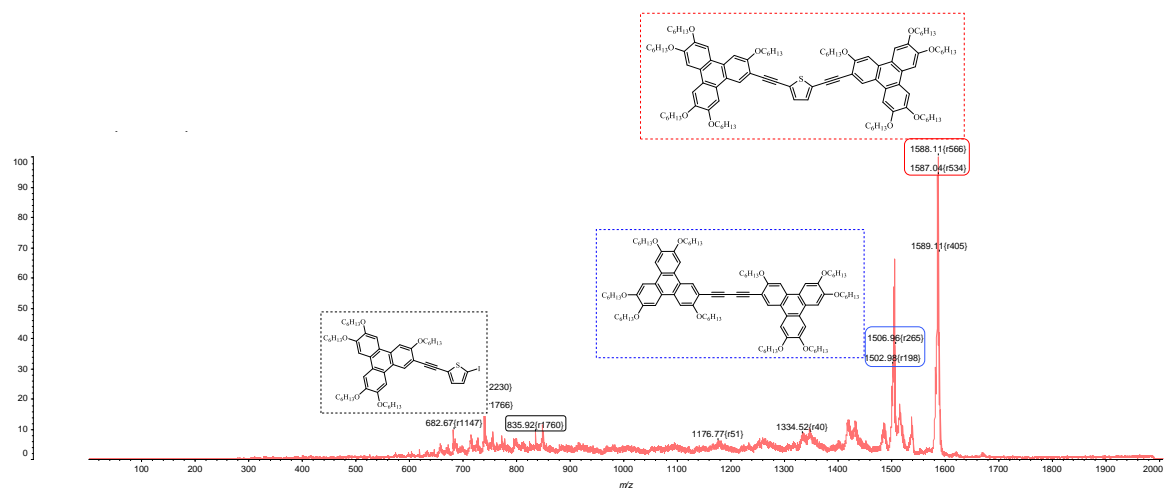


Figure 2.19 : Crude MALDI-MS showing the crude of the reaction.

The $^1\text{H-NMR}$ data obtained demonstrated this molecule with thiophene as singlet peak being hidden by the residual CHCl_3 peak and triphenylenes peaks being seen in the aromatic region (Figure 2.20).

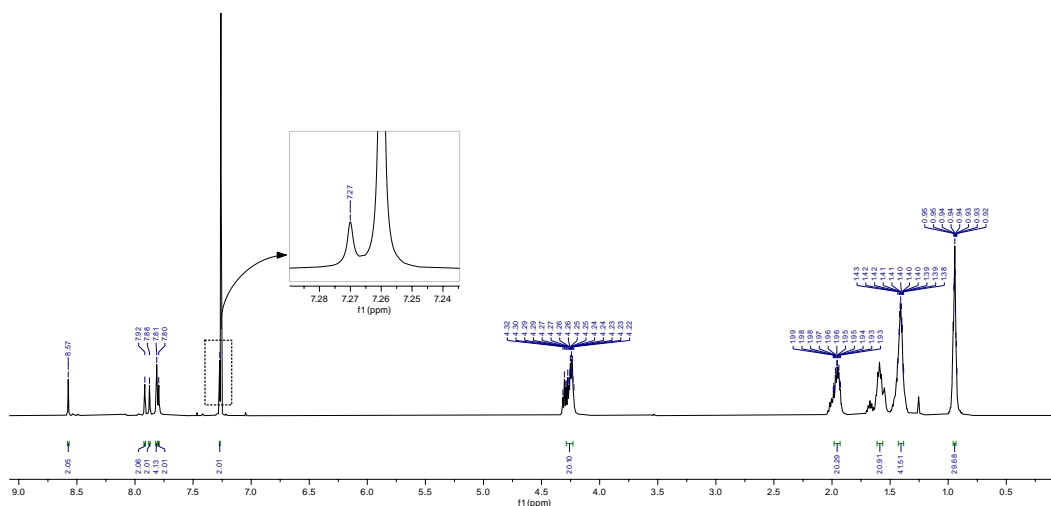


Figure 2.20: An expansion of the aromatic region for compound **113**.

Liquid crystals properties:

Compound was solid at room temperature and displayed liquid crystalline phase with heat, after melting transition to exhibit the unique transition mesophases as shown at 118°C and 200°C and emphasised the phase transition temperatures. Upon further heating, an isotropization phase was observed at 212°C. The DSC analysis obtained from heating and cooling cycles with diad and supported the earlier result. Pleasingly, the photomicrograph of compound 115 at 200 °C obtained during cooling from the isotropic liquid clearly displayed the N_D phase as well-defined schlieren texture. Regarding the fabrication of discotic nematic behaviour in our work, this was successfully achieved in this diad due to angle strain similar result to reported twin.

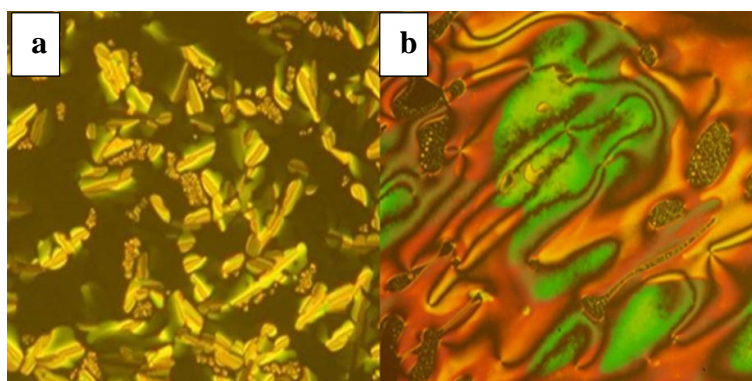


Figure 2.21: Compound **113** during a) columnar phase, b) nematic phase.

Both structures showed the nematic behaviour however in the diad structural feature, that displayed wide range columnar mesophase was also detected. In structure **112**, the nematic mesophase was observed due to the occupied void by the side chain in the neighbour unit which means the columnar behaviour could not observe. The liquid crystal resulting behaviour is dependent on the choice of linker which is balance between angle strain and conjugation. Thiophene unit was allowing the resonance through the structure with great angle that reduced the strain. However, 1,3-Phenylene bridge diad (compound **93**) was displayed similar feature but without the communication between the two halves.

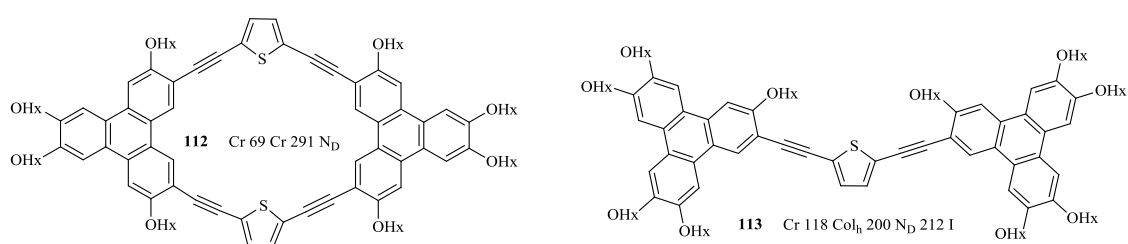


Figure 2.22: Comparison between the twin and the diad structures and mesophases.

In 2017 Yang et al synthesised triphenylene dimer with triazole bridge. The structure exhibit similar mesophase behaviour to earlier structure. However, the spacer between triphenylene moieties consists of the chain (O-(CH₂)₆) and the triazole linked diad has low melting point. Liquid crystal behaviour could be modified conveniently by the linker of the structure (figure 2.23). In addition, the spacer is crucial factor has effect on mesomorphic properties because whether if it rigid or flexible it will control the distance between the triphenylene units. Our group work to twinned triphenylene through ester linkages that break the symmetry and will investigate the effect on liquid crystal behaviour.

The work has been developed to synthesis diads with different connector and examined their mesophase behaviour. by 2,5-dicarboxylic thiophene spacer. Not only the spacer but also the angle of the linkage and the distance/ flexibility of the linker. Disorder in the discotic system it might lead to form nematic phase.

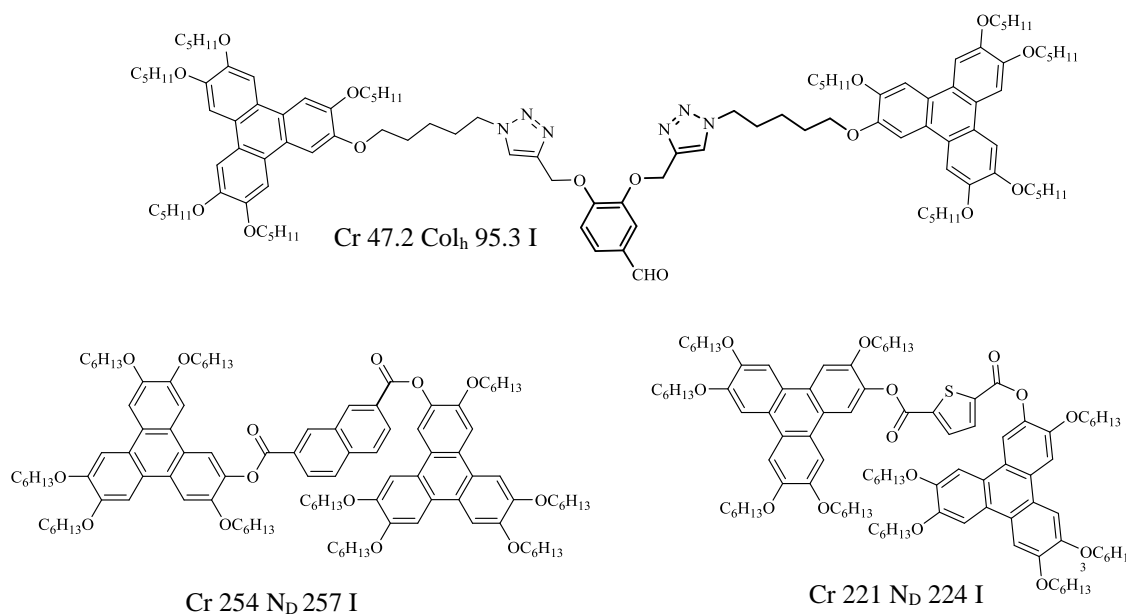


Figure 2.23: Other triphenylene diads mesophases

2.1.3.5. Optical properties

Figure 2.23 shows the UV-visible spectra of the 1st series in dichloromethane. All of them exhibited the typical triphenylene peak in the 300 nm range. The phenylene bridged diads have similar pattern however the para position linked shifted in the broad absorption. While the profile of thiophene bridged diad has a broad absorption between 360 and 450 nm with maximum absorption at 288 nm. On the other hand, mono substituted benzene structures the maximum absorption peak was at 250 nm and display broad peak at 300 nm range.

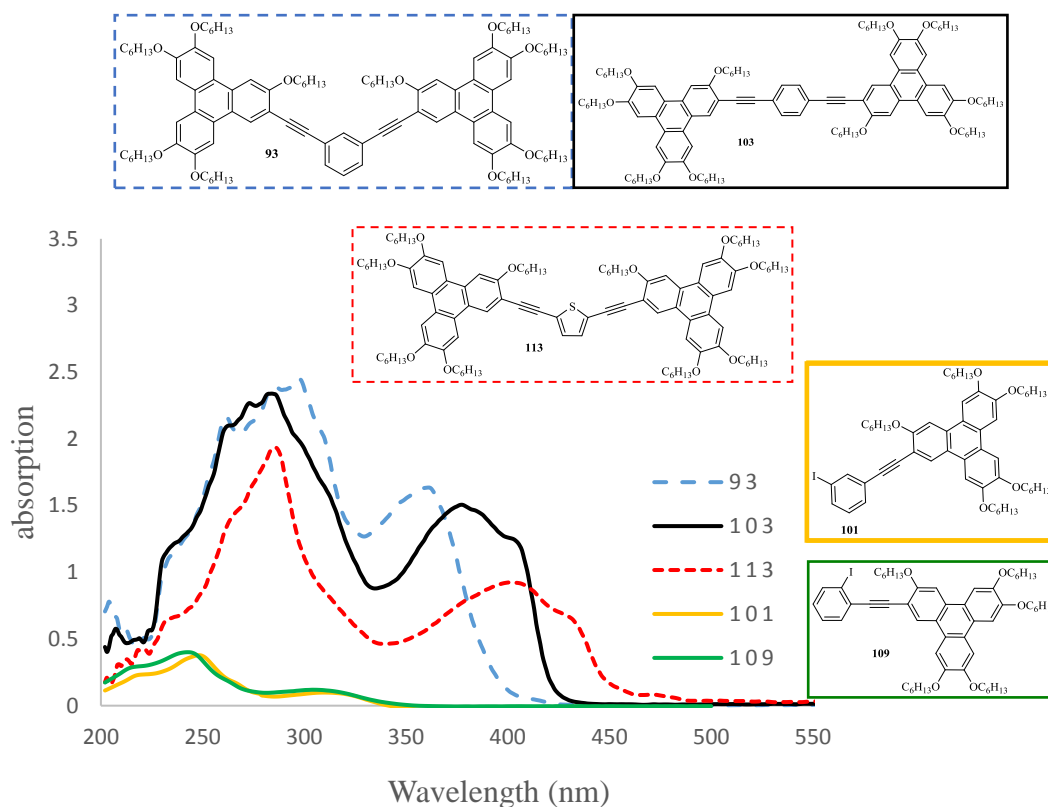
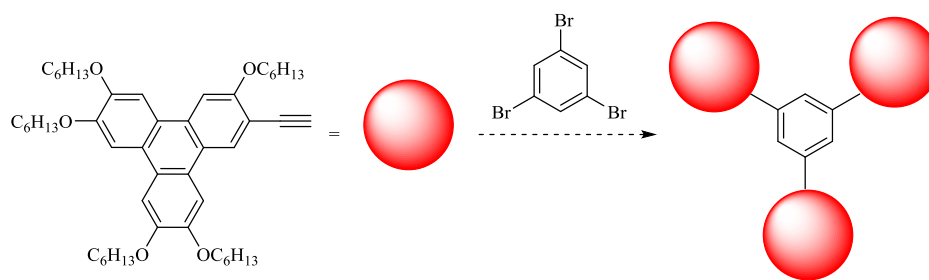


Figure 2.24: UV/Vis spectra of 1st series of triphenylene compounds.

2.2. Attempted synthesis of the triad of triphenylenes

Synthesising the triphenylene triad has been proposed after the earlier diads. The target structure has three positions to be substituted on the spacer to link TP units. The suggested bridge is the triiodobenzene but is known to be an unstable structure.^[84] Instead, tribromobenzene has been used because it is similar but is more stable and is a readily available reagent. 1, 3, 5-Tribromobenzene was used as a linker for the three triphenylene units under Sonogashira coupling conditions. As was done earlier in the series, the mixture was heated.



Scheme 2.15: attempted synthesis of 1, 3, 5-tri-triphenylene benzene.

A solution of 2-ethynyl- 3, 6, 7, 10, 11-pentakis (hexyloxy) triphenylene in TEA was added to the reaction mixture slowly after it had cooled down by syringe pump at a rate of 0.5ml/h. When the addition was finished, the mixture had been heated again, but this time to refluxing point overnight. The reaction TLC showed that there was a number of products, but very close to each other and there was no starting material left. Analysis of compound was conducted to ascertain whether or not the target compound was present. The MALDI results revealed the main peak, which gave 1504.46, corresponding to the homo-coupling product. Other peaks were apparent but could not be identified.

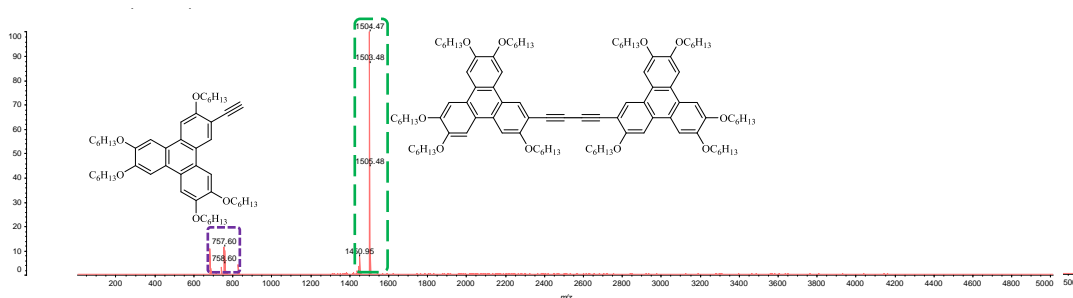


Figure 2.25: Crude MALDI-MS showing presence of compounds **97** and **102**.

A second attempt was made to produce the triad. The change made to improve the process aimed to reduce the production of homo-coupling by slower addition rate of the acetylene terminal in the reaction. Three equivalents of monoacetylene triphenylene were used with one equivalent of tribromobenzene, but some homo-coupling still occurred. It seems the triphenylene acetylene had a higher reactivity to couple with itself rather than couple with bromobenzene. Therefore, the synthesis of the triad was difficult and up to this point, it produced mainly the homo-coupling compound as shown in figure **2.25**. The reactivity of the Sonogashira catalytic system is mainly influenced by the choice of aryl halide or pseudohalide substrate. The choice of halide is important because different halides affect the process of the coupling procedure, for example, the iodine

group has the highest reactivity among the halides, which makes the reaction better. Therefore, using aryl iodides in the reaction is proven to be more successful. However, they are more expensive comparatively to the other halides. The aryl bromide starting materials were used in the subsequent reactions because of their availability in the lab but it made the coupling reaction less successful due to the reasons outlined above.

2.3. Introduction to BODIPY Compounds

In 1968, Treibs and Kreuzer were the first to synthesise 4,4-Difluoro-4-boro-3a,4a-diaza-s-indacenes (abbreviated as BODIPY) dyes.^[43] There are several substitution sites on a BODIPY moiety. One is on the α -position and two are on the β - position on each pyrrole. Other sites are on the meso-position. BODIPY compounds are highly fluorescent, UV-absorbing class of small organic molecules. They have the advantage of being relatively insensitive to such environmental conditions as polarity and pH. This characteristic makes BODIPY compounds useful fluorophores for labelling biological molecules, for example, proteins. In recent years, the potential for BODIPY dyes has begun to be understood as a result of biomedical imaging techniques.

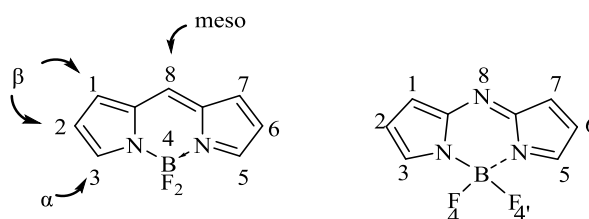


Figure 2.26: Boron dipyrromethene (BODIPY) (left) the aza-BODIPY core (right).

Research into the applicability of the aza-BODIPY structures has been reported only within the last decade, despite the foundations of the azadipyrromethene compound being reported in the early 1940s.^{[85] [85b]} The motivation behind the research was to discover compounds with red shifted photophysical properties. Aza-BODIPYs are part of BODIPY structures. However, they are differentiated by the nitrogen in the meso position. (see figure 2.25). There are 3 steps to synthesise aza-BODIPY structures which has been reported by Cammidge's group.^[14] The first step towards the synthesis of aminoisindolene is started by bromoamidine. The following step produce aza-(dibenzo)

dipyrrromethene by dimerization of this substituted aminoisoindolene in toluene. The third step is accomplished by forming the aza-BODIPY compound by treating it with BF_3 . Cantu et. al synthesised the Paddle-wheel BODIPY–hexaoxatriphenylene **115** which is an electron-rich donor-acceptor system and has both of these properties: the hexaoxatriphenylene group having donor properties and the BODIPY having acceptor properties.^[86] The electron-transfer process is ultra-fast when a suitable photosensitizer is used. These properties were established through electrochemical and computational studies of the molecule. In this one-step reaction, 2, 3, 6, 7, 10, 11-hexahydroxytriphenylene reacts with meso-aryl-functionalized BODIPY when dissolved in freshly distilled dichloromethane in the presence of dry aluminium chloride. This results in fluorine being replaced by oxygen atoms. Usually, the observation in the UV for BODIPY will show peaks at 500nm. However, the hexaoxatriphenylene showed a peak at 325 nm and these overlay each other in the UV/Vis spectrum. The methods used in this research are very different from those applied in our group but the results they have achieved form an interesting design and have the potential to inform some of our future activities.

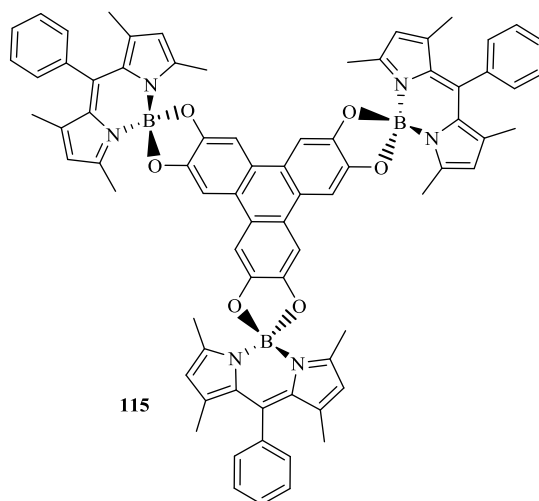


Figure 2.27: BODIPY–Hexaoxatriphenylene structure.

There is a research report that presents a new idea on design and synthesis of novel triphenylene Bodipy diad **116** which exhibited good liquid crystal properties. Under polarizing optical microscopy (POM) the novel diad exhibited a fan-like texture during the mesophase which is similar to triphenylene columnar liquid crystal.^[87] Additionally, the mesomorphic properties of triphenylene-Bodipy diads was confirmed by differential

scanning calorimetry (DSC). The transition temperature and the enthalpy change are shown in table 2.2 and figure 2.28, this displays a typical liquid crystal behaviour.^[9]

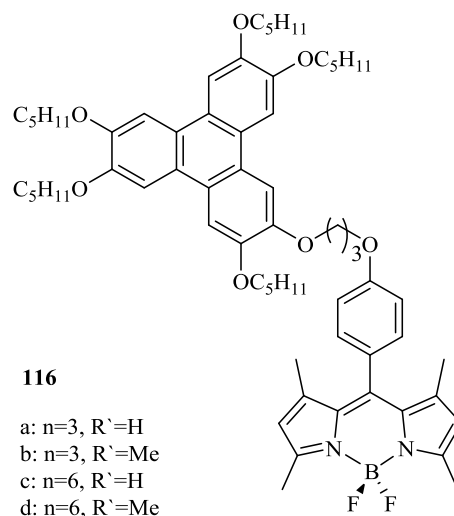


Figure 2.28: Triphenylene-Bodipy diad.

<i>Diads</i>	<i>Phase transition</i>	<i>T (ΔH) heating scan</i>	<i>T (ΔH) cooling scan</i>
A	Cr-Col	26.4 (5.35)	20.4 (5.98)
	Col-Iso	50.6 (23.28)	41.3 (24.61)
B	Cr-Col	17.9 (9.82)	16.6 (12.06)
	Col-Iso	52.7 (10.33)	43.7 (8.24)
C	Cr-Col	25.1 (8.68)	19.4 (8.85)
	Col-Iso	50.6 (9.86)	44.2 (10.01)
D	Cr-Col	27.1 (7.31)	23.8 (7.44)
	Col-Iso	58.5 (21.69)	52.4 (17.85)

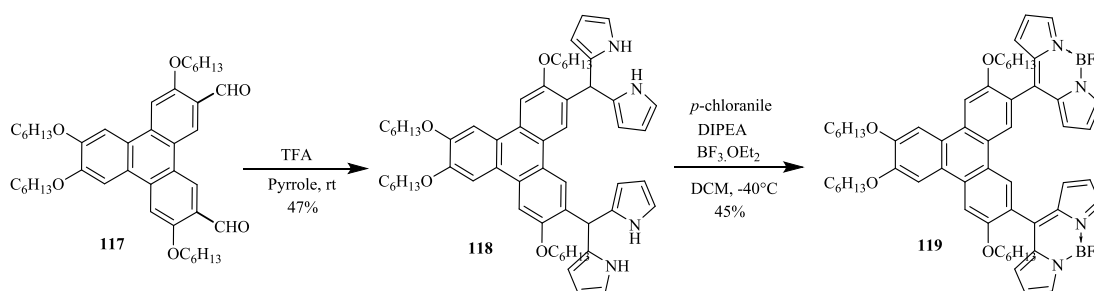
Cr = crystalline, Col = columnar, Iso = isotropic.

Table 2.2: Phase transfer temperature (°C) of compounds and enthalpy changes (KJ/mol in brackets).

2.3.1. Previous Work

The rationale for using the BODIPY in conjunction with the triphenylene was because our group had previously, successfully synthesised two BODIPY-triphenylene structures, triphenylene-bis BODIPY with different substitution positions. The most successful one was synthesised using dialdehyde triphenylene and freshly distilled

pyrrole in TFA. Dipyrromethane triphenylene **118** was produced as an intermediate, in the form of a light brown powder. However, it needed to be used quickly to avoid decomposition. It was therefore taken directly to form the Bis-BODIPY product **119**, which was more stable and obtained in the form of a highly coloured, dark red solid. This work had the BODIPY fragment attached at the meso position.^[43]



Scheme 2.16: Synthesis of BODIPY-triphenylene **119**.

Turner et al, then attempted to attach the BODIPY at the alpha position of the pyrrole.^[43] However, although the compounds could be formed and proved on the MALDI, they could not be isolated.

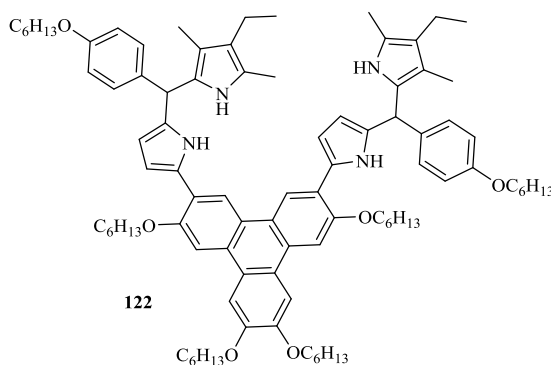
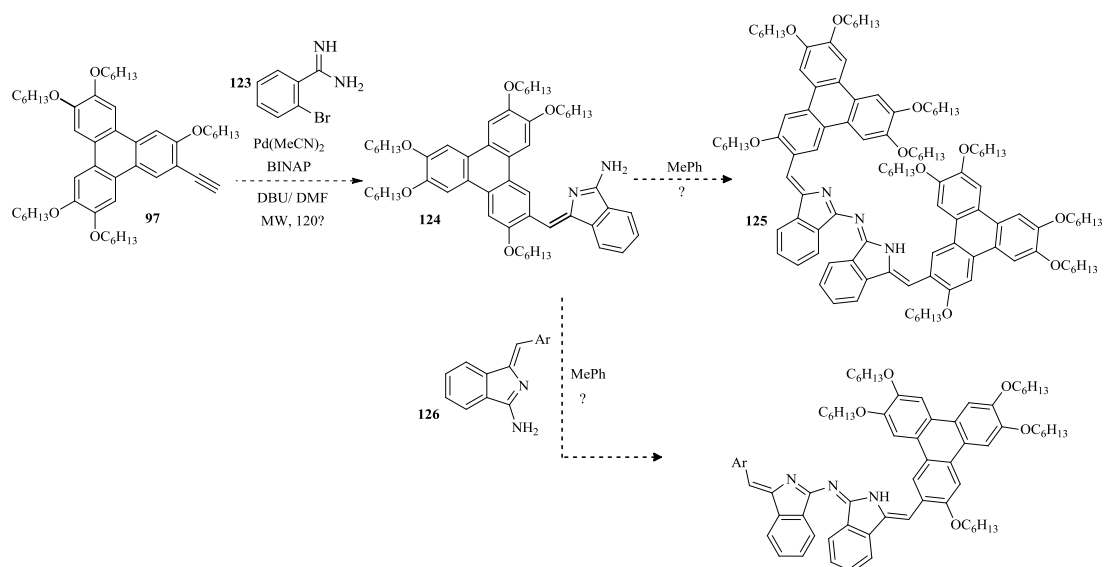


Figure 2.29: Dipyrromethane-triphenylene.

The benzofused aza-bodipy structures (and dipyrromethen) present an interesting architecture which logically they could be employed to link triphenylenes and other useful functional units. This series will focus on the formation of asymmetrical and symmetrical azadipyrromethene **125** molecules, by producing different aminoisindoline structures.

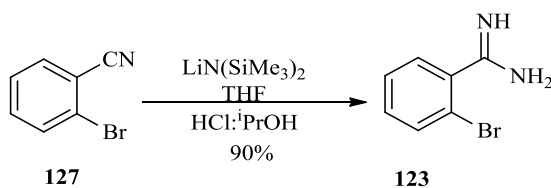


Scheme 2.17: outline plan in this series.

2.3.2. Synthesis of Aminoisoindolene

The preparation of aminoisoindolene **124** was the first step in the investigation of the synthesis of the target structure. Scheme **2.18** shows the synthetic route used. The route has initiated by preparing the amidine using the previously reported methodology.

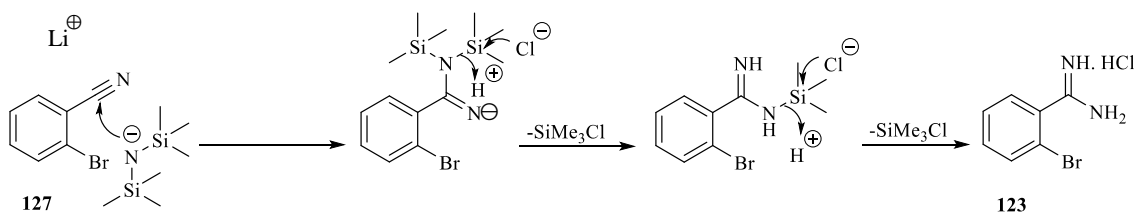
2-Bromobenzonitrile **127** was reacted with a solution of lithium bis(trimethylsilyl)amide in THF. The reaction was quenched using a solution of isopropanol and HCl. This produced a white solid, *o*-bromobenzamidine hydrochloride, at a yield of 90%.^[88]



Scheme 2.18: Synthesis of amidine **123**.

The conversion of 2-Bromobenzonitrile, **127**, to its corresponding amidine, **123**, was achieved through stirring with lithium bis(trimethylsilyl) amide in THF. The product was isolated by acid work up, precipitating a white solid. A procedure reported by the de Meijere group had followed, with few complications.^[88] The reaction has been carried out on two occasions, to high yields, allowing the accumulation of a stock of this key precursor. The identity of the product was confirmed by ¹H NMR spectroscopy, showing

the key amine and imine peaks at 9.5 ppm. All other peaks matched those quoted by the de Meijere group.



Scheme 2.19: The formation of 2-bromobenzamidine **123**.

This reaction involves a nucleophilic attack by the nitrogen bis trimethylsilyl anion (stabilised by a lithium cation) at the partially positive carbon atom of the nitrile group. Acid work up then removes the trimethylsilyl groups yielding 2-bromobenzamidine.

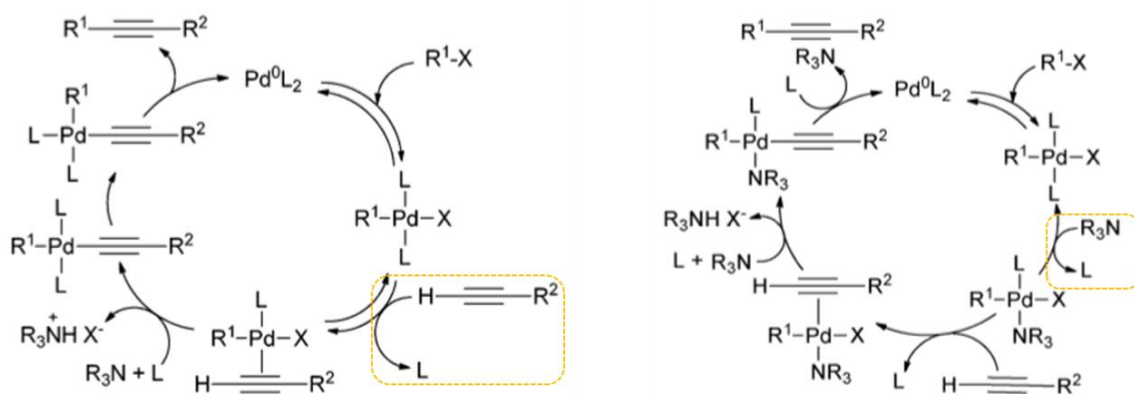
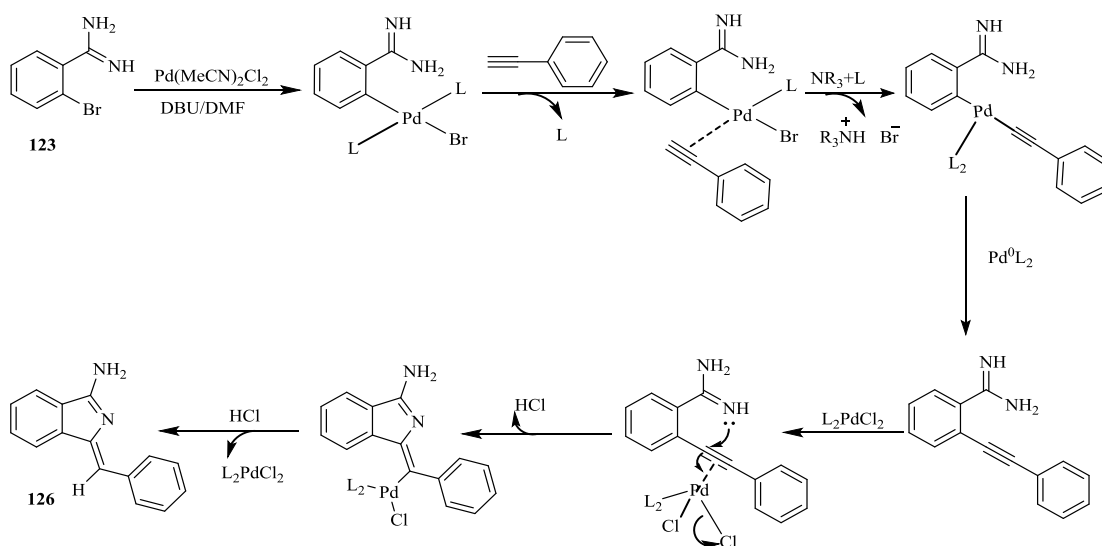


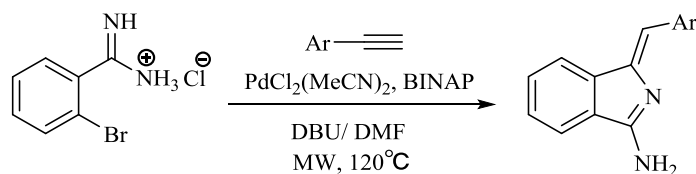
Figure 2.30: Possible mechanisms for the copper-free Sonogashira reaction.

The copper-free Sonogashira mechanism is frequently used if the alkyne is a better ligand for the palladium^[57] metal than the amine. If the amine that used in the reaction is the better ligand, the catalytic cycle is more complex and involves the amine in multiple roles during the process.^[89] The role of the amine, however, has not yet been fully elucidated. The catalytic cycle could be affected by using different acetylene derivatives or bases. There is still much to be investigated about this reaction. In our reaction, for the current work, after the coupling, a regioselective 5-exo-dig cycloisomerisation domino reaction takes place, through which the final product is obtained.



Scheme 2.20: Proposed mechanism for the aminoisoindolene.

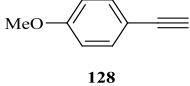
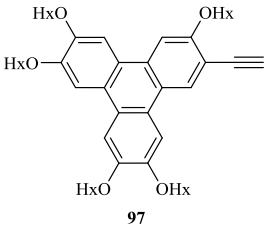
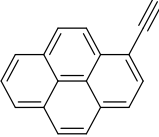
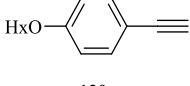
Scheme 2.20 illustrates the suggested mechanism. The first part of the mechanism is coupling step. The next part is to coordinate the palladium catalyst to the alkyne. The loss of HCl then occurs when the cyclisation takes place. Finally, the reductive elimination allows the catalyst to regenerate and the product to be formed.



Scheme 2.21: Synthesis of aminoisoindolene **126**.

Next, a palladium catalysed copper-free Sonogashira cross-coupling reaction was used followed by the microwave-assisted cycloisomerisation reaction protocol which was developed by Hellal and Cuny. This is a one pot synthesis method in which amidine **123**, phenyl acetylene, catalytic amounts of palladium catalyst and BINAP as ligand, are placed in a microwave vial, in the presence of DBU, which is a base.^[90] The solvent used for the reaction was DMF. The mixture was irradiated for 1 hour at 120 °C using a microwave set up. Following an aqueous work up, and column chromatography, the pure aminoisoindolene **126** was produced as a yellow powder. Using mass spectrometry, Compound **126** was characterised. The Sonogashira mechanism has already been explained (scheme 2.4). However, as mentioned above it is possible to use the same

procedure but omitting the copper.^{[91],[89]} The copper-free mechanism, was chosen for this step because it minimises the risk of homocoupling.^[89] The catalytic cycle begins with the aryl halide activating the catalyst [Pd(0)L₂], by oxidative addition. The alkyne undergoes a reversible π -coordination, which gives alkyne–Pd^[57] complex. It is easier for the acetylenic proton to be removed by the base because the proton has now become more acidic in nature. Next, the acetylene ligand coordinates to palladium metal. This produces a complex which undergoes isomerisation then releases the cross-coupled product in a reductive elimination step. The catalytic species [Pd(0)L₂] will be regenerated as a result of the previous step and will be ready to begin a new cycle, as shown in the scheme 2.20.

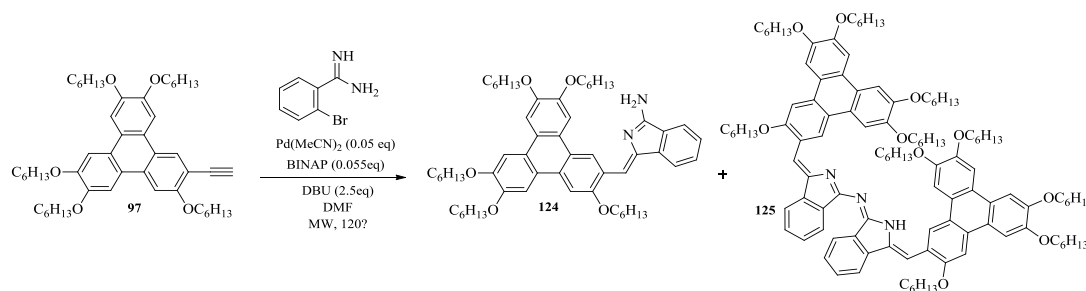
Entry	Ar	Yield	Product number
1	 128	72%	131
2	 97	21%	124
3	 129	46%	132
4	 130	42%	133

HxO = OC₂H₅

Table 2.3: Reaction of amidine with acetylenic precursors to produce aminoisindolene compounds.

Our first synthesis attempts towards aminoisindolene, were undertaken to introduce the desired functionalities. The reaction conditions used for each of the aminoisindolene compounds illustrated in the table, were those published by Hellal and Cuny, as mentioned earlier (scheme 2.21). The reaction was easy to perform at first and took only one hour. Aminoisindolene was produced.

The acetylenic precursor for product **131** was available. 4-Methoxyphenyl-aminoisindolene was created using the same copper free, palladium catalysed Sonogashira reaction.^[92] This reaction successfully converted amidine to aminoisindolene. The ¹H NMR spectrum of this molecule matched with the reference value.^[92] The MALDI showed that the expected structure had been produced. Our group had already reported the successful synthesis of aminoisindolene. This encouraged us to undertake the same procedure but using the mono-acetylene triphenylene in place of the 4-methoxyphenylacetylene.



Scheme 2.22: Synthesis of compound **124**.

Our next step was therefore synthesis of the triphenylene-aminoisindolene **124**. However, this proved challenging. The first attempt used an hour-long reaction. The TLC showed a number of products, one of which was the darker spot corresponding to self-condensation, as expected. There was a new yellow spot, but some starting materials were also left. Furthermore, analysis showed that homocoupling had taken place. The purification required two columns. Also, the recrystallisation showed the viscous nature of the product which was hard to filter because it became stuck in the filter paper. A different recrystallisation process, using PET, isolated a bright yellow solid. This was not the pure product but matched the expected NMR characterisation. The MALDI-MS showed the target product as in figure **2.31** but because a good quantity has been required to carry out the whole series, the reaction had been repeated. On this attempt, the reaction has been run for two hours, to ensure that all the starting material was consumed. However, with the longer reaction time, there was more self-condensation and some homocoupling. Eventually, the homo-coupling product has been isolated successfully by crystallisation using acetone. Nevertheless, the target compound, which had been solid, turned to a viscous substance when filtered.

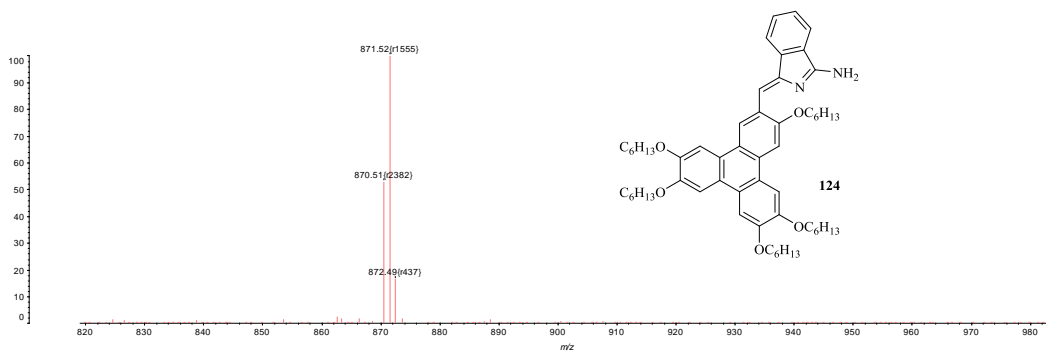


Figure 2.31: MALDI-TOF spectrum showing the mass for the target compound **124**.

The self-condensation was the second major product **125** as with the earlier reaction with the 4-methoxyphenylaminoisindolene. The self-condensation product had been isolated from triphenylene aminoisindolene reaction, by column chromatography. The structure was proven by the MALDI. However, the structure required crystallisation to form a pure, dark red solid.

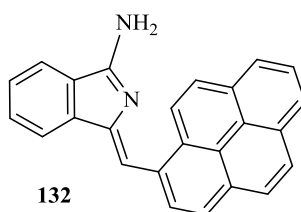
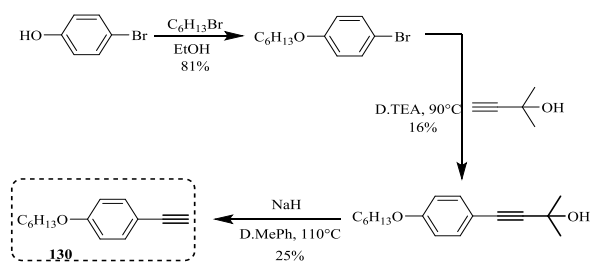


Figure 2.32: Pyrenyl-aminoisindolene.

Our group has already reported the successful synthesis of pyrenyl-aminoisindolene **132**, using the synthetic protocol which has been discussed earlier (Scheme **2.18**).^[93] This was a challenging synthesis partly due to problems with the solubility of the final product, and partly because, during the purification process, the product stuck to MgSO_4 and, it can be assumed, also to the silica gel. The column was flushed many times to recover all the material and it is likely that some of the product was lost in the process. Eventually, the product was isolated as yellow solid with both isomers as a mixture and a pure fraction of the Z -isomer.



Scheme 2.23: Preparation of 4-hexyloxyphenyl ethylene.

The last aminoisoindolene has been prepared to complete the series and to see if a smaller molecule than pyrenyl or triphenylene would produce clear NMR spectra and give a better analysis of the aza-dipyrromethene product. The 4-hexyloxyphenylacetylene had been selected **130** because it is similar to the 4-methoxy but had not been attempted before. It was necessary to prepare the 4-hexyloxyphenylacetylene due to its commercial unavailability. The scheme **2.23** above sets out the full synthetic route. Consequently, 4-hexyloxyphenylaminoisoindolene **133** was formed by reacting amidine with 4-hexyloxyphenylacetylene using the general procedure by microwave technique and yielded 42%. The TLC showed the self-condensation product along with the target compound and the starting materials. The $^1\text{H-NMR}$ spectrum showed, as expected, two distinctive peaks in the aromatic region, one corresponding to the alkene proton at 6.72 ppm, and the other corresponding to the two protons in the phenyl substituent at 6.94 ppm. The product was fully characterised by UV-Vis, Mass spectrometry and NMR spectroscopy, and full interpretation of the structure was possible after suitable crystals were grown slowly from pure methanol. The $^1\text{H-NMR}$ spectrum obtained proves the desired compound **133**, figure **2.33**. The aromatic regions of the target structure showed a singlet at 6.62 ppm, is corresponding to the alkene proton and the other corresponding to the two protons in the phenyl substituent at 6.90 ppm

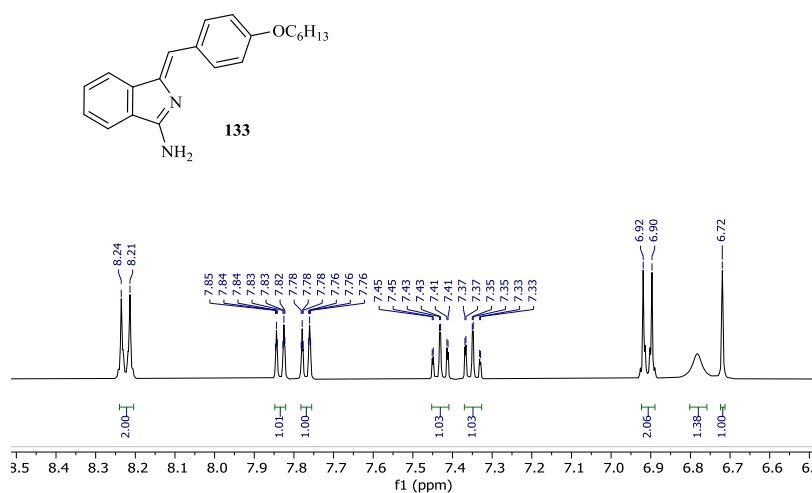
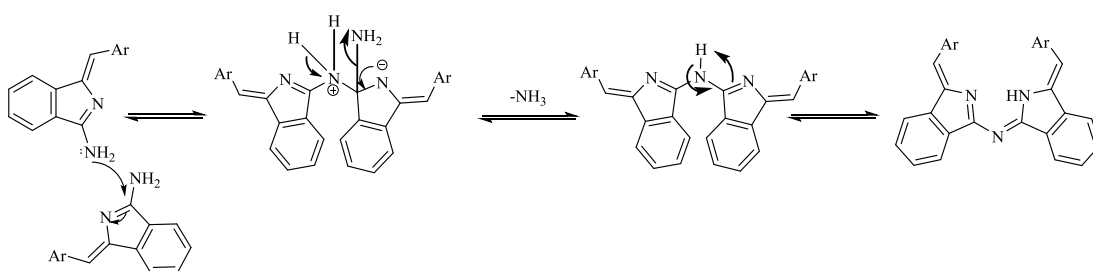


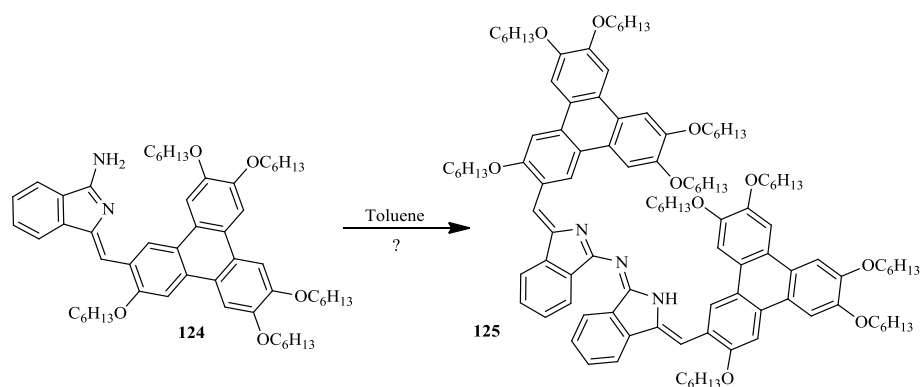
Figure 2.33: Aromatic region of ¹H-NMR spectrum of compound **133**.

2.3.3. Synthesis aza-BODIPY product



Scheme 2.24: Proposed mechanism for the formation of aza-dipyrrromethene.

The mechanism outlined above explains the formation of the aza-dipyrrromethene starting from a nucleophilic attack where an amine group of one molecule attacks the partially positive carbon between the two nitrogens on the other molecule followed by removing of ammonia and the desired product obtained after tautomerism.



Scheme 2.25: Synthesis of aza-dipyrrromethene triphenylene.

After producing the triphenylene aminoisoindole, a further reaction had been conducted to produce the symmetrical aza-dipyrrromethene triphenylene using just the triphenylene aminoisoindole and toluene as a solvent at a temperature of 120 °C. The main product was self-condensation. There was some starting material left, according to the TLC monitoring. It was left for 6h to give the starting materials a chance to be consumed. After the work up the MALDI-MS showed a peak at 1724, which proved the structure. The yield was 70%. Another attempt was made to improve the yield using 5ml p-xylene, at 140 °C, left for two days, but again some of the starting materials remained unconsumed. The desired product was formed but the yield had significantly reduced.

Time	Solvent	Yield
	Toluene	2 ml
	p-xylene	5 ml

Table 2.4: Solvent effect in aza-dipyrrromethene reaction.

However, the NMR was poor because of the aggregation. Purification was conducted by column chromatography. After carrying out a further NMR, with a different solvent, the spectra were still not clear. The NMR was who attempted at a temperature of 100°C. This gave in the same positions of peaks, similar to what was expected from the triphenylene moieties, but this time there was noise from the baseline and peaks were broader.

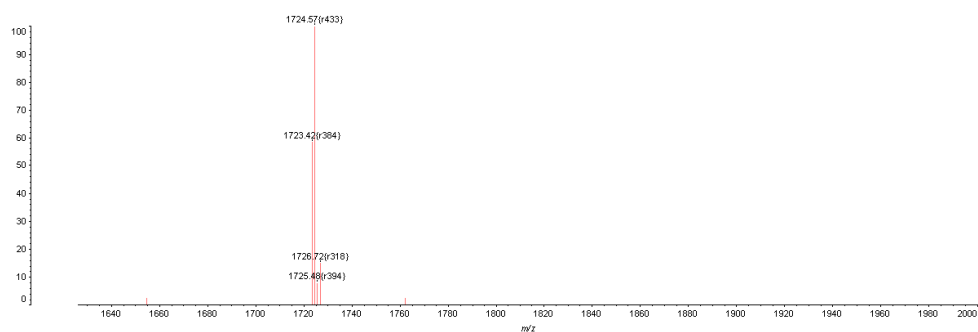
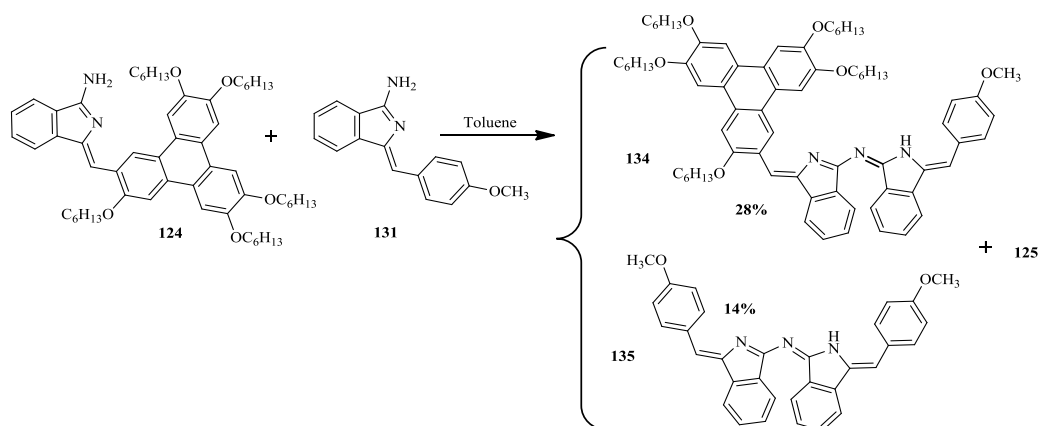


Figure 2.34: MALDI-MS spectra of aza-dipyromethene triphenylene **125**.

Next, our attention was turned to producing the unsymmetrical condensation product **134**, after the triphenylene-aminoisindolene had been dimerization. Then, the 4-methoxyphenylisindolene has used with the triphenylene aminoisindolene refluxing in 2 ml toluene. As a result of this reaction the TLC showed three main spots, corresponding to the triphenylene aminoisindolene dimerization product (the reference values were already available from the previous reaction) and the 4-methoxyphenylaminoisindolene self-condensation product **135**. The new spot formed between these two, corresponding to the new red product. Nevertheless, there were two minor spots close to the baseline which corresponded to the starting materials.



Scheme 2.26: Synthesis of the compound **134**.

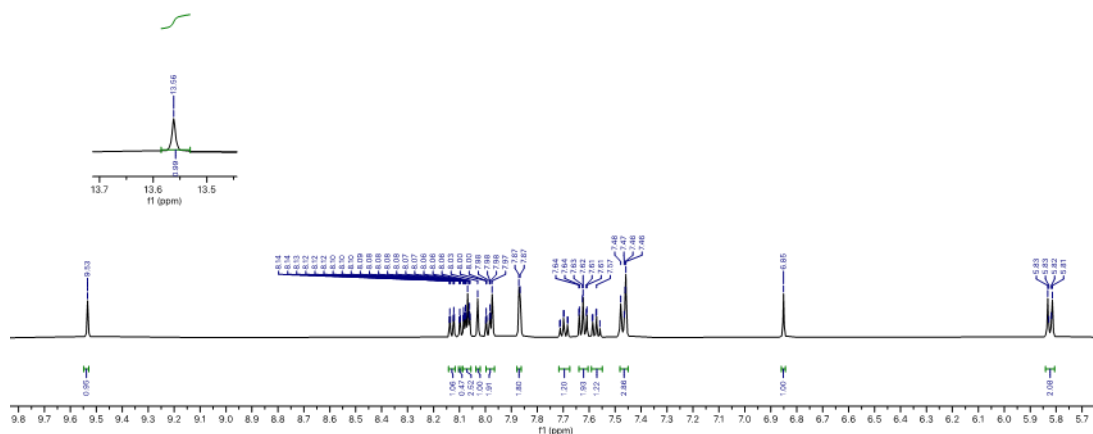


Figure 2.35: The expansion of the aromatic region for compound **134**.

However, more of this compound has been required in order to attempt the synthesis of unsymmetrical diaminoisindolene. This depended on the result of the Maldi spectroscopy that confirmed the formation of the target product. The $^1\text{H-NMR}$ spectrum showed something unexpected, the doublet peak at 5.8 ppm corresponded to aromatic protons. The COSY analysis method was used to help us assign the signals. This homonuclear analysis consists of a two-dimensional NMR spectrum. The f1 and f2 axes are used to highlight chemical shifts which occur from the nuclei. Signals where the chemical shifts are identical in both axes are shown on the diagonal of the spectrum. It depends on the 1D $^1\text{H-NMR}$ spectrum but is expanded to use two axes to show how coupling protons in the molecules link in the spectra to those other protons to which they couple. Cross peaks are shown by signals off the diagonal.^[94] Figure **2.36** shows COSY conducted at 263K in acetone. These spectra illustrate “through bonds” interactions and provided useful information about the protons that had couplings between them, for example the cross peaks shown between the doublets for phenyl substitution the latter overlapping with one of the triphenylene singlets. The set of triplets are coupled to other sets of doublets but the latter overlaps with the triphenylene singlets and so appears as an indistinguishable multiplet. However, the integration showed the expected number of protons for the structure. However, some uncertainty remains regarding assignment of the peaks.

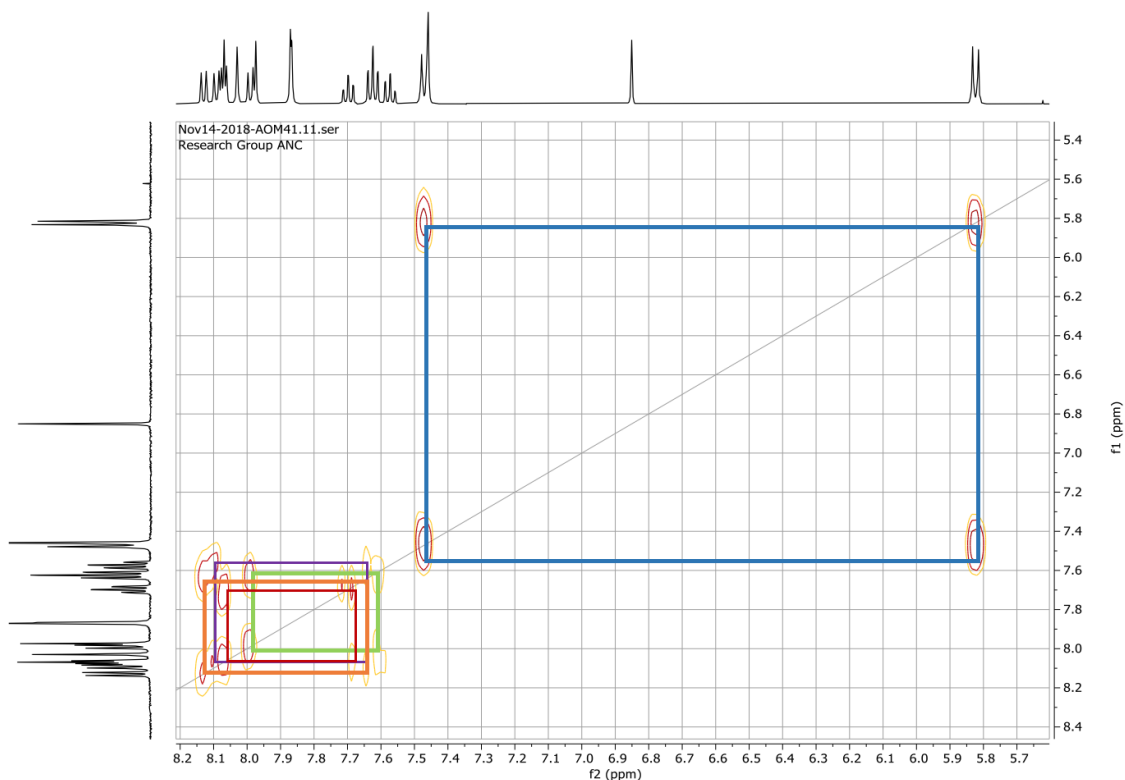


Figure 2.36: COSY experiment showing cross peaks in compound **134** at 263K.

Theoretically the aminoisoindole units sit below the triphenylene ring that is most likely to be influenced by π - π interactions between the aromatic systems. Optimised geometry, hydrogens omitted for clarity. The distance between the triphenylene and the end methoxy-phenyl unit is approx 4 Angstroms, perfect for pi-pi stacking interactions (**A**, **B** in figure **2.37**). Also, the one more with the hexyl chains removed (easier to see) as in **C** figure below **2.37**.

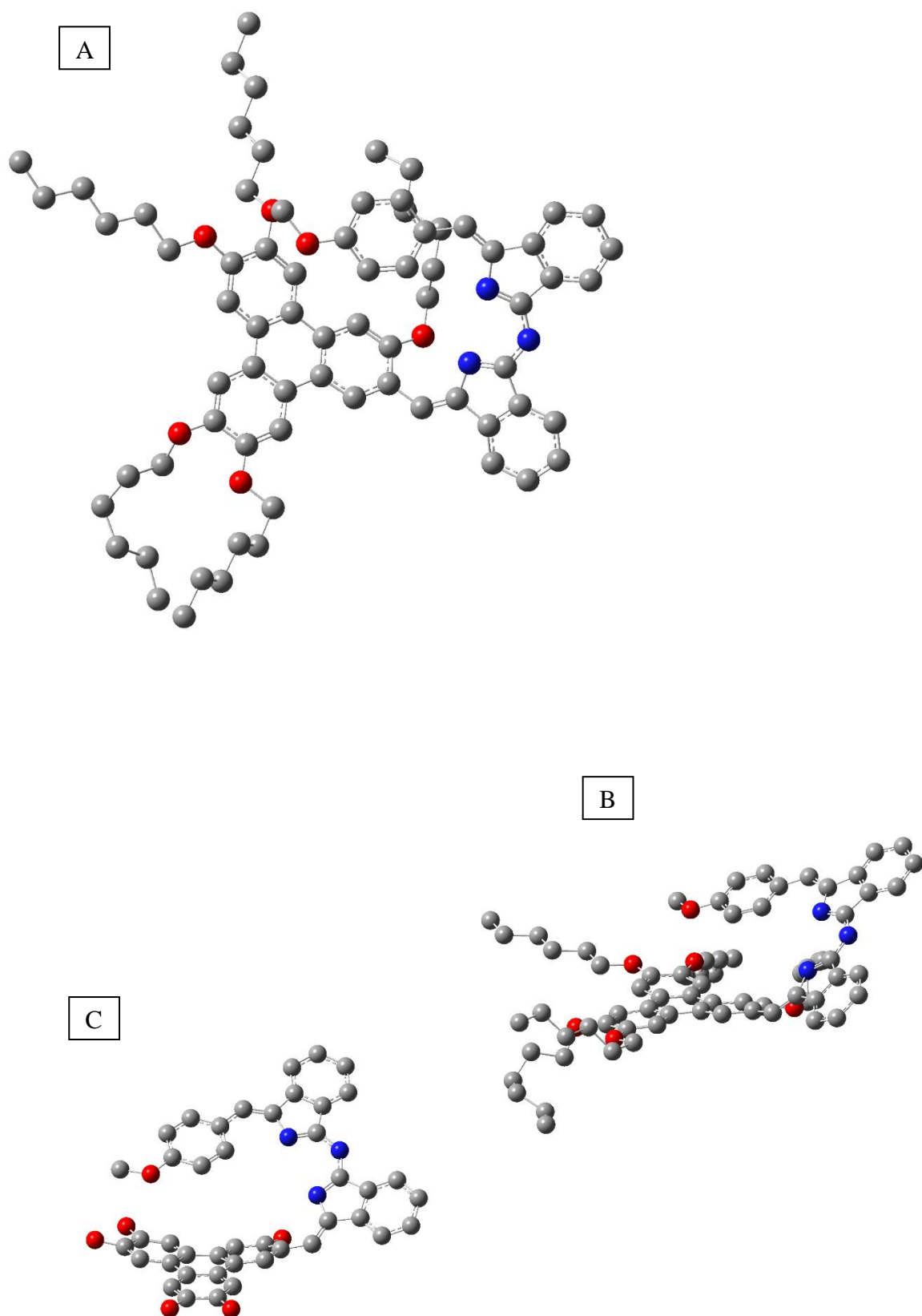
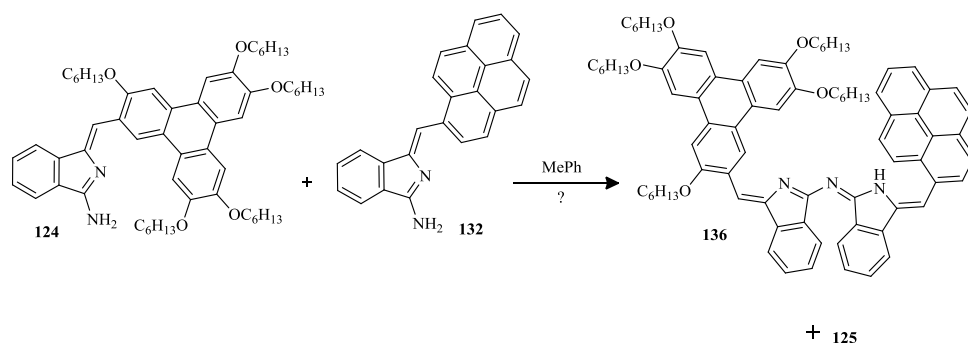


Figure 2.37: Modelling of compound 134.

The synthesis towards an aza-dipyrromethene compound bearing pyrenyl molecules started from the synthesis of pyrenyl-aminoisoindolene **132**. The reaction was carried out in toluene overnight.



Scheme 2.27: Synthesis of the compound **136**.

After that, TLC revealed the formation of three main spots, later confirmed by mass spectrometry to be the self-condensation product for both precursors and the desired structure. The purification process required two column chromatography separations on silica gel, which resulted in the pure compound as a dark brown solid in 60% yield. Despite the fact that clear NMR spectra was an issue due to solubility of the final product, great spectra had been obtained in THF with two different sets of peaks as expected which corresponded to the two components which are shown in the $^1\text{H-NMR}$ spectrum. (Figure 2.38).

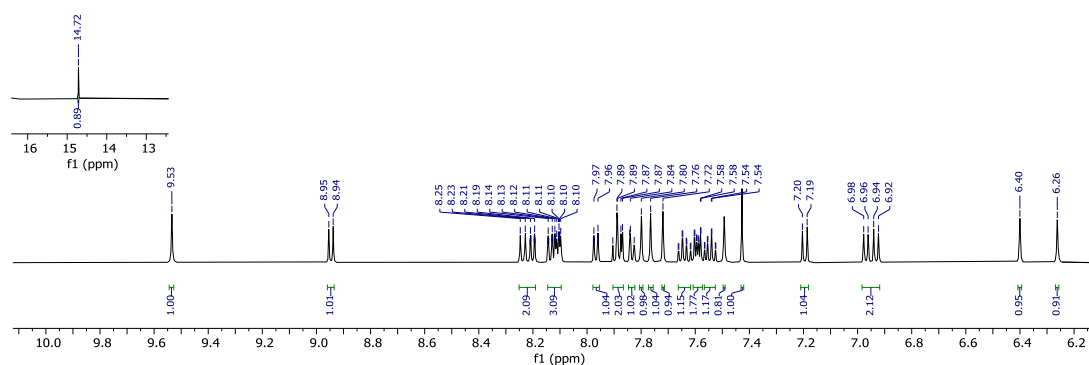
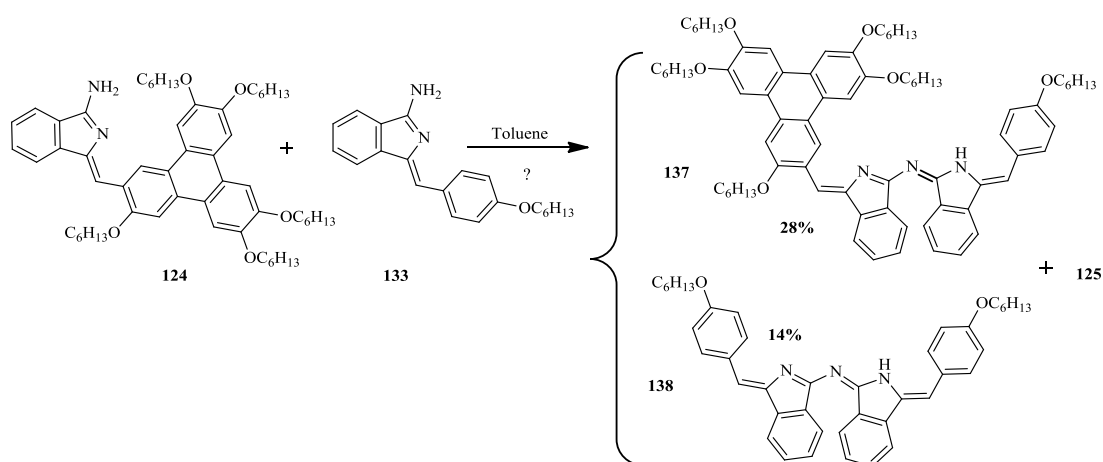


Figure 2.38: Aromatic region of $^1\text{H-NMR}$ spectra of compound **136**.

The spectrum showed the integration of the protons as expected in the aromatic region and the distinctive singlet at 14.72 ppm characteristic for (NH). In addition, the aryl peaks which shifted upfield is similar the suggesting helical structure as in compound **134**. The mass spectroscopy is supporting the existence of the target compound. To conclude the series of synthesis an unsymmetrical aza-dipyrromethene products, 4-hexyloxyphenyl aminoisindolene was reacted with the triphenylene aminoisindolene in 2ml toluene at reflux. To monitor the reaction, TLC was used. It showed three main spots which corresponded to the 4-hexyloxyphenyl-aminoisindolene self-condensation, 14%, the target compound with triphenylene aminoisindolene yielded at 28% and the aminoisindolene triphenylene self-condensation product.



Scheme 2.28: Synthesis of compound **137**.

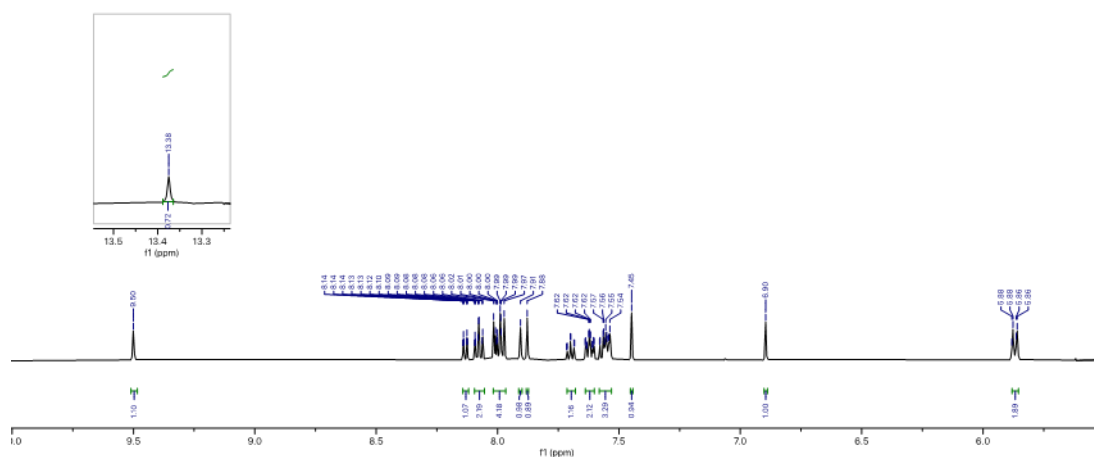


Figure 2.39: aromatic region of the compound **137**.

$^1\text{H-NMR}$ spectroscopy showed similar spectra of the compound **134**, also the assistance obtained from COSY experiment made possible the interpretation of the structure. COSY analysis was conducted to confirm the structure of the aza-dipyrromethene product which paired the triphenylene aminoisindolene with the hexyloxy-aminoisindolene. Figure 2.30 below shows the overlapping of the peaks on the aromatic area and their interactions.

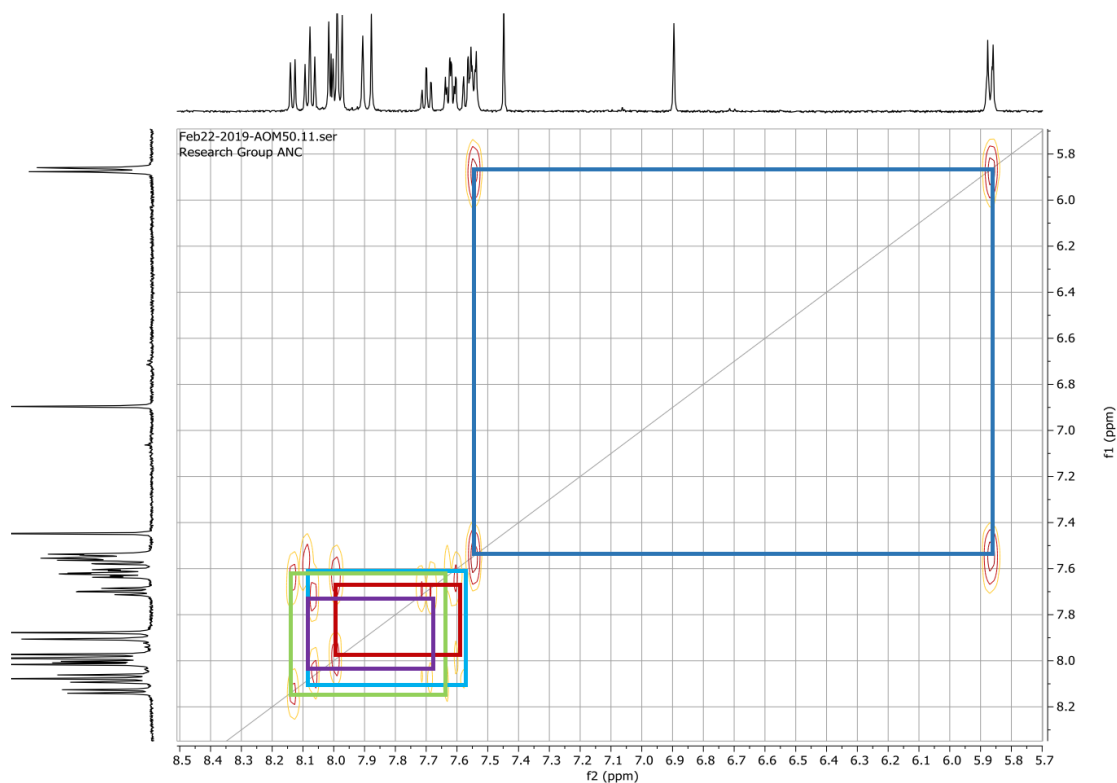


Figure 2.40: COSY experiment showing cross peaks in compound **137** at 263K.

Optical properties

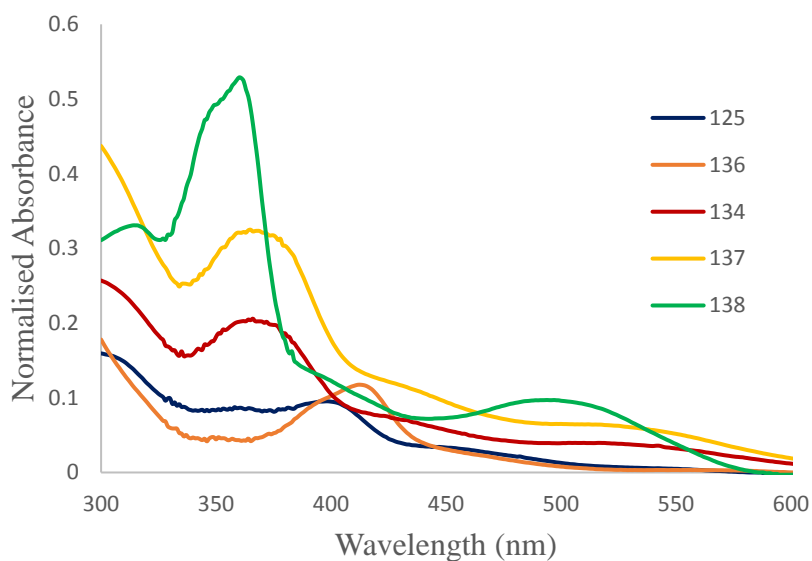
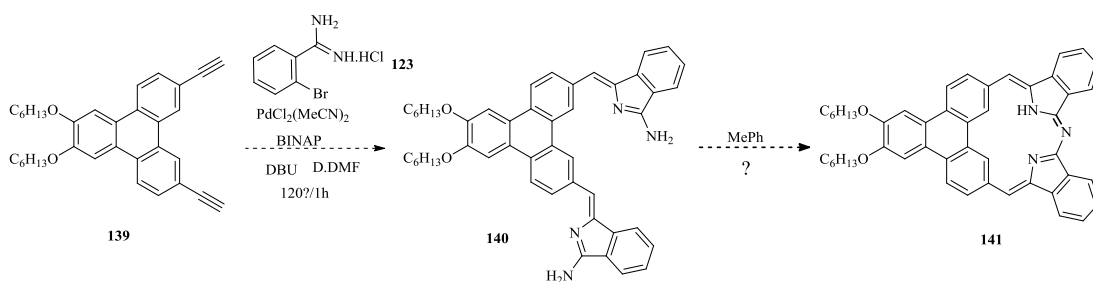


Figure 2.41: UV-Vis spectra of compounds 2nd series in dichloromethane.

The UV-Vis absorption spectra in dichloromethane were obtained and shown in Figure 2.41. There were about three absorption bands at 300nm, 360-420nm and shoulders from 450 - 560nm. All the first four products which have the triphenylene molecule moiety contain larger π -conjugate area than other molecules. The absorption peaks for them at 360-420nm is stronger than the BODIPY moiety absorption peak in TP-BODIPY. While azadipyrromethene **138** is red in color and its absorption as shown in figure below displays broad profile with a visible region maximum at 500 nm.

2.4. Attempted synthesis of aza(ditriphenylene) dipyrromethene

After the synthesis of triphenylene aminoisoindolene was followed by formation of aza-dipyrromethene compounds which have been prepared earlier. Our attention was move to design structures have antiaromatic feature that expected to exhibit mesophase behaviour. Structures between antiaromatic and aza-dipyrromethene had been suggested to produced. This part of project will focus on the synthesis of diaminoisoindolene triphenylene. In structure **141** there is some similarity with porphyrin in the right side of the structure such as core geometry. In porphyrin there is (CH) bridge while in the target molecule NH is the bridge in one site.



Scheme 2.29: Plan to synthesise aza(ditriphenylene)dipyrromethene.

2.4.1. Synthesis of Diacetylene-Triphenylene 139

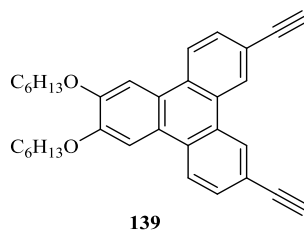
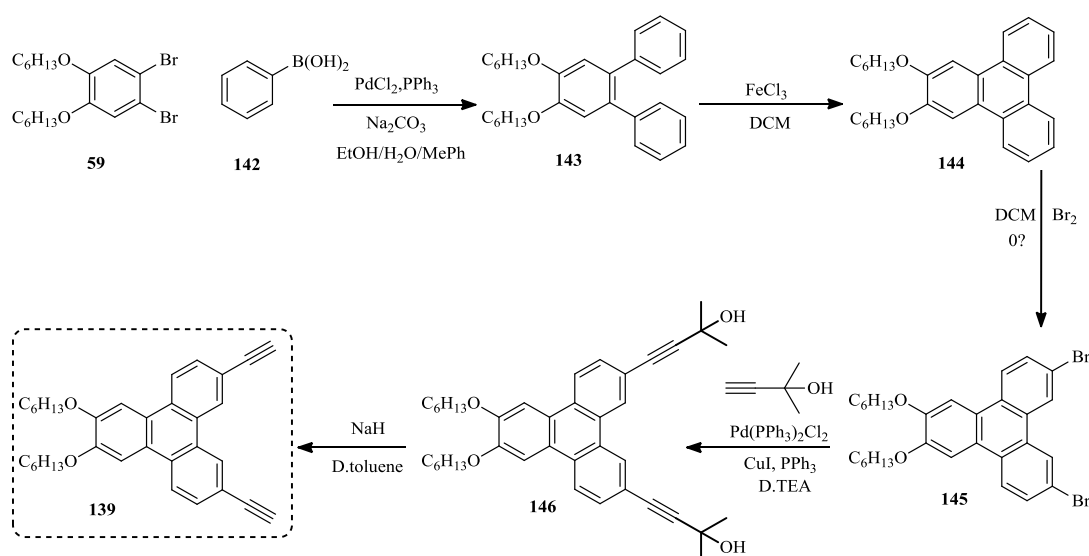


Figure 2.42: The precursor structure.

Turner (2015) had already successfully reported the attempted synthesis of Diacetylene-triphenylene, the necessary starting material to make diaminosoindolene-triphenylene, from 7, 10-dibromo-2, 3-bis (hexyloxy) triphenylene **145**. However, only a small quantity of the compound was available for our use, so the decision was taken to synthesise more and compare it with Turner (2015)'s reference. The protocol used earlier by our group was followed and using the four alkoxy chain in addition to the two other substituents. This involved a Sonogashira reaction using 2-methyl-but-3-yn-2-ol. This produced 4, 4'-(6, 7-bis (hexyloxy) triphenylene-2, 11-diyl) bis (2- methylbut-3-yn-2-ol) **146** in good yield. The purification was carried out by column chromatography. A mixture of dichloromethane, petroleum ether and ethyl acetate (3:1:1) allowed us to isolate the product. Sodium hydride in dry toluene was the condition for the deprotection step. The work- up and purification were carried out using column chromatography and showed that 7, 10-diethyne-2, 3- bis(hexyloxy)triphenylene **139** had been produced.^[43]



Scheme 2.30: Full synthetic route to compound **139**.

It was now possible to use the diacetylene triphenylene with *o*-bromobenzamidine hydrochloride. Therefore, the next structure to be synthesised was Triphenylene-bisaminosindolene **140**.

2.4.2. Attempted synthesis of Diaminoisindolene triphenylene

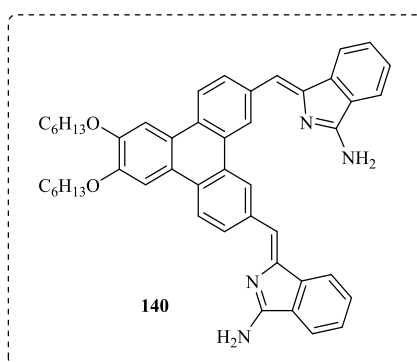


Figure 2.43: The target compound.

Hellal and Cuny's general condition for the reaction was followed, as explained earlier. The reaction was performed in (3ml) anhydrous DMF. Diacetylene triphenylene, and amidine, in presence of palladium, as a catalyst, with copper as a co-catalyst and DBU, formed the reaction mixture. This was degassed with nitrogen and stirred at room temperature for 5 minutes, to ensure that all the components had been thoroughly mixed.

The reaction was conducted in a microwave reactor for one hour. After this time a sample was taken and analysed by MALDI-MS. The spectra for the crude showed evidence of the desired Triphenylene-bisaminoindolene (Figure 2.29). A peak at 712, which corresponded to the di-substituted triphenylene, and 595 was the monosubstituted triphenylene significant peak at 476 m/z was also observed, which corresponded to the starting material, diacetylene triphenylene, and a peak at 950 m/z which showed the condensation product had taken place and the reaction had not proceeded as required. Purification was attempted but proved ineffective. It was not possible to isolate the products.

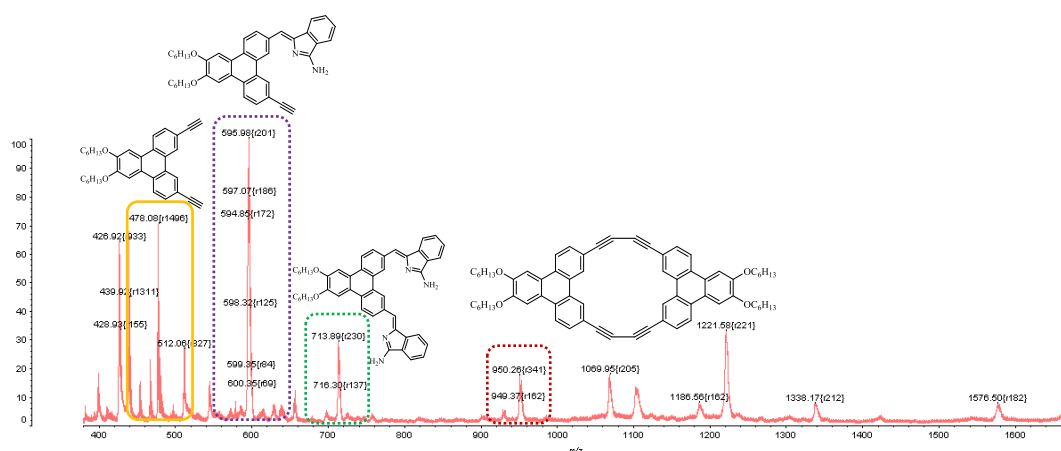
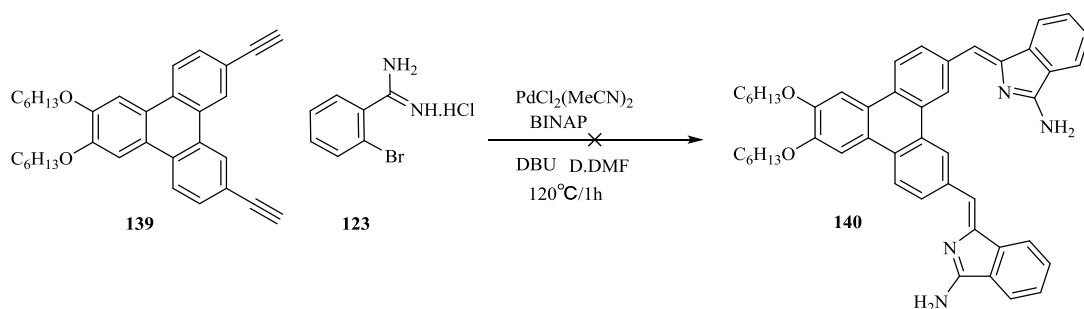


Figure 2.44: Maldi-TOF spectrum of the crude.

The column was flushed to recover all the materials present and another MALDI was conducted to make sure all the materials had been recovered. However, the same peaks were not apparent. Another attempt was made to consume the diacetylene-triphenylene totally, using the same scale as before but leaving it for longer to give it a chance to react with the amidine. However, the solvent had decreased, using only 1.5ml DMF, thus increasing the concentration and the reactivity of the mixture. The monitoring was kept the reaction each hour. After six hours, the amount of amidine had increased by 2 equivalents and doubled the quantity of the palladium catalyst because not all the starting material had been reacted. The mixture was then left for a further hour, after which the MALDI was checked. There was a small peak of 595, corresponding to the mono-substituted product. The main peak was the starting material. A peak at 577 started to appear after the seventh hour. The TLC showed that were no starting materials left. There were two possibilities. Either homocoupling had occurred or the target compound had been produced. The MALDI showed no interesting peak, which suggested that polymerisation might have occurred. The third attempt was made using 10 equivalents

amidine, at a temperature which was decreased to 80 °C. The mixture was a yellow colour, and the TLC was once again checked hourly. After five hours the TLC showed the starting materials and a spot at the baseline.

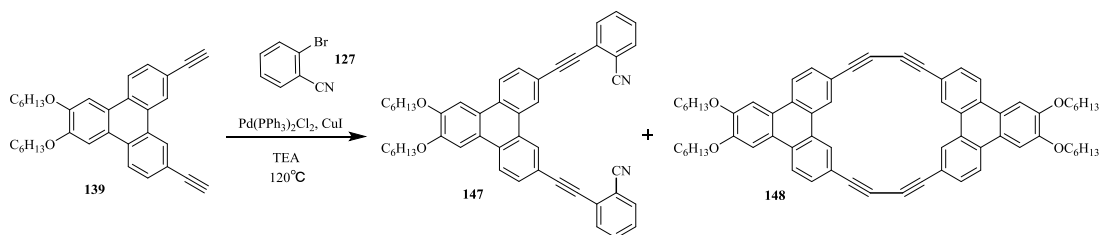


Scheme 2.31: Attempted synthesis of diaminoisoindolene triphenylene.

The quantity of the palladium catalyst had been doubled and increased the temperature to 120°C, at which point the colour of the mixture was brown and the MALDI-MS showed nothing of interest. A final attempt was made to conclude this reaction. After one hour the mass spectrometry had been checked for the crude. It showed the mono-substituted product and the starting material. There was little to gain from purifying this crude because the target compound was clearly not present.

The unsuccessful reaction led us to replace the amidine with 2-bromobenzonitrile which is the precursor of the amidine. By using this precursor, it was expected that bis-benzonitrile triphenylene would be formed under Sonogoshira coupling condition. This might have allowed the formation of liquid crystal phases of the in the intermediate product. Bisaminoisoindolene triphenylene would be formed after reacting the bis(benzonitrile) triphenylene with a solution of lithium bis(trimethylsilyl)amide in THF. This might allow the formation of the self-condensation in the advanced stage of this series.

2.4.3. Synthesis of 6, 7-bis (hexyloxy)-2, 11-bis (2-benzonitrile) triphenylene



Scheme 2.32: Synthesis bisbenzocyanide triphenylene **147**.

This reaction successfully produced the target structure, although there was still some homocoupling product. The reaction was conducted in a sealed tube using 3 equivalent bromobenzonitrile with the diacetylene triphenylene dissolved in normal TEA heated to 120°C in an oil bath, overnight. The TLC was checked the next day and showed the homocoupling product with the target product. The MALDI was checked and a peak of 678 was found. The starting material peak of 477 was not showing, demonstrating that all these materials had been consumed. The use of petroleum ether and DCM for crystallisation would bring out both products together as a mixture which was not desirable. Therefore, acetone crystallisation was used to cause the homo-coupling compound to crystallise out of the solution while the target product remained in solution. Later the petroleum ether and DCM were used to recrystallise the target product. The ¹H-NMR spectrum of the structure **147** showed 16 protons in the aromatic region. However, there is chemical shift of the inner proton at 8.89 ppm, from 8.75 ppm in starting material.

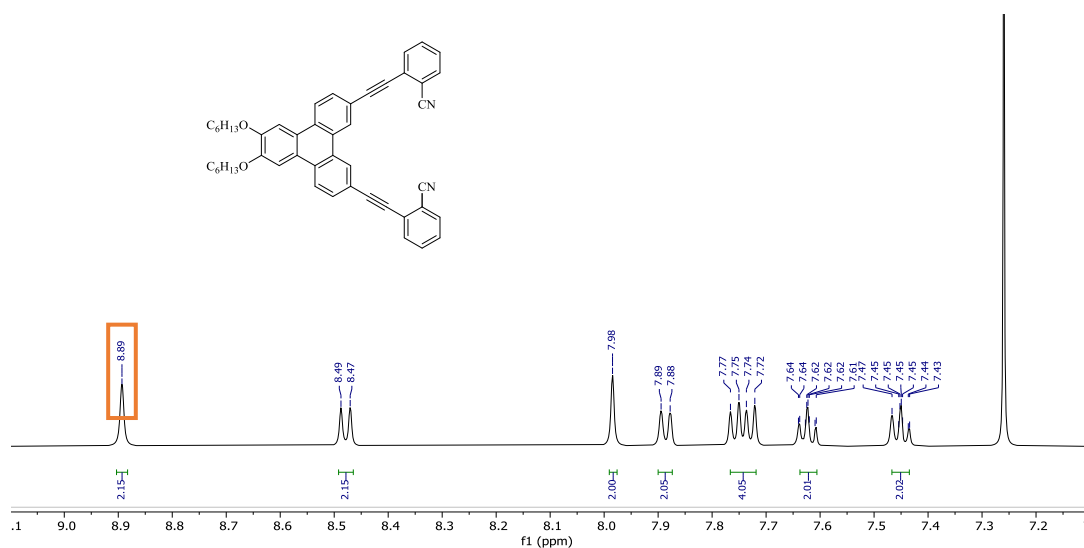
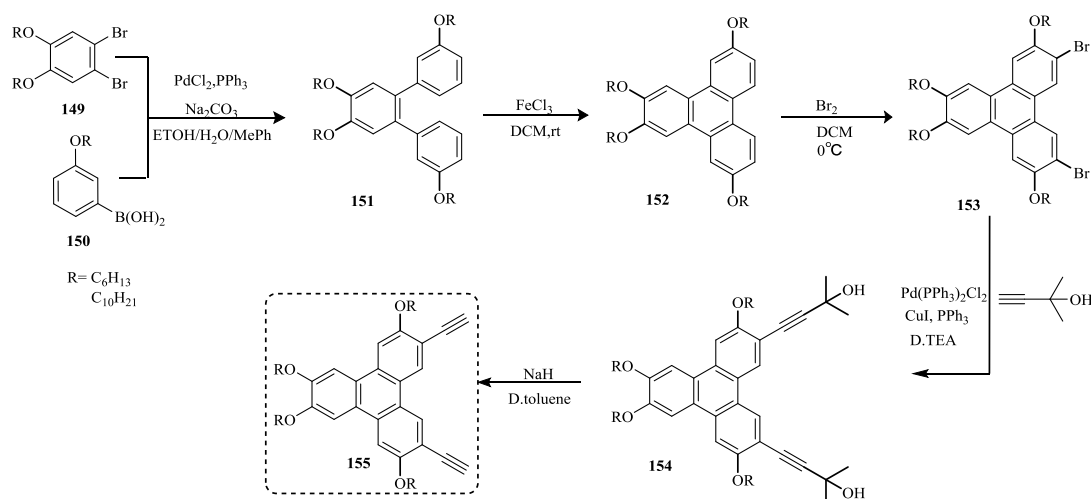


Figure 2.45: $^1\text{H-NMR}$ aromatic regions of compound **147**.

2.4.4. Synthesis of tetra (alkoxy)-diacetylene triphenylene

Another substitution was then attempted, synthesising the diacetylene triphenylene core with the four alkoxy chains. Diacetylene triphenylene is the key precursor to dibenzonitrile triphenylene. The full synthesis is shown in Scheme **2.33**. For the synthesis of the triphenylene moiety followed the procedure the first developed by our group in 2001. The starting point for the synthesis was 3-Bromophenol and catechol, which are relatively inexpensive and easy to use. Catechol, 1-bromohexane and potassium carbonate were mixed in ethanol at refluxing temperature. This produced diether. Bromination can be used at this point to give 1, 2-dibromo-4, 5-bisalkoxybenzene **149** ($\text{R}=\text{C}_6\text{H}_{13}$, $\text{C}_{10}\text{H}_{21}$). However, for the current research this step was not necessary as there were adequate supplies of compounds **150**. Compounds **150** were also available. Had it been necessary to synthesise it, this would have been done by means of alkylation of 3-bromophenol following the same conditions and yielding the compound. 3-hexyloxyphenol would have been purified by vacuum distillation, then reacted with magnesium turnings to form the Grignard reagent which would have been reacted with trimethylborate to produce the boronic acid **150**. A Suzuki-Miyaura cross coupling reaction was conducted between **149** and **150**. This produced 1, 2-bisalkoxy-4, 5-bis (3-dialkoxyphenyl) benzene **151**. Later, the cyclisation was carried out by using ferric chloride to induce oxidative ring closure of terphenyl **151** and obtain the corresponding triphenylene **152**.



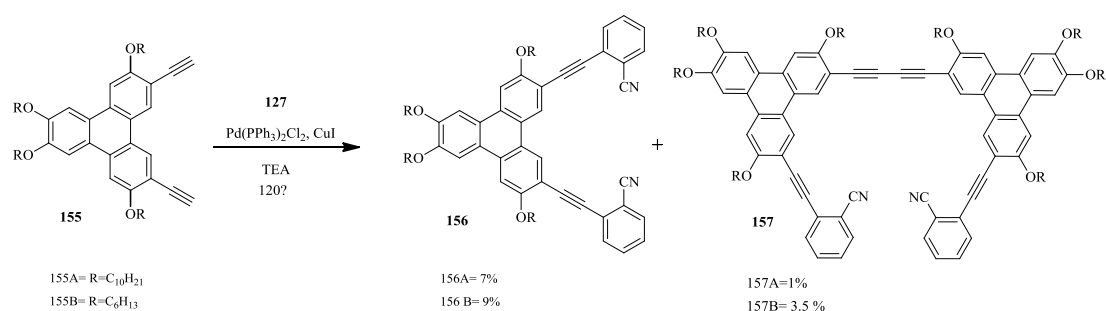
Scheme 2.33: Synthesis of diacetylene-triphenylene **155**.

A further bromination produced 3, 6- dibromo-2, 7, 10, 11-tetrakis (alkoxy) triphenylene **153**. At this point a Sonogashira cross-coupling reaction was applied to introduce the alkyne terminal then deprotect it, as mentioned earlier.

The next step used diacetylene triphenylene with four decyloxy chains, which was already available in the laboratory because it had been produced earlier by our group. The same procedure was used as in the previous step. However, the homo-coupling product was less on this occasion.

2.4.5. Synthesis of 3, 6, 7, 10-tetrakis (alkoxy)-2, 11-ethynl-(bis (2-benzonitrile)) triphenylene **156**

The earlier procedure was followed for reacting bromobenzonitrile with the diacetylene triphenylene, but this time with four decyloxy chains, which was already available in the laboratory because it had been produced earlier by our group. The reaction was starting by using the same equivalent of bromobenzonitrile and the Sonogashira method was used as mentioned earlier (Scheme **2.34**). The reaction was monitored by TLC and three new spots had appeared. After the work up for the reaction, there was a bright yellow precipitate. This was filtered to isolate it. The NMR revealed that this was the homocoupling product. The crude was still a mixture of two components. The column chromatography did not prove helpful because the spots were too close together. Recrystallisation was then attempted, using a different solvent but, on each occasion, the two compounds came out as a mixture.



Scheme 2.34: Synthesis of compound **156**.

Eventually, when the NMR was conducted using acetone, it showed that the material was partly dissolved and gave a clear NMR value for the target compound. Later, Recrystallisation from the acetone was carried out. The light brown crystal growth corresponded to the new structure, with homo-coupling product from one of the acetylene terminals. The pure material was produced as a bright yellow solid. However, this was a time-consuming process because it was difficult to find the right crystallisation system after the column chromatography. Another reaction using diacetylene triphenylene with four hexyloxy chains was applied in the same previous reaction with some changes to improve the yield of the target. The quantity of bromo-benzonitrile was increased to 4 equivalents to avoid the formation of the other product with the homo-coupling at the top. However, the homo-coupling product was more on this occasion.

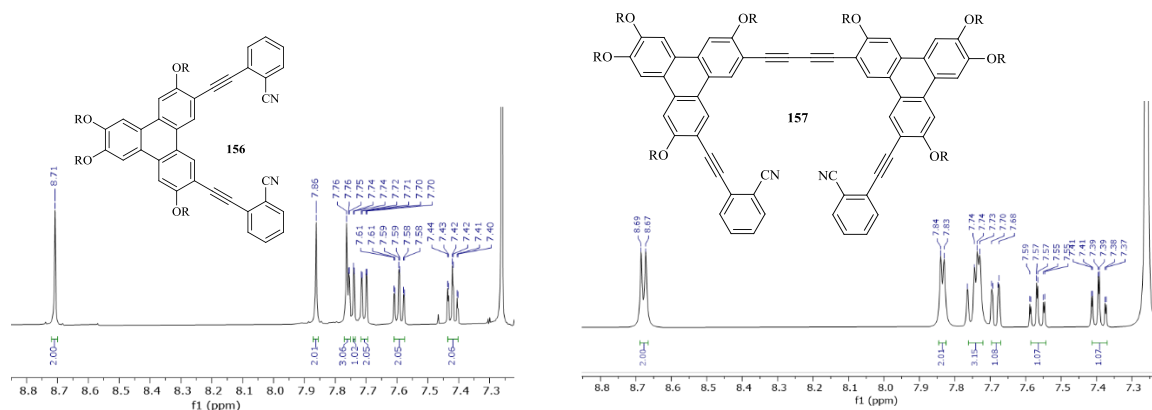


Figure 2.46: Comparison of the aromatic region of $^1\text{H-NMR}$ of compounds **156A** and **157A** respectively.

In the $^1\text{H-NMR}$ spectrum three aromatic proton signals were present, indicating the triphenylene protons, also the substituted phenyl protons. However, a closer look for the number of protons of compound **157A** indicate to one phenyl coupled to the triphenylene unit without any appearance of terminal proton at 3.37 ppm. The suggested diad structure was confirmed by Mass spectroscopy.

2.4.6. Characterisation of liquid crystal properties

This new structure was solid at room temperature and showed columnar mesophase behaviour, which was observed under a polarising optical microscope. The transition temperature from solid crystal to liquid crystal behaviour for **156A** at 52°C , the isotropation occurred at 140°C . In compound **156B**, the melting temperature is 95°C to displayed mesophase state before changing to clear liquid at 209°C (Figure 2.47).

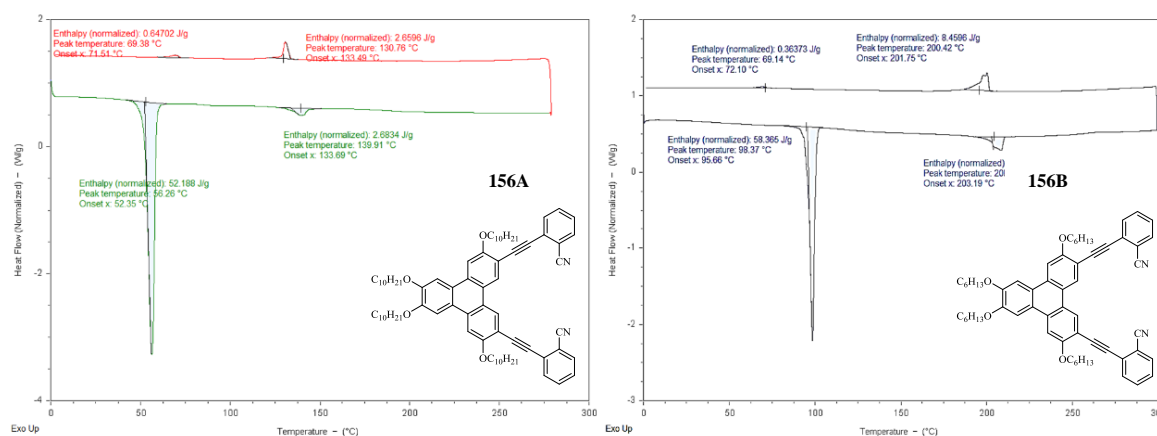
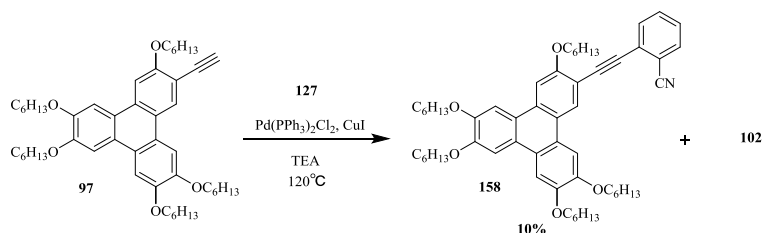


Figure 2.47: DSC thermograph of compounds **156A**, **156B**.

2.4.7. Synthesis of compound 158

The same condition and the same procedure were used to yield mono-benzonitrile triphenylene. The mono-acetylene triphenylene that had already been prepared in the first series was used as the starting material. The reaction was monitored by TLC which showed two main spots which did not correspond to the precursor. It was expected that some self-coupling product would form alongside with the target

product. However, in practice, after crystallisation, it was found that the homocoupling structure was the major product.



Scheme 2.35: Synthesis of compound **158**.

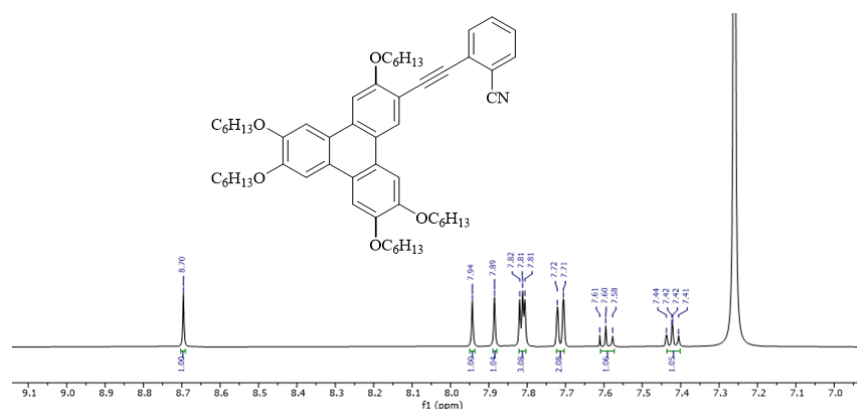


Figure 2.48: $^1\text{H-NMR}$ spectra for aromatic regions of compound **158**.

The $^1\text{H-NMR}$ -data of benzonitrile-triphenylene **158** was simple to analyse. The spectrum significantly confirms the structure giving six aromatic singlets for the triphenylene protons overlapping with, four peaks for the benzene protons. MALDI spectra exhibited the target compound as well as isotopes pattern was matched. However, the liquid crystal analysis was hard due to the solubility of the compound, trying another crystallisations system is the selected option.

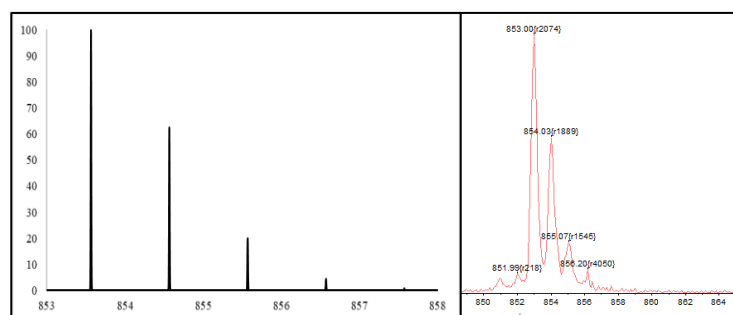
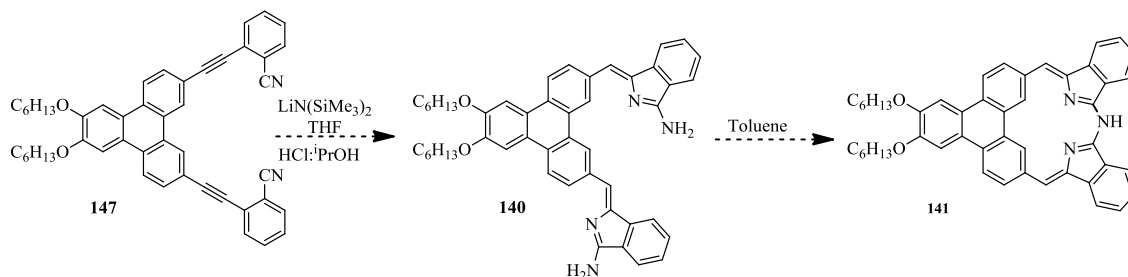


Figure 2.49: MALDI-TOF desired structure **158** with isotopes pattern.

2.5. Future work

The other schemes that have been proposed but were not able to complete it include:

- Synthesis and cyclisation of the diaminoisindolene **140** (scheme 2.36).



Scheme 2.36: Proposed synthesis of compound **140**

- Additionally, further analyses are pending because of insufficient yield for an earlier new compounds such as symmetrical diads **157** and molecule **158**.

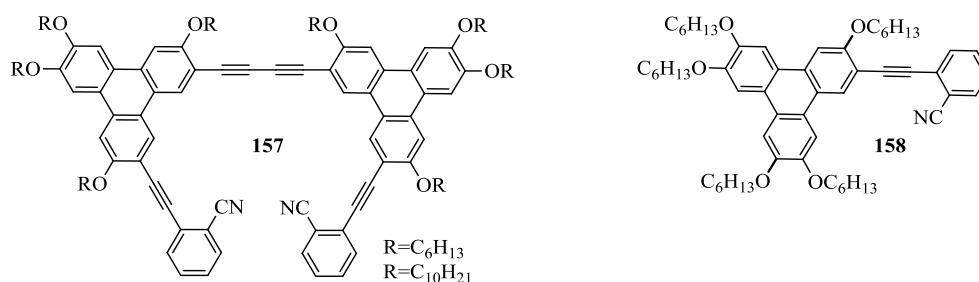


Figure 2.50: The structure of compounds **157** and **158**.

2.6. Conclusion

The project had started with a diad as the target compound to investigate its liquid crystal properties. Previous work involving a twin with two terminal alkynes, required a two-step process. In our case, one step reaction was required because it has one terminal on each side. The method was to link the alkyne with the diiodobenzene in different positions (meta, para and ortho). However, the monoacetylene is quite reactive and had a tendency towards the homo-coupling structure, which has been reported previously, and purification was problematic. The investigation showed the target nematic behaviour in the structure of 1, 3-phenylene bridged triphenylene **93** and in the last diad in the series with 2, -thiophene bridge. In addition, the precursors **101** for meta diad and **109** for ortho diad displayed only columnar behaviour.

As expected, our yield was higher than in the case of the twin, partly because it involved only a single step and the Sonogashira coupling is a good reaction method to follow. The triad also proved difficult to synthesise at this stage, so it was decided to stop the series at this point and focus on using another functional group with the triphenylene structure to synthesise liquid crystal structures. A number of routes could be investigated from this point. Our attention had been turned for the next stage to investigate the use of BODIPY to synthesise triphenylene-BODIPY hybrids. It was synthesised from monoacetylene triphenylene with amidine. Then another diad series was synthesised linked by azadipyrromethene molecules that bear triphenylene aminoisindolene with itself and with another aminoisindolene such as (pyrenyl-aminoisindolene, 4-methoxyphenyl aminoisindolene and 4-hexyloxyphenyl aminoisindolene). All diads in this collection have no liquid crystals properties and spectroscopy revealed an unexpected helical structure in these molecules.

The later work aimed to incorporate antiaromatic structures with additional functional units into discotic mesophases. Such amidine structure had been employed by our group in the past and was therefore used in the current work. To this point, an attempt was made to couple amidine with diacetylene triphenylene to form the target product, but the plan was changed, and the first product was an intermediate dibenzonitrile triphenylene which displays liquid crystal properties. The planned synthesis route was changed to focus on

the synthesis and characterisation of the symmetrical disubstituted dibenzonitrile triphenylene and derivatives were completed. Both **156A** and **156B** have showed columnar mesophase. However, the quantity of the homocoupling products inadequate to complete the full investigation. The goal of this series was to synthesise diaminoisindolene in a triphenylene core and potential mesophase behaviour could be observed.

Chapter 3

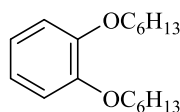
Experimental

3.1. General Information

Solvents and reagents were obtained from commercial supplies. Unless otherwise stated no further purification was carried out. Dichloromethane (DCM), triethylamine (TEA) and toluene (MePh) were all dried using MgSO₄. Aluminium sheets coated with Silica gel/UV254 (Macherey-Nagel) were used for the thin layer chromatography (TLC) and UV light was used for visualization. A Büchi rotary evaporator was used to evaporate the solvents and the process was carried out at reduced pressure. A Bruker 500 recorded the NMR spectra (for ¹H NMR 500 MHz was used, while for ¹³C NMR, 126 MHz was used). The residual solvent peak was used as reference. This was carried out at room temperature. The signals for both ¹H and ¹³C NMR are given as ppm, while coupling constants J are reported in Hertz. A Perkin-Elmer Spectrum 100 FT-IR spectrometer was used to record the IR spectra. Absorption bands are shown in cm⁻¹. A Shimadzu Biotech Axima spectrometer was used to record the MALDI-TOF analyses. A Reichert Thermovar microscope containing a thermopar based temperature control was used to measure melting points. UV-vis spectra were measured in the stated solvents using a Perkin Elmer Lambda 35 UV/VIS. Silica gel Material Harvest 40-63 micron was used for column chromatography. Polarizing Optical microscope (POM) was used to identify the mesophases and phase transition of liquid crystal compound. Differential Scanning Calorimetry (DSC) analyses were recorded on DSC 2500 device from TA instruments.

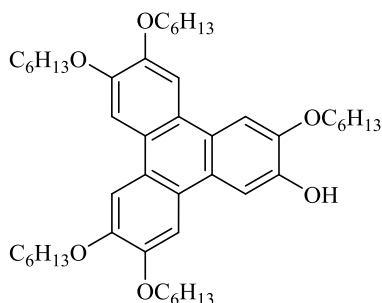
3.2. Synthetic procedures and characterization data:

3.2.1. 1,2-Dihexyloxybenzene 55



Catechol (26 g, 0.24 mol), 1-iodohexane (21 g, 15 mol) and potassium carbonate (79 g, 0.57 mol) were stirred in ethanol (250 ml) under nitrogen. The reaction mixture was heated at reflux for 36 hours. On completion the mixture was filtered under suction and washed with dichloromethane. The filtrate was collected, and the solvent removed in vacuo. The crude product was distilled, collecting the fraction giving the pure product as a clear yellow oil (39 g, 60%). ¹H-NMR (500 MHz, CDCl₃) δ 6.91 (s, 4H), 4.01 (t, J = 6.63 Hz, 4H), 1.7-1.81 (m, 4H), 1.53-1.48 (m, 4H), 1.39-1.37 (m, 8H), 0.95-0.92 (m, 6H) ppm.

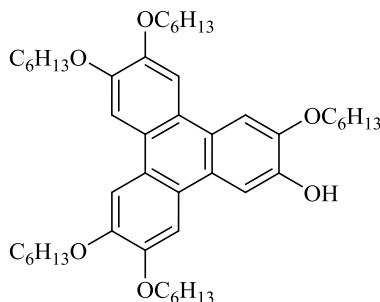
3.2.2. Synthesis of 2-hydroxy- 3, 6, 7, 10, 11- penta-hexyloxy-triphenylene^[95] 94



To a stirred solution of DHB (4 g, 14.4 mmol, 1 eq) in CH_2Cl_2 (70 ml) was added anhydrous FeCl_3 (7 g, 43mmol, 3 eq) at 0 °C. After 1 hour, another portion of FeCl_3 (5 g, 29 mmol, 2eq) was added, and the reaction mixture was stirred for 2.5 h. The reaction was quenched by the addition of CH_3OH (50 ml) and water (200 ml). The aqueous phase was further extracted with DCM (3 x 15 ml), and the combined organic layers were washed with water (50 ml), dried with anhydrous MgSO_4 and filtered. The solvent was removed under reduced pressure. Purification by column chromatography on silica gel (petroleum ether/EtOAc, 1:80) gave MHT product (1.90 g, 18 %) as a pale purple solid. $^1\text{H NMR}$ (500 MHz, CDCl_3) δ 7.96 (s, 1H), 7.83 (s, 3H), 7.82 (s, 1H), 7.77 (s, 1H), 5.90 (s, 1H), 4.31 – 4.19 (m, 10H), 1.96 – 1.90 (m, 10H), 1.54 – 1.55 (m, 10H), 1.40 – 1.38 (m, 20H), 0.97-0.90 (m, 15H) ppm.

$^{13}\text{C NMR}$ (126 MHz, CDCl_3): δ = 149.2, 149.1, 148.9, 148.8, 145.9, 145.3, 124.0, 123.8, 123.7, 123.6, 123.3, 123.0, 107.7, 107.5, 107.4, 106.6, 104.4, 70.0, 69.9, 69.7, 69.2, 31.7, 31.6, 29.5, 29.4, 29.3, 25.9, 25.8, 22.7, 22.6, 14.1 ppm.

3.2.3. Synthesis of 2-hydroxy- 3, 6, 7, 10, 11- penta-hexyloxy-triphenylene^[81] 94

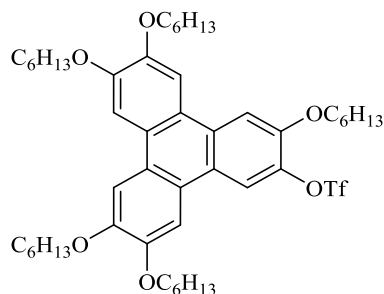


Anhydrous FeCl_3 (3.4g, 21 mmol, 10.50 eq) was dissolved in a mixture of DCM (20 ml) and nitromethane (MeNO_2) (2 ml). The mixture of solution of DHB (1.11 g, 4 mmol, 2 eq) and 2-hexyloxy phenol (0.4 g, 2 mmol, 1eq) was dissolved in CH_2Cl_2 (15ml) then added to the reaction mixture at 0°C , dropwise over 30 min. The reaction mixture was stirred for 2.5 h. The reaction was quenched by the addition of CH_3OH (50 ml) and water (200 ml). The aqueous phase was further extracted with DCM (3 x 15 ml), and the combined organic layers were washed with water (50 ml), dried with anhydrous MgSO_4 and filtered. The solvent was removed under reduced pressure. Purification by column chromatography on silica gel (petroleum ether/ EtOAc , 1:30) gave the title product as a white solid (0.5 g, 34 %).

$^1\text{H NMR}$ (500 MHz, CDCl_3) δ 7.96 (s, 1H), 7.83 (s, 3H), 7.82 (s, 1H), 7.77 (s, 1H), 5.90 (s, 1H), 4.31 – 4.19 (m, 10H), 1.96 – 1.90 (m, 10H), 1.54 – 1.55 (m, 10H), 1.40 – 1.38 (m, 20H), 0.97-0.90 (m, 15H) ppm.

$^{13}\text{C NMR}$ (126 MHz, CDCl_3): δ = 149.2, 149.1, 148.9, 148.8, 145.9, 145.3, 124.0, 123.8, 123.7, 123.6, 123.3, 123.0, 107.7, 107.5, 107.4, 106.6, 104.4, 70.0, 69.9, 69.7, 69.2, 31.7, 31.6, 29.5, 29.4, 29.3, 25.9, 25.8, 22.7, 22.6, 14.1 ppm.

3.2.4. Synthesis of 2-trifluoromethylsulfonyl - 3, 6, 7, 10, 11-penta-hexyloxy-triphenylene^[82] **95**

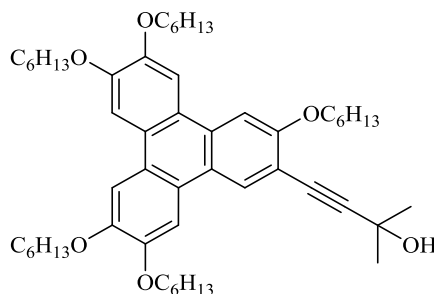


According to the procedure our group to a stirred solution of compound **94** (0.9 g, 1.2 mmol, 1 eq) and pyridine (0.7 ml, 9 mmol, 7.5 eq) in dry DCM (75 ml) was added dropwise trifluoromethanesulfonic anhydride (1.5 ml, 9 mmol, 7.5 eq) at $-20\text{ }^{\circ}\text{C}$ for 30 min under nitrogen. The resulting mixture was allowed to warm at room temperature overnight. Dilute hydrochloric acid (150 ml) was added and the mixture was extracted with DCM (3x15 ml). The solvent was evaporated in vacuo and the obtained product was purified by column chromatography (eluting with petroleum ether/DCM, 4:1) and recrystallized from DCM and EtOH to give the title product as an off-white solid (1 g, 94 %).

¹H NMR (500 MHz, CDCl_3) δ 8.21 (s, 1H), 7.90 (s, 1H), 7.83 (s, 1H), 7.81 (s, 1H), 7.80 (s, 1H), 7.73 (s, 1H), 4.26 – 4.20 (m, 10H), 1.95 – 1.91 (m, 10H), 1.62 – 1.52 (m, 10H), 1.43 – 1.38 (m, 20H), 0.95 - 0.91 (m, 15H) ppm.

¹³C NMR (126 MHz, CDCl_3): δ = 150.2, 149.4, 148.8, 148.7, 138.1, 129.4, 125.1, 123.3, 123.0, 122.7, 122.1, 120.1, 117.6, 116.4, 107.8, 107.1, 106.4, 106.3, 69.8, 69.7, 69.3, 69.2, 31.7, 31.6, 29.4, 29.3, 29.1, 25.9, 25.6, 22.7, 22.6, 14.0 ppm.

3.2.5. Synthesis of 2- (3-methyl-3-hydroxybutynyl)- 3, 6, 7, 10, 11- penta- hexyloxy-triphenylene^{[82], [96]} **96**

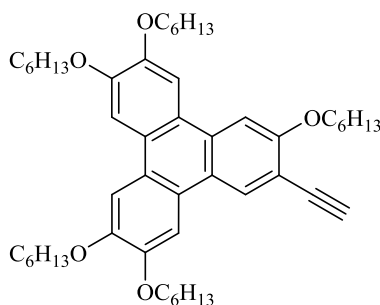


Following a literature procedure using Sonogashira cross-coupling method, 2-trifluoromethylsulfonyl - 3, 6, 7, 10, 11- penta-hexyloxy-triphenylene **95** (2.4 g, 2.7 mmol, 1eq), CuI (0.04g, 0.2 mmol, 0.07 eq), Pd(PPh₃)₂Cl₂ (0.11 g, 0.16 mmol, 0.06 eq) and PPh₃(0.085 g, 0.33 mmol, 0.12eq) were stirred in refluxing freshly distilled triethylamine (50 ml) for 15 min under nitrogen. 2-Methyl-but-3-yn-2-ol (1.4g, 16.3 mmol, 6 eq) was added slowly to the mixture by syringe pump. The resulting solution was refluxed for a further 24 h. After the reaction was completed, the solution was worked up by addition of water and then was further extracted with DCM (3x100 ml). The solvent was evaporated in *vacuo*, to give a crude product, which was subjected to column chromatography over silica gel using (EtOAc/petroleum ether,1:4) to give the desired compound that was recrystallized from DCM/MeOH (1:1) to obtain the compound (1.5 g, 70 %) as an off-white solid.

¹H NMR (500 MHz, CDCl₃) δ 8.47 (s, 1H), 7.86 (s, 1H), 7.85 (s, 1H), 7.80 (s, 1H), 7.79 (s, 1H), 7.73 (s, 1H), 4.26 – 4.21 (m, 10H), 1.96 – 1.93 (m, 10H), 1.72 (s, 6H), 1.60 – 1.55 (m, 10H), 1.42– 1.40(m, 20H), 0.95- 0.93 (m, 15H) ppm.

¹³C NMR (126 MHz, CDCl₃): δ = 157.9, 150.4,149.7, 149.2, 149.1,130.6, 128.7, 125.6, 123.7, 123.2, 123.1, 122.9, 112.1, 108.3, 107.7, 107.1, 106.7, 104.7, 98.2, 70.1, 69.8, 69.6, 66.1, 66.2, 32.0, 31.9, 31.8, 29.7, 26.1, 22.9, 14.3 ppm.

3.2.6. Synthesis of 2- ethynyl- 3, 6, 7, 10, 11- penta-hexyloxy- triphenylene^[96] 97

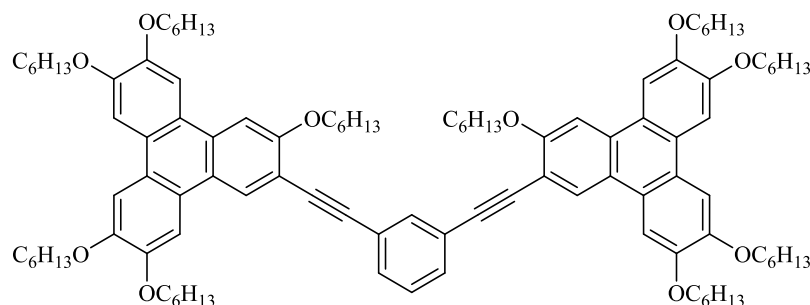


In a 50 ml round bottom flask, the 2-(3-methyl-3-hydroxybutynyl) - 3, 6, 7, 10, 11- penta-hexyloxy-triphenylene (2.60 g, 3.20 mmol, 1 eq) was refluxed in dry toluene (50 ml) under nitrogen. Then, NaH (60% dispersion in oil) (0.93 g, 9.6 mmol, 3 eq) was added in small portion and the mixture was heated at reflux for 4 h. After completion (monitored by TLC), the mixture was poured onto ice-cold water, and extracted with DCM. The combined organic extracts were concentrated under reduced pressure. Purification by column chromatography on silica gel (pet ether/EtOAc, 1:9) gave the product (2.1 g, 86 %) as a pale-yellow solid; m.p. 140 °C.

¹H NMR (500 MHz, CDCl₃) δ 8.56 (s, 1H), 7.86 (s, 1H), 7.85 (s, 1H), 7.80 (s, 1H), 7.79 (s, 1H), 7.76 (s, 1H), 4.25 – 4.21 (m, 10H), 3.40 (s, 1H), 1.97 – 1.94 (m, 10H), 1.64 – 1.55 (m, 10H), 1.44 – 1.39 (m, 20H), 0.95- 0.92 (m, 15H).

¹³C NMR (126 MHz, CDCl₃): δ = 158.1, 150.5, 149.8, 149.2, 148.8, 139.7, 129.5, 124.3, 123.5, 123.2, 123.0, 122.9, 112.1, 108.3, 107.7, 107.1, 106.5, 104.9, 103.7, 82.3, 81.4, 70.1, 69.8, 69.5, 69.4, 33.0, 32.2, 32.0, 31.8, 30.8, 30.0, 29.7, 29.6, 26.1, 23.0, 22.9, 14.4, 14.3 ppm.

3.2.7. 1, 3-phenylene bridged triphenylene **93**



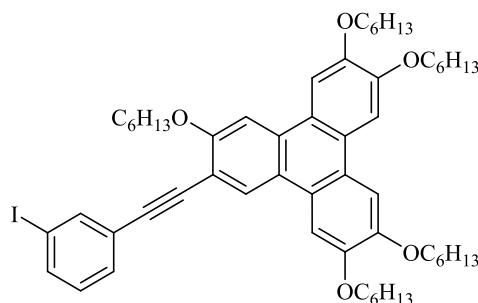
In a 100 ml 2-neck round bottom flask, Pd (PPh₃)₂Cl₂ (0.007 g, 0.0099 mmol, 0.06 eq.), CuI (0.0022 g, 0.011 mmol, 0.07 eq.) and PPh₃ (0.0052 g, 0.0199 mmol, 0.12 eq.) with 1, 3-diiodobenzene (0.055 g, 0.166 mmol, 1 eq.) were stirred in freshly distilled triethylamine (40 ml) under nitrogen. 2-ethynyl- 3,6,7,10,11-Penta-hexyloxy triphenylene (0.275 g, 0.365 mmol, 2.2 eq.) was dissolved in dry TEA (10ml) and added slowly by syringe pump at 0.5 ml per hour to the above mixture. The resulting solution was refluxed overnight. The reaction was worked up by addition of water and then extracted with DCM (3x100 ml), dried over anhydrous MgSO₄ and the solvent was evaporated under reduced pressure, to give a crude product which was purified using column chromatography on silica gel with the system DCM: PE (1:3) to give a solid which was recrystallized from DCM/EtOH (1:1) to obtain compound **93** (0.0754 g, 29 %) as a pale-yellow solid.

Transition temperatures Cr 87 Col 143 N_D152 I. **MS** (MALDI-TOF): m/z = 1578. [M⁺] (100%). **IR** (thin film, cm⁻¹): 2926, 2855, 2210, 1510, 1260, 1240, 1025, 1049, (725-820). **UV-Vis** (CH₂Cl₂) λ_{max}/nm (ε/dm³.mol⁻¹.cm⁻¹): 204 (2.1 × 10⁵), 261 (6 × 10⁵), 297 (6.8 × 10⁵), 361 (4.5 × 10⁵).

¹H NMR (500 MHz, CDCl₃) δ 8.60 (s, 2H), 7.93 (s, 2H), 7.89 (m, 3H), 7.82 (m, 6H), 7.61 (dd, J = 7.7, 1.6 Hz, 2H), 7.41 (t, J = 7.7 Hz, 1H), 4.32 (t, J = 6.4 Hz, 4H), 4.25 (m, 16H), 2.04 – 1.90 (m, 20H), 1.72 – 1.50 (m, 20H), 1.49 – 1.36 (m, 40H), 0.96 – 0.81 (m, 30H).

¹³C NMR (126 MHz, CDCl₃) δ 157.79, 150.34, 149.64, 149.09, 148.99, 131.43, 130.63, 125.49, 124.30, 123.58, 123.16, 123.02, 112.46, 108.16, 107.01, 104.87, 92.99, 87.34, 77.16, 70.02, 69.64, 69.42, 69.32, 31.89, 31.84, 31.83, 29.59, 29.57, 29.53, 26.10, 26.00, 22.88, 22.81, 14.22, 14.20.

3.2.8. 2- (3-iodophenyl) ethynyl-3, 6, 7, 10, 11-Penta-hexyloxy-triphenylene **101**

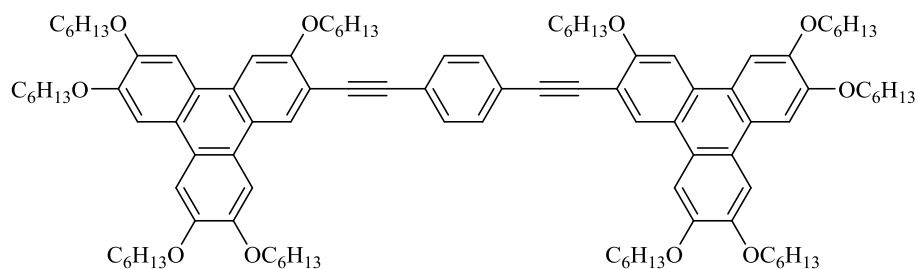


The above compound was also isolated from the previous reaction as a side-product **101** (0.020 g, 13%); **Transition temperatures** Cr 75 Col 185 I. **MS** (MALDI-TOF): $m/z = 828 [M^-]$ (100%). **IR** (thin film, cm^{-1}): 2934, 2861, 2216, 725. **UV-Vis** (CH_2Cl_2) $\lambda_{\text{max}}/\text{nm}$ ($\epsilon/\text{dm}^3 \cdot \text{mol}^{-1} \cdot \text{cm}^{-1}$): 268 (6.2×10^4), 297 (10×10^4), 361 (2.6×10^4).

^1H NMR (500 MHz, CDCl_3) δ 8.55 (s, 1H), 7.99 (t, $J = 1.6$ Hz, 1H), 7.89 (m, 2H), 7.80 (m, 3H), 7.68 (ddd, $J = 8.0, 1.7, 1.1$ Hz, 1H), 7.61 – 7.53 (m, 1H), 7.12 (t, $J = 7.8$ Hz, 1H), 4.34 – 4.19 (m, 10H), 2.03 – 1.88 (m, 10H), 1.70 – 1.52 (m, 10H), 1.50 – 1.36 (m, 20H), 0.94 (m, 15H).

^{13}C NMR (126 MHz, CDCl_3) δ 157.78, 153.81, 149.66, 147.68, 140.31, 131.78, 130.80, 130.63, 130.00, 115.22, 112.12, 111.00, 106.52, 97.63, 93.87, 89.43, 77.41, 77.16, 76.91, 71.61, 70.04, 69.47, 69.35, 69.28, 31.88, 31.84, 29.59, 29.52, 26.12, 26.00, 22.89, 22.81, 14.26, 14.20.

3.2.9. 1, 4-phenylene bridged diad 103

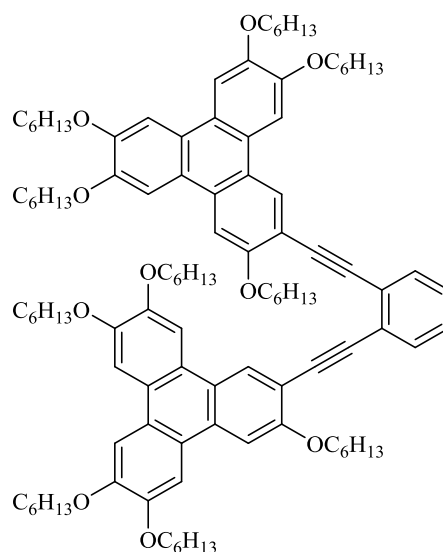


In a 100 ml 2-neck round bottom flask, Pd(PPh₃)₂Cl₂ (0.0046 g, 0.0066 mmol, 0.06 eq.), CuI (0.0015 g, 0.0077 mmol, 0.07 eq.) and PPh₃ (0.0035 g, 0.01328 mmol, 0.12 eq.) with 1,4-diiodobenzene (0.0365 g, 0.11 mmol, 1 equiv.) were stirred in freshly distilled triethylamine (20 ml) under nitrogen. 2-ethynyl-3,6,7,10,11-Penta-hexyloxy triphenylene (0.250 g, 0.332 mmol, 3 eq.) was dissolved in dry TEA (10 ml) and added slowly by syringe pump at 0.5 ml per hour to the above mixture. The resulting solution was refluxed overnight. The reaction was worked up by addition of water and then extracted with DCM (3x100 ml), dried over anhydrous MgSO₄ and filtered. Then the solvent was evaporated under reduced pressure, to give a crude product, which was purified using column chromatography on silica gel with the system DCM: PE (1:3) to give the desired product which was recrystallized from DCM/EtOH (1:1) to obtain compound **103** (0.045 g, 26%) as a yellow solid; **Transition temperatures** Cr 98 Cr 237 Col 247 I. **MS** (MALDI-TOF): m/z = 1578 [M⁺] (100%). **IR** (thin film, cm⁻¹): 2955, 2932, 2861, 2214, 1736, 1615, 1516, 1263, 1174, 1046, 836. **UV-Vis** (DCM) λ_{max}/nm (ε/dm³.mol⁻¹.cm⁻¹): 207 (2.2 × 10⁵), 219 (1.9 × 10⁵), 284 (9 × 10⁵), 377 (5.7 × 10⁵).

¹H NMR (500 MHz, CDCl₃) δ 8.60 (s, 2H), 7.93 (s, 2H), 7.89 (s, 2H), 7.82 (d, *J* = 4.4 Hz, 6H), 7.64 (s, 4H), 4.32 (t, *J* = 6.4 Hz, 4H), 4.28 – 4.21 (m, 16H), 2.05 – 1.91 (m, 20H), 1.65 – 1.51 (m, 20H), 1.49 – 1.37 (m, 40H), 0.98 – 0.92 (m, 30H).

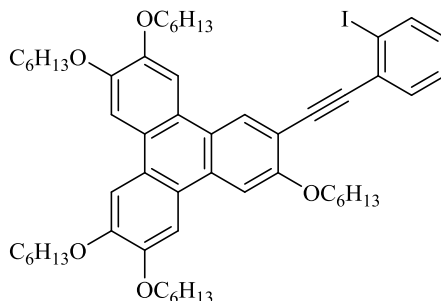
¹³C NMR (126 MHz, CDCl₃) δ 157.74, 150.34, 149.62, 149.10, 148.99, 131.68, 130.66, 128.46, 125.50, 123.56, 123.16, 123.00, 122.95, 112.42, 108.15, 106.99, 106.53, 104.79, 93.67, 88.77, 77.16, 70.03, 69.63, 69.47, 69.27, 31.89, 31.85, 31.83, 29.59, 29.56, 29.53, 29.51, 26.08, 26.00, 22.86, 22.81, 14.23, 14.20.

3.2.10. 1, 2- Phenylene bridged diad 108



In a 100 ml 2-neck round bottom flask, Pd (PPh₃)₂Cl₂ (0.0050 g, 0.0072 mmol, 0.06 eq.), CuI (0.00161 g, 0.00845 mmol, 0.07 eq.) and PPh₃ (0.0038 g, 0.0145 mmol, 0.12 eq.) with 1,2-diiodobenzene (0.039 g, 0.121 mmol, 1 eq.) were stirred in freshly distilled triethylamine (40 ml) under nitrogen. 2-ethynyl -3,6,7,10,11-Penta-hexyloxy triphenylene (0.20 g, 0.26 mmol, 2.2 eq.) was dissolved in dry TEA (10ml) and added slowly by syringe pump at 0.25 ml per hour to the above mixture. The resulting solution was refluxed overnight. The reaction was worked up by addition of water and then extracted with DCM (3x100 ml), dried with anhydrous MgSO₄ and the solvent was evaporated under reduced pressure, to give a crude product which was purified using column chromatography on silica gel with the system DCM: PE (1:3) to give a solid which was recrystallized from DCM/EtOH (1:1) to obtain compound **108** (0.1 g, 53%). **Mp.** 77 °C. **MS** (MALDI-TOF): m/z = 1578 [M⁺] (100%). **IR** (Thin film, cm⁻¹): 2954, 2926, 2855, 2204, 1608, 1508, 1258, 1165, 1031, 720, 758. **UV-Vis** (DCM) λ_{max}/nm (ε/dm³.mol⁻¹.cm⁻¹): 264 (2.5 × 10⁵), 290 (3.6 × 10⁵), 339 (1.1 × 10⁵), 361 (4.5 × 10⁵). **¹H NMR** (500 MHz, CDCl₃) δ 8.70 (s, 2H), 7.83 (s, 2H), 7.76 (d, J = 9.7 Hz, 4H), 7.70 – 7.67 (m, 4H), 7.50 (s, 2H), 7.38 – 7.33 (m, 2H), 4.27 – 4.17 (m, 12H), 4.00 (t, J = 6.6 Hz, 4H), 3.39 (t, J = 6.6 Hz, 4H), 2.00 – 1.90 (m, 10H), 1.88 – 1.78 (m, 10H), 1.62 – 1.55 (m, 20H), 1.52 – 1.46 (m, 8H), 1.45 – 1.34 (m, 32H), 0.96 – 0.91 (m, 20H), 0.86 – 0.79 (m, 10H). **¹³C NMR** (126 MHz, CDCl₃) δ 157.74, 150.30, 149.64, 148.88, 148.70, 131.93, 130.70, 128.91, 126.46, 125.61, 123.64, 123.17, 122.86, 122.79, 112.89, 108.27, 105.68, 104.92, 93.01, 91.32, 77.16, 70.33, 69.95, 69.58, 69.46, 68.57, 31.88, 31.86, 31.84, 31.07, 29.72, 29.61, 29.55, 29.43, 29.23, 26.02, 25.97, 25.95, 25.65, 22.81, 22.77, 22.72, 14.19.

3.2.11. (2-iodophenyl) ethynyl-3, 6, 7, 10, 11-Penta-hexyloxy-triphenylene 109

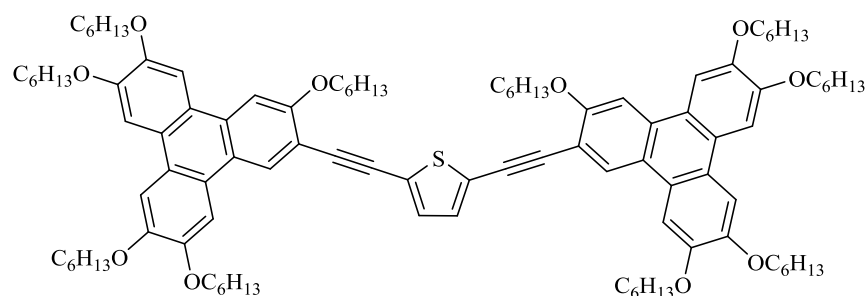


The above compound was also isolated from the previous reaction as a minor product as a brown solid (0.030 g, 26%); **Transition temperatures.** Cr 49 Col 171 I. **MS** (MALDI-TOF): $m/z = 827[M^{-1}]$ (100%). **UV-Vis** (CH_2Cl_2) $\lambda_{\text{max}}/\text{nm}$ ($\epsilon/\text{dm}^3 \cdot \text{mol}^{-1} \cdot \text{cm}^{-1}$): 265 (7×10^4), 293 (9.5×10^4), 355 (2.8×10^4). **IR** (thin film, cm^{-1}): 2939, 2934, 2856, 2213, 1044, 755.

$^1\text{H NMR}$ (500 MHz, Chloroform-*d*) δ 8.64 (s, 1H), 7.94 – 7.90 (m, 2H), 7.88 (s, 1H), 7.82 (d, $J = 2.4$ Hz, 2H), 7.80 (s, 1H), 7.64 (dd, $J = 7.7, 1.7$ Hz, 1H), 7.37 (td, $J = 7.6, 1.2$ Hz, 1H), 7.03 (td, $J = 7.7, 1.6$ Hz, 1H), 4.31 (t, $J = 6.5$ Hz, 2H), 4.27 – 4.21 (m, 8H), 2.03 – 1.91 (m, 10H), 1.70 – 1.55 (m, 10H), 1.45 – 1.34 (m, 20H), 0.96 – 0.89 (m, 15H).

$^{13}\text{C NMR}$ (126 MHz, CDCl_3) δ 157.77, 149.58, 149.01, 138.95, 132.90, 129.34, 128.94, 127.94, 123.04, 108.24, 108.04, 107.59, 107.12, 107.04, 105.15, 104.81, 103.30, 100.83, 77.16, 70.05, 69.65, 69.51, 69.40, 31.84, 31.83, 29.59, 26.00, 22.85, 22.81, 14.20.

3.2.12. 2, 5-thiophene bridged diad 113



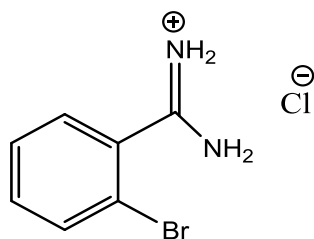
In a 100 ml 2-neck round bottom flask, Pd (PPh₃)₂Cl₂ (0.0103g, 0.0148 mmol, 0.06 eq.), CuI (0.0032g, 0.017 mmol, 0.07eq.) and PPh₃ (0.0078g, 0.029 mmol, 0.12eq.) with 2, 5-diiodothiophene (0.08g, 0.24 mmol, 1 eq) were stirred in freshly distilled triethylamine (40 ml) under nitrogen. 2-ethynyl-3,6,7,10,11-Penta-hexyloxy triphenylene (0.41g, 0.543 mmol, 2.2 eq.) was dissolved in dry TEA (10ml) and added slowly by syringe pump at 0.25 ml per hour to the above mixture. The resulting solution was refluxed overnight. The solution was worked up by addition of water and then extracted with DCM (3x100 ml), dried with anhydrous MgSO₄, and the solvent was evaporated under reduced pressure, to give a crude product, which was purified using column chromatography on silica gel with the system DCM: PE (1:3) to give the product which was recrystallized from DCM/EtOH (1:1) to obtain compound **113** (0.056 g, 14%) as a fluorescent solid;

Transition temperature Cr118 Col 200 N 212 I. **MS** (MALDI-TOF): $m/z = 1588 [M^{+2}]$ (100%). **IR** (thin film, cm⁻¹): 2925, 2857, 1611, 1513, 1466, 1430, 1388, 1260, 1171, 1036, 925, 872, 836, 796, 725. **UV-Vis** (DCM) λ_{max}/nm ($\epsilon/dm^3 \cdot mol^{-1} \cdot cm^{-1}$): 400 (6.9×10^4), 284 (1.4×10^4).

¹H NMR (500 MHz, Chloroform-*d*) δ 8.57 (s, 2H), 7.92 (s, 2H), 7.88 (s, 2H), 7.80 (m, 6H), 7.27 (s, 2H), 4.29 – 4.22 (m, 20H), 2.01 – 1.93 (m, 20H), 1.62 – 1.56 (m, 20H), 1.45 – 1.35 (m, 40H), 1.01 – 0.91 (m, 30H).

¹³C NMR (126 MHz, Chloroform-*d*) δ 157.64, 150.39, 149.65, 149.11, 148.98, 131.88, 130.80, 128.32, 125.55, 125.23, 123.51, 123.15, 122.96, 112.02, 108.13, 107.54, 106.94, 106.46, 104.79, 86.73, 70.02, 69.61, 69.45, 69.29, 31.85, 31.83, 29.58, 29.52, 29.50, 29.46, 26.00, 22.85, 22.81, 14.25, 14.21.

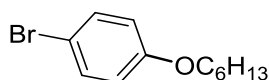
3.2.13. *O*-Bromobenzamidinium Hydrochloride 123^[88]



2-Bromobenzonitrile (4.179 g, 22.7 mmol, 1 eq) was dissolved in tetrahydrofuran (3.4 ml). This mixture was added to lithium bis (trimethylsilyl) amide (1M in THF) (25 ml, 1.1 eq) and stirred for 4 hours at room temperature. The reaction was cooled down on an ice bath and 15 mL of a 1:1 mixture of HCl (5N) and isopropanol was added dropwise, and then it was left to stir overnight. The reaction mixture was filtered in cold and the resultant solid was washed with diethyl ether (10 mL x 2) and dried under vacuum to yield the title compound (4.2 g, 80%) as a white solid.

¹H NMR (500 MHz, DMSO-*d*⁶) δ 9.51 (s, 4H), 7.83 (dd, *J* = 7.6, 1.6 Hz, 1H), 7.63 (dd, *J* = 7.3, 2.1 Hz, 1H), 7.60 – 7.54 (m, 2H) ppm.

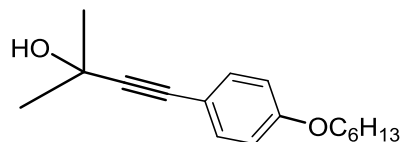
3.2.14. 1-Bromo-4-hexyloxybenzene^[97]



A mixture of 4-bromophenol (20 g, 0.12 mol, 1 eq), 1-bromohexane (28.6 g, 0.17 mmol, 1.5 eq), and potassium carbonate anhydrous (24 g, 0.17 mol, 1.5 eq) were added to ethanol (150 ml) with potassium iodide as catalyst and refluxed at 80 °C overnight. The crude was cooled and filtered and washed with DCM, removal of the solvent in vacuum and the residue was purified by distillation, collecting the pure compound as a colourless oil (24 g, 81%) **B.p.** 155°C. **R_f** 0.14 (1:6, EtOAc: Pet.ether), **IR** (thin film) ν 641, 1072 cm⁻¹.

¹H NMR (500 MHz, Chloroform-*d*) δ 7.36 (d, *J* = 8.9 Hz, 2H), 6.78 (d, *J* = 8.9 Hz, 2H), 3.91 (t, *J* = 6.6 Hz, 2H), 1.82 – 1.73 (m, 2H), 1.49 – 1.42 (m, 2H), 1.38 – 1.31 (m, 4H), 0.94 – 0.90 (m, 3H) ppm.

3.2.15. 4-(p-hexyloxyphenyl)-2-methyl-3-butyn-2-ol ^[97]

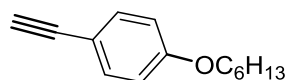


Under a nitrogen atmosphere 1-Bromo-4-hexyloxybenzene (10 g, 39 mmol, 1eq), copper iodide (0.52g, 2.7 mmol, 0.07eq), PPh₃ (0.41 g, 1.56 mmol, 0.04eq) and Pd (PPh₃)₂Cl₂ (0.55 g, 0.78 mmol, 0.02 eq) were dissolved in freshly distilled triethylamine (95 mL). The mixture was then stirred and refluxed at 90 °C for 15 min. A solution of 2-methyl-3-butyn-2-ol (8.23g, 97.3 mol, 2.5 eq) in dry TEA (30 ml) was added slowly by syringe pump by a rate of 0.5 ml per hour. The reaction was left at room temperature then water was added and extracted with dichloromethane three times, and then dried (MgSO₄). The solvent was evaporated to afford an oil. The crude product was purified by column chromatography (petroleum ether / EtOAc = 20:1) to afford a yellow oil (1.5 g, 16%).

R_f 0.14 (1:6, EtOAc: Pet.ether).

¹H NMR (500 MHz, Chloroform-*d*) δ 7.33 (d, *J* = 8.9 Hz, 2H), 6.81 (d, *J* = 8.8 Hz, 2H), 3.94 (t, *J* = 6.6 Hz, 2H), 1.80 – 1.74 (m, 2H), 1.61 (s, 6H), 1.48 – 1.41 (m, 2H), 1.37 – 1.30 (m, 4H), 0.92 – 0.88 (m, 3H) ppm.

3.2.16. 1-ethynyl-4-hexyloxybenzene ^[97]



Under a nitrogen atmosphere 4-(p-hexyloxy-phenyl)-2-methyl-3-butyn-2-ol (3 g, 12 mmol, 1 eq) was dissolved in freshly distilled toluene (50 ml) and sodium hydride dispersion in oil (60%) (0.33 g, 8.4 mmol, 2 eq) was added slowly. The stirred suspension was slowly heated and refluxed for 4h. The crude was poured onto ice-cold water, and the extracted with DCM. The residue solvents were evaporated crude was required two column chromatography using system 1:30 Pet.ether: EtOAc» 2:1 pet.ether: Dcm to afford the title product as a clear yellow oil. (0.6 g, 25%). ¹H NMR (400 MHz,

Chloroform-*d*) δ 7.41 (d, $J = 8.9$ Hz, 2H), 6.83 (d, $J = 8.8$ Hz, 2H), 3.95 (t, $J = 6.6$ Hz, 2H), 2.99 (s, 1H), 1.83 – 1.73 (m, 2H), 1.50 – 1.39 (m, 2H), 1.38 – 1.28 (m, 4H), 0.95 – 0.87 (m, 3H) ppm.

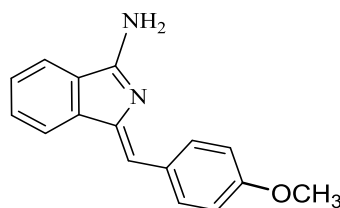
^{13}C NMR (101 MHz, Chloroform-*d*) δ 159.7, 133.7, 114.6, 114.0, 83.9, 75.7, 68.2, 31.7, 29.2, 25.8, 22.7, 14.1 ppm.

3.3. Synthesis of Aminoisoindolene

3.3.1. General procedure A

A mixture of *o*-bromobenzamidine hydrochloride (1eq), BINAP (0.055 eq.) and $\text{PdCl}_2(\text{MeCN})_2$ (0.05 eq.) was sealed in a microwave vessel with a magnetic bar and then purged and refilled with N_2 three times. Then, a solution of the acetylene-derivative (1.2 eq.) and DBU (2.5 eq.) in dry DMF (12 ml) was added. The mixture was stirred under nitrogen for 5min. Finally, the mixture was irradiated in a microwave reactor at 120 °C for 1 h. After cooling, ethyl acetate (50 ml) was added and the mixture washed with a saturated solution of NaHCO_3 (75 mL) three times. The organic layer was dried over MgSO_4 , filtered and concentrated. The residue was finally purified by column chromatography using 100% dichloromethane to 1:1 ethyl acetate/petroleum ether to 100% ethyl acetate as solvent gradient. The resulting solid was recrystallised from a 1:1 mixture of dichloromethane/petroleum ether to yield the desired compounds.

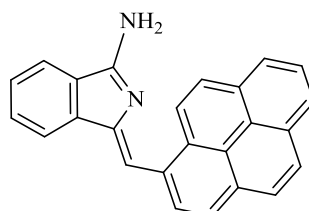
3.3.1.1. 1-(4-Methoxyphenylmethylene)-1H-isoindol-3-amine 131 [92]



Synthesised following the general procedure A from *o*-bromobenzamidine hydrochloride (0.71 g, 3 mmol, 1eq), BINAP (0.103 g, 0.17 mmol, 0.055 eq.), $\text{PdCl}_2(\text{MeCN})_2$ (0.039 g, 0.151 mmol, 0.05 eq.), 4-ethynylanisole (0.47 mL, 3.6 mmol, 1.2 eq.), and DBU (1.15 mL, 7.5 mmol, 2.5 eq.) in DMF (12 ml). Work-up and purification process yielded the title compound as a yellow solid (0.36g, 48%). **Mp.** 163 °C (lit. 156 – 157 °C)^[92]. **MS** (MALDI-TOF): $m/z = 252$ [$\text{M}+2$, 100%]; **IR** (thin film) ν 3446, 2085, 1656 cm^{-1} .

¹H NMR (500 MHz, Acetone-*d*₆) δ 7.29 – 7.23 (m, 2H), 6.86 (dt, *J* = 7.6, 0.9 Hz, 1H), 6.79 (dt, *J* = 7.5, 0.9 Hz, 1H), 6.45 (td, *J* = 7.4, 1.0 Hz, 1H), 6.37 (td, *J* = 7.4, 1.0 Hz, 1H), 5.94 (d, *J* = 8.9 Hz, 2H), 5.84 (s, 2H), 5.75 (s, 1H), 1.09 – 1.05 (m, 3H).

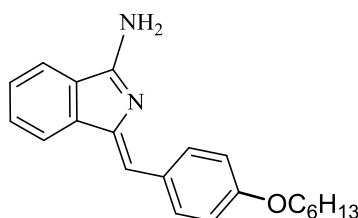
3.3.1.2. (Z)-1(1-Pyrenylmethylene)-1H-isoindol-3-amine 132 ^[93]



Synthesised following the general procedure A from *o*-bromobenzamidine hydrochloride (0.523 g, 2.21 mmol, 1 eq), BINAP (0.78 g, 0.122 mmol, 0.055 eq), PdCl₂(MeCN)₂ (0.31 g, 0.11 mmol, 0.05 eq), 1-ethynylpyrene (0.60 g, 2.7 mmol, 1.2 eq), and DBU (0.84 mL, 5.52 mmol, 2.5 eq) in DMF (10 ml). The work-up and purification process yielded the title compound as an orange/brown powder (0.35 g, 46%). **Mp** 285 °C (dec) (lit. 280 – 282 °C) ⁽⁶⁾; **MS** (MALDI-TOF): *m/z* = 345.7 [M+1, 100%]; **IR** (thin film) ν 3433, 2087, 1653, 1636 cm⁻¹.

¹H NMR (500 MHz, Methanol-*d*₄) δ 8.87 (d, *J* = 8.1 Hz, 1H), 8.59 (d, *J* = 9.3 Hz, 1H), 8.27 – 8.16 (m, 5H), 8.11 (s, 2H), 8.03 (t, *J* = 7.6 Hz, 1H), 7.89 (d, *J* = 7.6 Hz, 1H), 7.86 (s, 1H), 7.67 (td, *J* = 7.5, 1.1 Hz, 1H), 7.53 (td, *J* = 7.5, 0.9 Hz, 1H) ppm.

3.3.1.3. 1-(4-hexyloxyphenylmethylene)-1H-isoindol-3-amine 133



Synthesised following the general procedure A from *O*-bromobenzamidine hydrochloride (0.346 g, 1.5 mmol, 1eq), BINAP (0.051 g, 0.082 mmol, 0.055 eq), PdCl₂(MeCN)₂ (0.019 mg, 0.074 mmol, 0.05 eq), 1-ethynyl-4-hexyloxybenzene (0.35 g, 1.5 mmol, 1.2 eq), and DBU (0.56 mL, 3.70 mmol, 2.5 eq) in DMF (10 ml). Work-up and

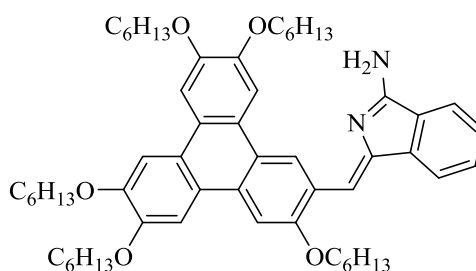
purification process yielded the title compound as a yellow solid (0.2 g, 42%). **Mp** 115°C; **MS** (MALDI-TOF): $m/z = 322.13$ [$M+2$, 100%].

IR (thin film) ν 3432, 2916, 2849, 2086, 1729, 1644 cm^{-1} . **UV-Vis** (DCM) $\lambda_{\text{max}}/\text{nm}$ ($\epsilon/\text{dm}^3 \cdot \text{mol}^{-1} \cdot \text{cm}^{-1}$): 397 (2.6×10^4), 378 (3.4×10^4), 359 (2.7×10^4), 286 (0.8×10^4), 233 (0.2×10^5).

^1H NMR (400 MHz, Acetone- d_6) δ 8.27 – 8.18 (m, 2H), 7.83 (dt, $J = 7.6, 1.0$ Hz, 1H), 7.77 (dt, $J = 7.5, 1.0$ Hz, 1H), 7.43 (td, $J = 7.4, 1.1$ Hz, 1H), 7.35 (td, $J = 7.4, 1.0$ Hz, 1H), 6.95 – 6.87 (m, 2H), 6.78 (s, 2H), 6.72 (s, 1H), 4.02 (t, $J = 6.5$ Hz, 2H), 1.84 – 1.72 (m, 2H), 1.53 – 1.43 (m, 2H), 1.43 – 1.31 (m, 4H), 0.96 – 0.86 (m, 3H).

^{13}C NMR (126 MHz, Chloroform- d) δ 164.31, 158.98, 144.69, 142.98, 134.15, 132.09, 130.35, 129.34, 129.16, 127.00, 119.73, 119.21, 115.96, 114.80, 68.18, 31.76, 29.38, 25.87, 22.76, 14.19.

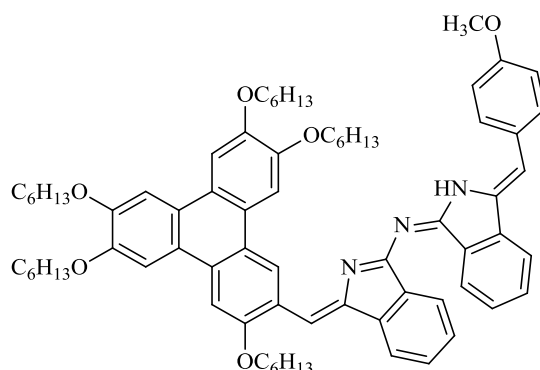
3.3.1.4. 1-(4-triphenylenemethylene)-1H-isoindol-3-amine 124



Synthesised following the general procedure A from *o*-bromobenzamidine hydrochloride (0.10 g, 0.55 mmol, 1eq), BINAP (0.018g, 0.030 mmol, 0.055 eq), $\text{PdCl}_2(\text{MeCN})_2$ (0.007g, 0.0276 mmol, 0.05 eq), 2- ethynyl- 3, 6, 7, 10, 11- penta-hexyloxy-triphenylene (0.5g, 0.664 mmol, 1.2 eq), and DBU (0.21 mL, 2.5 eq) in DMF (2ml). Work-up and purification process yielded the title compound as a yellow solid (0.1g, 21%). **Mp** 125 °C; **MS** (MALDI-TOF): $m/z = 870.60$ [M , 100 %]; **IR** (thin film) ν 3398, 2954, 2919, 2851, 1660 cm^{-1} ; **UV-Vis** (DCM) $\lambda_{\text{max}}/\text{nm}$ (ϵ) 411 (3×10^4), 438 (shoulder) (2×10^4).

^1H NMR (500 MHz, Acetone- d_6) δ 10.40 (s, 1H), 8.21 (s, 1H), 8.10 (s, 1H), 8.03 (d, $J = 3.7$ Hz, 1H), 7.99 (s, 1H), 7.88 (d, $J = 7.7$ Hz, 1H), 7.84 (d, $J = 7.5$ Hz, 1H), 7.51 (td, $J = 7.4, 1.0$ Hz, 1H), 7.42 (td, $J = 7.4, 0.9$ Hz, 1H), 7.40 (s, 1H), 4.36- 4.27 (m, 10H), 1.98 – 1.85 (m, 10H), 1.68 – 1.58 (m, 10H), 1.43 (m, 20H), 0.98 – 0.90 (m, 15H) ppm.

3.3.2. Azadipyrromethene compound 134



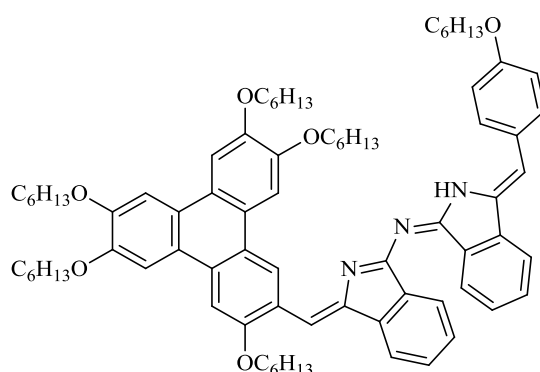
Triphenylene-Aminoisoindolene **124** (0.1g, 0.114 mmol, 1eq) and compound **131** (0.06g, 0.23 mmol, 2eq) were dissolved in toluene (2 mL) and heated to reflux at 120°C under an inert atmosphere, overnight. Purification carried out by chromatography on silica gel using solvent system 4:1 petroleum ether to dichloromethane yielded the title compound as a red solid. This was washed with ethanol and recrystallized from DCM, ethanol (1:1) (0.017g, 27 %).

R_f 0.40 (6:1) Pet.ether: EtOAc; **Mp**.162°C; **MS** (MALDI-TOF): $m/z = 1105.50$ [M, 100%]. **IR** (thin film) ν 3447, 2955, 2929, 2861, 1599, 1580 cm^{-1} ; **UV-Vis** (DCM) $\lambda_{\text{max}}/\text{nm}$ (ϵ) 368 (5.1×10^4), 403(shoulder) (1.5×10^4), 530 (9.2×10^3).

¹H NMR (500 MHz, Acetone-*d*₆) δ 13.56 (s, 1H), 9.54 (s, 1H), 8.13 (dt, $J = 7.5, 1.0$ Hz, 1H), 8.10 – 8.05 (m, 3H), 8.03 (s, 1H), 7.99 (dt, $J = 7.8, 1.0$ Hz, 1H), 7.97 (s, 1H), 7.87 (d, $J = 2.1$ Hz, 2H), 7.70 (td, $J = 7.4, 1.1$ Hz, 1H), 7.62 (td, $J = 7.3, 1.1$ Hz, 2H), 7.57 (td, $J = 7.3, 1.0$ Hz, 1H), 7.47 (d, $J = 8.6$ Hz, 2H), 7.46 (s, 1H), 6.85 (s, 1H), 5.83 (dd, $J = 8.8, 1.7$ Hz, 2H), 4.38 (t, $J = 6.5$ Hz, 2H), 4.29 (dt, $J = 7.7, 6.3$ Hz, 4H), 4.21 (t, $J = 6.4$ Hz, 2H), 3.72 (t, $J = 6.5$ Hz, 2H), 2.93 (s, 3H), 2.01 – 1.83 (m, 10H), 1.67 – 1.56 (m, 10H), 1.48 – 1.35 (m, 20H), 0.98 – 0.83 (m, 15H) ppm.

¹³C NMR (126 MHz, Acetone-*d*₆) δ 141.44, 141.19, 131.21, 130.79, 129.23, 128.63, 127.36, 126.34, 124.95, 124.68, 167.03, 159.52, 156.45, 151.15, 150.29, 149.79, 149.55, 140.23, 135.59, 131.34, 124.58, 123.74, 123.00, 122.66, 120.71, 120.47, 117.06, 114.14, 108.71, 108.45, 107.56, 106.33, 105.52, 70.26, 70.08, 69.77, 69.60, 68.74, 54.53, 32.48, 26.75, 26.69, 26.31, 23.41, 23.33, 23.29, 14.40 ppm.

3.3.3. Azadipyrromethene compound 137

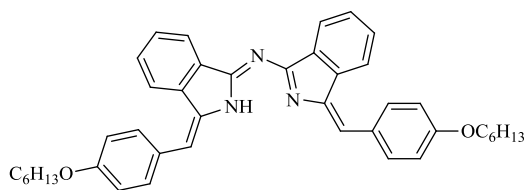


Triphenylene-Aminoisoindolene **124** (0.1g, 0.17 mmol, 1eq) and compound **133** (0.10g, 0.34 mmol, 2eq) were dissolved in toluene (2 mL) and heated to reflux at 120°C under an inert atmosphere overnight. Purification carried out by chromatography on silica gel using solvent system 4:1 petroleum ether to dichloromethane yielded as a red solid. This was washed with ethanol and recrystallized from DCM, ethanol (1:1) (0.028g, 28 %). **Rf** 0.50 (6:1) Pet.ether: EtOAc; **Mp.** 170°C. **MS** (MALDI-TOF): $m/z = 1175.11$ [M+2]; **IR** (thin film) ν 3433, 2929, 2857, 1599, 1577 cm^{-1} ; **UV-Vis** (DCM) $\lambda_{\text{max}}/\text{nm}$ (ϵ) 371 (8.6×10^4), 403(shoulder) (3.1×10^4), 525 (1.6×10^4).

$^1\text{H NMR}$ (500 MHz, Acetone- d_6) δ 13.38 (s, 1H, NH), 9.50 (s, 1H), 8.13 (d, $J = 7.5$ Hz, 1H), 8.08 (dd, $J = 8.4, 7.5$ Hz, 2H), 8.03 – 7.95 (m, 4H), 7.91 (s, 1H), 7.88 (s, 1H), 7.70 (td, $J = 7.4, 1.1$ Hz, 1H), 7.62 (tdd, $J = 7.4, 2.6, 1.1$ Hz, 2H), 7.57 (td, $J = 7.4, 1.0$ Hz, 1H), 7.55 (d, $J = 8.8$ Hz, 2H), 7.45 (s, 1H), 6.90 (s, 1H), 5.87 (d, $J = 8.7$ Hz, 2H), 4.34 (t, $J = 6.5$ Hz, 2H), 4.28 (dt, $J = 12.8, 6.4$ Hz, 4H), 4.21 (t, $J = 6.4$ Hz, 2H), 3.79 (t, $J = 6.5$ Hz, 2H), 2.93 (t, $J = 6.8$ Hz, 2H), 1.91 – 1.53 (m, 12H), 1.50 – 1.39 (m, 12H), 1.38 – 1.03 (m, 24H), 1.00 – 0.83 (m, 18H).

$^{13}\text{C NMR}$ (126 MHz, Chloroform- d & THF) δ 157.23, 154.47, 149.24, 148.60, 147.92, 147.66, 139.45, 129.51, 125.27, 124.54, 123.13, 122.87, 121.99, 118.53, 118.24, 112.66, 106.86, 106.57, 105.64, 104.58, 103.41, 83.12, 74.87, 58.24, 49.97, 41.16, 30.88, 30.84, 29.02, 28.77, 28.72, 28.67, 28.41, 28.35, 28.13, 21.76, 16.28, 12.80.

3.3.4. Azadipyrromethene compound 138



The above compound was also isolated from the above reaction. This was washed with ethanol, and recrystallization was performed using DCM, ethanol (1:1) to obtain a red solid (0.08 g, 14 %).

R_f 0.50 (6:1) Pet.ether: EtOAc; **Mp.** 155 °C; **MS** (MALDI-TOF): $m/z = 624 [M+2]$;

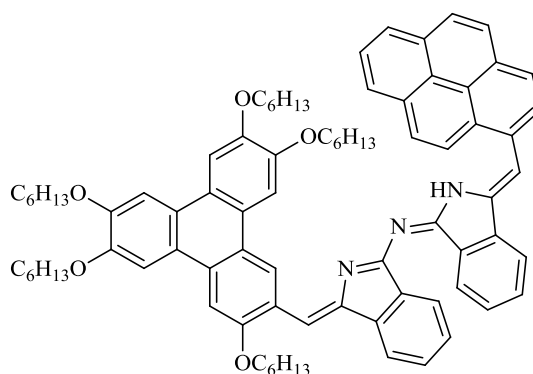
UV-Vis (DCM) λ_{\max}/nm (ϵ) 362 (6.8×10^4), 403(shoulder) (1.5×10^4), 498 (1.2×10^4);

IR (thin film) ν 3434, 2950, 2856, 2089, 1645 cm^{-1} .

¹H NMR (500 MHz, Acetone-*d*₆) δ 12.92 (s, 1H-NH), 8.08 – 7.99 (m, 4H), 7.94 (d, $J = 8.7$ Hz, 4H), 7.62 (td, $J = 7.5, 1.2$ Hz, 2H), 7.55 (td, $J = 7.4, 1.0$ Hz, 2H), 7.07 (s, 2H), 6.71 (d, $J = 8.7$ Hz, 4H), 3.89 (t, $J = 6.6$ Hz, 4H), 1.77 (m, 4H), 1.49 (m, 4H), 1.41 – 1.34 (m, 8H), 0.96 – 0.90 (m, 6H) ppm.

¹³C NMR (126 MHz, Chloroform-*d*₃ & THF) δ 164.77, 158.19, 139.31, 139.19, 133.91, 130.42, 129.11, 127.60, 126.98, 121.43, 118.48, 114.33, 113.37, 83.59, 75.31, 70.12, 69.09, 58.73, 50.46, 41.48, 31.06, 29.43, 29.04, 28.64, 21.98, 13.19.

3.3.5. Azadipyrromethene compound 136

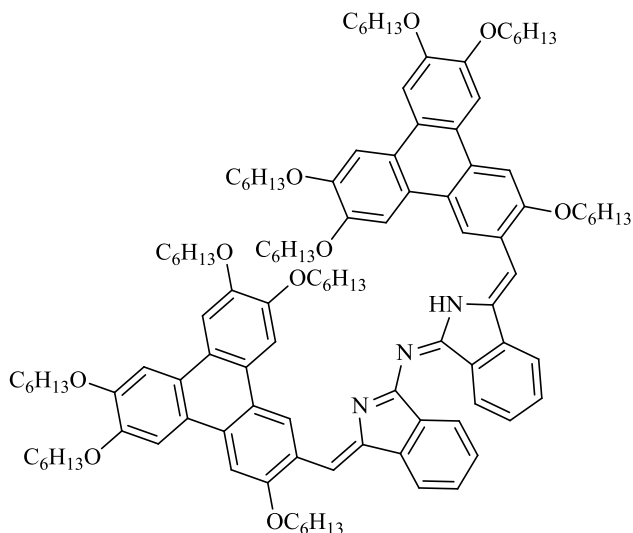


Triphenylene-Aminoisoidolene **124** (0.1g, 0.114mmol, 1eq) and pyrenyl-Aminoisoidolene (0.06g, 0.172 mmol, 1.5 eq) were dissolved in toluene (2 mL) and heated to reflux at 120°C under an inert atmosphere overnight. After cooling, the solvent was allowed to slowly evaporate, the residue was purified by column chromatography using solvent system 4:1 petroleum ether to ethyl acetate to yield the title compound. This was washed with ethanol and recrystallized from DCM, ethanol (1:1) to afford a dark brown solid (0.042g, 60%). **R_f** 0.43 (6:1) Pet.ether: EtOAc; **Mp** 187°C; **MS** (MALDI-TOF): $m/z = 1199.12$ [$M+2$, 100%]. **IR** (thin film) ν 3434, 2925, 2089, 1641 cm^{-1} ; **UV-Vis** (DCM) $\lambda_{\text{max}}/\text{nm}$ (ϵ) 400 (3.7×10^4), 455(shoulder) (1.2×10^4), 550 (0.2×10^4).

¹H NMR (500 MHz, THF-*d*₈) δ 13.94 (s, 1H), 8.75 (s, 1H), 8.17 (d, $J = 8.1$ Hz, 1H), 7.48 – 7.39 (m, 2H), 7.38 – 7.30 (m, 3H), 7.19 (d, $J = 7.6$ Hz, 1H), 7.13 – 7.07 (m, 2H), 7.08 – 7.03 (m, 1H), 7.02 (s, 1H), 6.99 (s, 1H), 6.94 (s, 1H), 6.90 – 6.78 (m, 3H), 6.82 – 6.73 (m, 1H), 6.71 (s, 1H), 6.65 (s, 1H), 6.42 (d, $J = 8.8$ Hz, 1H), 6.17 (dd, $J = 18.8, 8.5$ Hz, 2H), 5.62 (s, 1H), 5.48 (s, 1H), 3.49 (t, $J = 6.3$ Hz, 2H), 3.12 (t, $J = 6.2$ Hz, 2H), 3.01 (t, $J = 6.3$ Hz, 2H), 2.91 (t, $J = 6.8$ Hz, 2H), 2.75 – 2.70 (m, 2H), 1.35 – 1.29 (m, 2H), 1.25 – 1.06 (m, 8H), 0.89 – 0.83 (m, 2H), 0.78 – 0.66 (m, 20H), 0.57 – 0.50 (m, 2H), 0.45 – 0.39 (m, 2H), 0.32 (t, $J = 7.0$ Hz, 4H), 0.28 – 0.20 (m, 15H).

¹³C NMR (126 MHz, Chloroform-*d*) δ 154.40, 148.64, 147.33, 147.13, 146.70, 141.09, 138.81, 138.61, 130.31, 129.92, 128.94, 128.02, 127.50, 126.83, 125.97, 125.83, 125.66, 124.92, 124.09, 123.99, 123.81, 123.20, 121.58, 121.30, 121.13, 120.44, 118.92, 118.40, 107.09, 103.72, 103.18, 102.92, 82.96, 74.69, 58.09, 49.83, 41.04, 30.86, 28.51, 28.33, 21.53, 16.18, 12.72, 7.89 ppm.

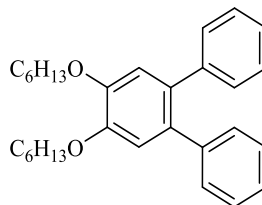
3.3.6. Aza-(ditriphenylene) dipyrromethenes (Self-Condensation of triphenylene-Aminoisoindoline) compound 125



Triphenylene-Aminoisoindoline **124** (0.5g, 0.55 mmol, 1eq) was dissolved in toluene (2 mL) and heated to reflux at 120°C under an inert atmosphere overnight. After cooling, the solvent was allowed to slowly evaporate, the residue was purified by column chromatography using 4:1 petroleum ether to dichloromethane solvent system to yield the title compound. This was washed with ethanol and recrystallized from DCM, ethanol (1:1) to obtain a dark red solid (0.07g, 70 %).

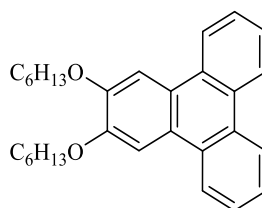
R_f 0.65 (6:1) Pet.ether: EtOAc; **MS** (MALDI-TOF): $m/z = 1724 [M^+, 100\%]$; **Mp** 265°C; **IR** (thin film) ν 3426, 2956, 2930, 2862, 1608 cm^{-1} ; **UV-Vis** (DCM) $\lambda_{\text{max}}/\text{nm}$ (ϵ) 400 (3.7×10^4), 455(shoulder) (1.2×10^4), 550 (0.2×10^4). **¹H NMR** not clear due to aggregation.

3.3.7. Compound 143 ^[47]



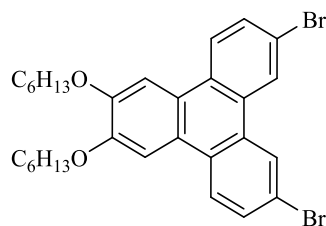
1,2-Dibromo-4,5-bis(hexyloxy)benzene (5 g, 11.5 mmol, 1 eq.), benzene boronic acid (4.2 g, 34.4 mmol, 3 eq.), palladium chloride (0.163 g, 0.92 mmol, 0.08 eq.), triphenylphosphine (0.96 g, 3.7 mmol, 0.32 eq.) and sodium carbonate (3.65 g, 34.4 mmol, 3 eq.) were stirred in a mixture of toluene, ethanol and water in ratio 1:1:1 (120 ml). The reaction mixture was refluxed for 16 hours. After that a second portion of benzene boronic acid (4.2 g, 34.4 mmol, and 3 eq.), palladium chloride (0.163 g, 0.92 mmol, 0.08 eq.), triphenylphosphine (0.96 g, 3.7 mmol, 0.32 eq.) and sodium carbonate (3.65 g, 34.4 mmol, 3 eq.) was added to the reaction. The reaction was stopped and quenched after 40 hours by adding hydrochloric acid (100 ml, 2M). The residue was extracted with dichloromethane and dried with magnesium sulphate. The solvents were removed in vacuo and the crude was purified by column chromatography which was eluted using 1:9 dichloromethane to petroleum ether. The pure product was obtained as bright white crystals (1.6 g, 33%).

¹H NMR (500 MHz, Chloroform-d) δ 7.20 – 7.11 (m, 10H), 6.94 (s, 2H), 4.06 (t, *J* 6.6 Hz, 4H), 1.89 – 1.80 (m, 4H), 1.52 – 1.46 (m, 4H), 1.37 – 1.34 (m, 8H), 0.92 – 0.89 (m, 6H) ppm.

3.3.8. 2,3-Bis(hexyloxy)triphenylene 144^[47]

A solution of 1, 2-bis (hexyloxy)-4, 5-diphenylbenzene (1 g, 2.324 mmol, 1eq.) in dichloromethane (50 mL) was stirred at room temperature. Iron (III) chloride (1.9 g, 11.62 mmol, 5 eq.) was added and the reaction mixture was stirred for two hours. The reaction mixture was cooled to -10°C and methanol (50 mL) was added. The solvents were removed in vacuo, and the resulting crude residue dissolved in dichloromethane. This was then washed with water (4 x 100 mL) and the organics were collected then dried over magnesium sulphate. The solvents were removed in vacuo and the crude product was loaded onto a silica gel column (pore size 40-63 μ). The column was eluted using a 1:9 mixture of dichloromethane/petroleum ether. After removal of solvents, the pure product was obtained as a white solid (0.54 g, 55%).

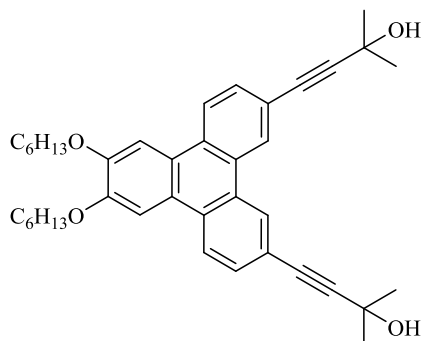
¹H NMR (500 MHz, Chloroform-d) δ 8.65 (dd, *J* 7.9, 1.7 Hz, 2H), 8.50 (dd, *J* 8.0, 1.6 Hz, 2H), 8.03 (s, 2H), 7.66 – 7.59 (m, 4H), 4.25 (t, *J* 6.6 Hz, 4H), 2.00 – 1.93 (m, 4H), 1.62 – 1.56 (m, 4H), 1.46 – 1.34 (m, 8H), 0.97 – 0.91 (m, 6H) ppm.

3.3.9. 2,11-Dibromo-6,7-bis(hexyloxy)triphenylene 145 ^[98]

2, 3-Bis (hexyloxy) triphenylene (0.90 g, 2.10 mmol, and 1 eq.) was stirred in dichloromethane (45 ml) at 0°C. Bromine (0.23 mL, 0.72 g, 4.50 mmol, 2.14 eq.) was added dropwise via pipette and the mixture stirred for a further 2 hours at 0°C and then allowed to warm to room temperature. The reaction mixture was washed with sodium metabisulphite solution (20%, 100 ml) and the crude product extracted with dichloromethane. The combined organic layer was dried over magnesium sulphate, and the solvents removed in *vacuo*. The crude product was recrystallized from pentanol, giving the pure product as a white powder (0.90 g, 72%).

¹H NMR (500 MHz, Chloroform-d) δ 8.63 (d, *J* 2.0 Hz, 2H), 8.31 (d, *J* 8.9 Hz, 2H), 7.90 (s, 2H), 7.72 (dd, *J* 8.8 Hz, 2.0 Hz, 2H), 4.23 (t, *J* 6.6 Hz, 4H), 1.98 – 1.91 (m, 4H), 1.61 – 1.53 (m, 4H), 1.45 – 1.34 (m, 8H), 0.96 – 0.92 (m, 6H) ppm.

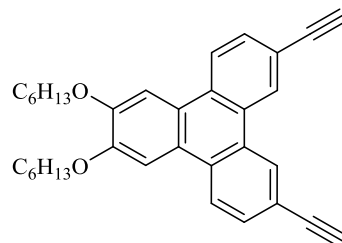
3.3.10. 4, 4'-(6, 7-Bis (hexyloxy) triphenylene-2, 11-diyl) bis(2-methylbut-3-yn-2-ol) 146



A mixture of 7,10-dibromo-2,3-bis(hexyloxy)triphenylene (1.8 g, 3.10 mmol, 1 eq), copper iodide (0.083 g, 0.43 mmol, 0.14 eq) and bis(triphenylphosphine)palladium ^[57] dichloride (0.13 g, 0.19 mmol, 0.06 eq) were stirred in degassed triethylamine (30 mL) under nitrogen. The reaction mixture was heated at reflux for 30 minutes. 2-Methyl-but-3-yn-2-ol (1.3 g, 16 mmol, 5 eq) was added via syringe and the reaction heated under reflux for overnight. On completion, the crude mixture was washed with water and the organics were extracted with dichloromethane. The organic extracts were combined and dried over magnesium sulphate. The solvent was removed in vacuo and the crude product loaded onto a silica gel column. The column was eluted using a 3:1:1 mixture of dichloromethane, ethyl acetate and petroleum ether respectively. After removal of solvents, the pure product was obtained as a pale-yellow solid (0.94 g, 51%).

¹H-NMR (500 MHz, CDCl₃) δ 8.66 (s, 2H), 8.37 (d, J = 8.6 Hz, 2H), 7.92 (s, 2H), 7.64 (d, J = 8.6 Hz, 2H), 4.23 (t, J = 6.6 Hz, 4H), 2.14 (br s, 2H), 1.97-1.92 (m, 4H), 1.72 (s, 12H), 1.59- 1.55 (m, 4H), 1.42-1.38 (m, 8H), 0.94 (t, J = 7.1 Hz, 6H) ppm.

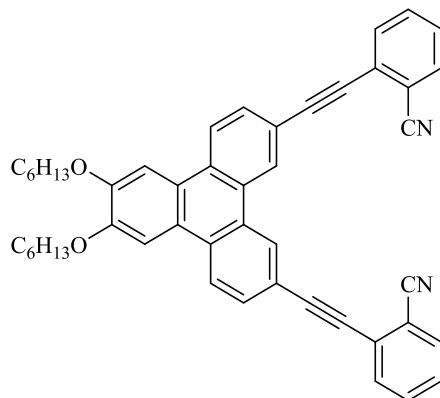
3.3.11. Synthesis of 2, 11-Diethynyl-6, 7-bis (hexyloxy) triphenylene 139



4,4'-(6,7-Bis(hexyloxy)triphenylene-2,11-diyl) bis(2-methylbut-3-yn-2-ol) (0.90 g, 1.6 mmol, 1 eq) was stirred in anhydrous toluene (16 mL) under nitrogen, and the mixture heated to reflux. Sodium hydride (0.32 g, 8 mmol, 5 eq) was added portion-wise, and after the addition was complete, the reaction was heated at reflux for overnight. Upon completion the reaction was poured onto cold water and extracted with dichloromethane. The organic extracts were combined and dried over magnesium sulphate, and the solvent removed in vacuo. The crude product was loaded onto a silica gel column and the column was eluted with a 1:9 mixture of ethyl acetate/petroleum ether. After removal of solvents, the pure product was obtained as a yellow solid (0.40 g, 54%).

¹H-NMR (500 MHz, CDCl₃) δ 8.75 (s, 2H), 8.40 (d, J = 8.4 Hz, 2H), 7.93 (s, 2H), 7.72 (d, J = 8.4 Hz, 2H), 4.24 (t, J = 6.6 Hz, 4H), 1.98- 1.92 (m, 4H), 1.61-1.56 (m, 4H), 1.42-1.39 (m, 8H), 0.94 (t, J = 7.1 Hz, 6H) ppm.

3.3.12. Synthesis of 6, 7-bis (hexyloxy)-2, 11-bis yn-bis (2-benzonitrile) triphenylene 147



A mixture of 2-bromobenzonitrile (0.115g, 0.63 mmol, 3 eq.), 3, 6-diethynyl-10, 11-di (hexyloxy) triphenylene (0.1 g, 0.21 mmol, 1 eq.), Pd (PPh₃)₂Cl₂ (0.006 g, 0.008 mmol, 0.04 eq.), CuI (0.003g, 0.0142mmol, 0.07 eq.), and TEA (2 ml) was heated in a sealed tube at 120 °C overnight. The reaction mixture was diluted with H₂O and extracted with diethyl ether. The organic layer obtained from ethereal extract was purified by column chromatography using ethyl acetate-petroleum ether (1:4) as solvent. Recrystallization from petroleum ether afforded the product as a dark yellow solid (0.06 g, 4%), **IR** (thin film) ν 2930, 2858, 2213 cm⁻¹; **R_f** 0.25 (1:1) DCM: Pet. ether.

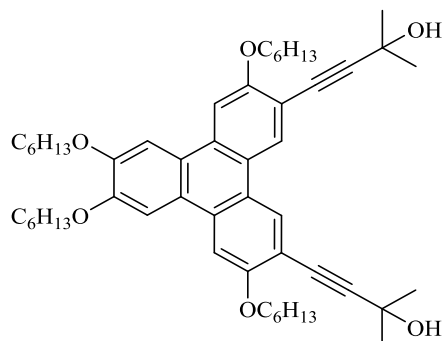
UV-Vis (CH₂Cl₂) λ_{max} /nm (ϵ) 353(4×10⁴), 328(5×10⁴), 299 (5.3×10⁴), 266 (4.5×10⁴) nm.

MS (MALDI-TOF): m/z calculated for C₄₈H₄₂N₂O₂: 678.86, found (M, 100 %): (678.22).

¹H NMR (500 MHz, Chloroform-*d*) δ 8.67 (d, J = 1.7 Hz, 2H), 8.29 (d, J = 8.6 Hz, 2H), 7.80 – 7.76 (m, 4H), 7.74 – 7.65 (m, 4H), 7.56 (td, J = 7.7, 1.4 Hz, 2H), 7.39 (td, J = 7.7, 1.2 Hz, 2H), 4.19 (t, J = 6.6 Hz, 4H), 1.99 – 1.89 (m, 4H), 1.62 – 1.52 (m, 4H), 1.46 – 1.33 (m, 8H), 0.99 – 0.90 (m, 6H).

¹³C NMR (126 MHz, Chloroform-*d*) δ 150.3, 132.8, 132.58, 132.50, 130.4, 128.37, 128.36, 127.48, 127.43, 124.3, 123.2, 119.9, 117.8, 115.3, 106.8, 96.6, 86.5, 69.4, 31.8, 29.3, 25.9, 22.8, 14.20 ppm.

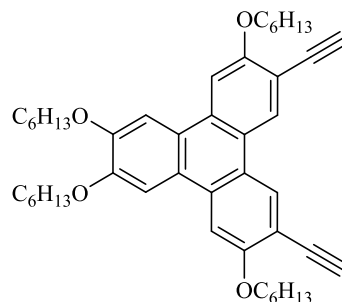
3.3.13. 4,4'-(3,6,7,10-tetrakis(hexyloxy)triphenylene-2,11-diyl)bis(2-methylbut-3-yn-2-ol) 154^[77]



2, 11-Dibromo-3, 6, 7, 10-tetrakis (hexyloxy) triphenylene (1 g, 1.3 mmol, 1 eq.), CuI (0.03 g, 0.17 mmol, 0.14 eq.), Pd (PPh₃)₂Cl₂ (0.05 g, 0.07 mmol, 0.06 eq.) and PPh₃ (0.08 g, 0.3 mmol, 0.24 eq.) were stirred in freshly distilled triethylamine (16 mL) under an atmosphere of nitrogen. The reaction mixture was heated at reflux for 15 min then the heating source was removed and 2-methyl-but-3-yn-2-ol (0.5 g, 6.7 mmol, 5.25 eq.) dissolved in dry triethylamine (8 ml) was added dropwise to the mixture by syringe pump for 16 h. Then the mixture was heated under reflux for 3h. The mixture was cooled to room temperature and water was added. The mixture was extracted with dichloromethane (3×100 mL) and the solvent removed in vacuo to leave a dark-brown solid which was purified by column chromatography (ethyl acetate/petroleum ether 1:4) to give the pure title compound (0.86 g, 85%) as a pale-yellow solid.

¹H NMR (500 MHz, Chloroform-d) δ 8.52 (s, 2H), 7.83 (s, 2H), 7.70 (s, 2H), 4.24 (td, *J* 6.5 Hz, 4.4 Hz, 8H), 2.17 (br, 2 H), 1.99 – 1.90 (m, 8H), 1.71 (s, 12H), 1.66 – 1.56 (m, 8H), 1.46 – 1.33 (m, 16H), 0.97 – 0.89 (m, 12H).

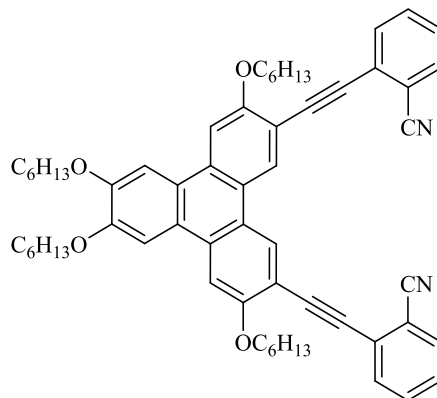
3.3.14. 2,11-Diethynyl-3,6,7,10-tetrakis (hexyloxy)triphenylene
155 ^[77]



3,6,7,10-Tetrakis(hexyloxy)-2,11-bis(3-methyl-3-hydroxybutynyl) triphenylene (1.5 g, 1.9 mmol, 1 eq.) was dissolved in refluxing dry toluene (25mL) under an atmosphere of nitrogen. Sodium hydride (60% dispersion in oil) (0.34 g, 8.50 mmol, 4.5 eq.) was added in small portions and the mixture heated under reflux for 2 h. The reaction mixture was then poured onto ice-cold water and the organic layer was extracted with dichloromethane (3×100 mL) and dried over magnesium sulphate. The solvent was removed in vacuo to leave a dark-brown oil which was purified by column chromatography (ethyl acetate/petroleum ether 1:9) to obtain the pure compound (0.60 g, 47%) as a pale-yellow solid.

¹H NMR (500 MHz, Chloroform-d) δ 8.58 (s, 2H), 7.82 (s, 2H), 7.72 (s, 2H), 4.25 (m, 8H), 3.37 (s, 2H), 2.00 – 1.90 (m, 8H), 1.63 – 1.55 (m, 8H), 1.47 – 1.33 (m, 16H), 0.97 – 0.90 (m, 12H).

3.3.15. Synthesis of 3, 6, 7, 10-tetrakis (hexyloxy)-2, 11-diethynyl – (bis (2-benzonitrile)) triphenylene 156B



A mixture of 2-bromobenzonitrile (0.323 g, 1.80 mmol, 3 eq.), 3, 6-diethynyl-2, 7, 10, 11-tetrakis (hexyloxy) triphenylene (0.4 g, 0.60 mmol, 1 eq.), CuI (0.007g, 0.041 mmol, 0.07 eq.), PdCl₂ (PPh₃)₂ (0.017g, 0.024 mmol, 0.04 eq.) in triethylamine (2 ml) was heated in a sealed tube at 120°C overnight. The reaction mixture was diluted with H₂O and extracted with diethyl ether. The organic layer obtained from ethereal extract was purified by column chromatography using system EtOAc: Pet. Ether 1:20, then DCM: Pet. Ether 1:4 then recrystallization from dichloromethane/petroleum ether (1:1) to afford the product as major product (0.045 g, 9 %). **R_f** 0.166 (1:5) EtOAc: Pet. ether.

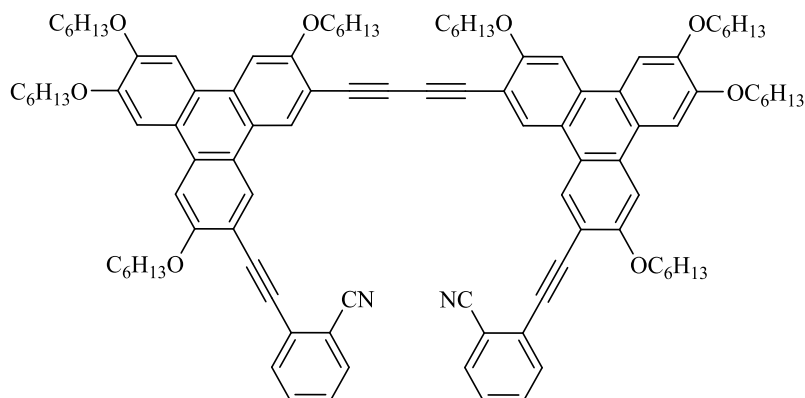
Transition temperature: Cr 98 Col 208 **IIR** (thin film) ν 2928, 2861, 2211, 1607 cm⁻¹

UV-Vis (CH₂Cl₂) λ_{max} /nm (ϵ) 405(1.3×10⁴), 383(3.4×10⁴), 352 (5.2×10⁴), 304 (7.6×10⁴), 276 (5.7×10⁴) nm, **MS** (MALDI-TOF): m/z calculated for C₆₀H₆₆N₂O₄: 879.17, found (M, 100 %): (879.20).

¹H NMR (500 MHz, Chloroform-*d*) δ 8.62 (d, J = 2.3 Hz, 2H), 7.82 (s, 2H), 7.75 (dd, J = 8.0, 1.2 Hz, 2H), 7.72 – 7.69 (m, 4H), 7.59 (td, J = 7.7, 1.3 Hz, 2H), 7.42 (td, J = 7.7, 1.2 Hz, 2H), 4.30 (t, J = 6.5 Hz, 4H), 4.26 (t, J = 6.5 Hz, 4H), 2.05 – 1.99 (m, 4H), 1.97 – 1.90 (m, 4H), 1.67 – 1.53 (m, 8H), 1.46 – 1.33 (m, 18H), 0.96 – 0.92 (m, 12H).

¹³C NMR (126 MHz, Chloroform-*d*) δ 158.2, 150.2, 132.89, 132.82, 132.3, 130.8, 129.0, 128.1, 127.88, 124.7, 122.3, 117.8, 115.0, 111.8, 107.6, 104.4, 93.3, 89.9, 69.7, 69.3, 31.8, 29.5, 29.3, 26.06, 26.0, 22.8, 14.2.

3.3.16. bisBenzonitrile substituted diad 157B

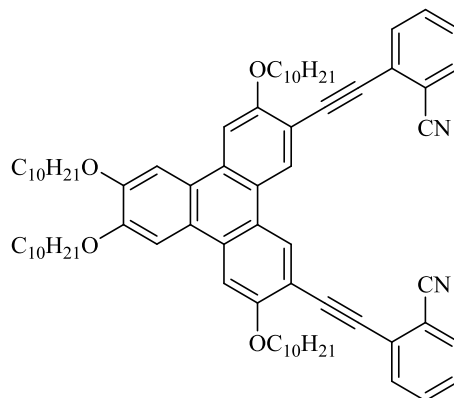


The above compound was also isolated from the previous reaction as minor product as a yellow solid. **Yield** (0.0163 g, 3.5 %). **Mp.** The quantity of pure compound is insufficient. **IR** (thin film) ν 2955, 2930, 2858, 2210, 1607 cm^{-1} . **UV-Vis** (CH_2Cl_2) λ_{max} /nm (ϵ) 419(4.8×10^4), 356(1.2×10^5), 295 (1.7×10^5) nm. **MS** (MALDI-TOF): m/z calculated for $\text{C}_{106}\text{H}_{124}\text{N}_2\text{O}_8$:1554.12, found (M, 100 %): (1552.59).

$^1\text{H NMR}$ (400 MHz, Chloroform-*d*) δ 8.64 (s, 4H), 7.81 (s, 4H), 7.76 (d, $J = 7.8$ Hz, 2H) 7.72 – 7.65 (m, 6H), 7.57 (td, $J = 7.7, 1.4$ Hz, 2H), 7.40 (td, $J = 7.7, 1.2$ Hz, 2H), 4.33 – 4.23 (m, 16H), 2.06 – 1.92 (m, 16H), 1.69 – 1.57 (m, 16H), 1.44 – 1.33 (m, 32H), 0.98 – 0.86 (m, 24H).

$^{13}\text{C NMR}$ (101 MHz, Chloroform-*d*) δ 150.07, 149.97, 132.72, 132.25, 127.93, 122.16, 122.01, 117.64, 114.91, 93.26, 69.53, 69.31, 31.73, 31.71, 31.69, 29.41, 29.24, 25.94, 25.90, 25.80, 22.68, 14.10, 14.07.

3.3.17. Synthesis of 3, 6, 7, 10-tetrakis (decyloxy)-2, 11-diethynyl (bis (2-benzonitrile)) triphenylene 156A

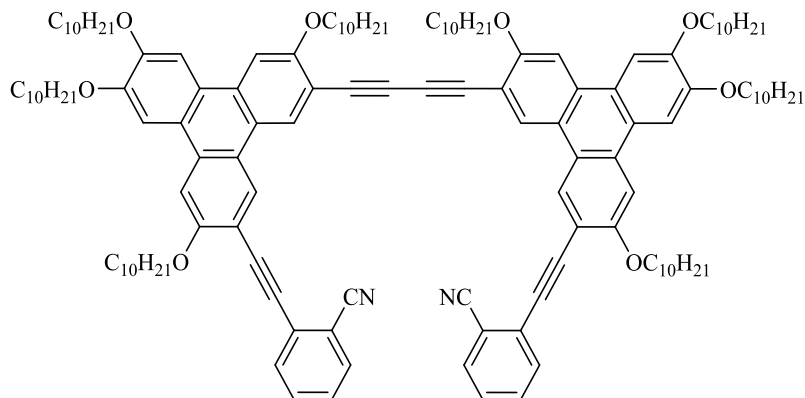


A mixture of 2-bromobenzonitrile (0.156 g, 0.832 mmol, 3 eq.), 3, 6-diethynyl-2, 7, 10, 11-tetrakis (decyloxy) triphenylene (0.25 g, 0.28 mmol, 1 eq.), CuI (0.004 g, 0.02 mmol, 0.07 eq.), PdCl₂ (PPh₃)₂ (0.0078 g, 0.0111 mmol, 0.04 eq.) in trimethylamine (2 ml) was heated in a sealed tube at 120 °C overnight. The mixture was cooled at room temperature. The reaction crude was diluted with H₂O and extracted with diethyl ether. The crude was required two column chromatography to be purified starting with eluent system EtOAc /pet. Ether 1:30, then pet. Ether: DCM 1:4 *R_f* 0.36 (1:5) EtOAc: Pet.ether. Yield (0.023 g, 7 %). **Transition temperatures:** Cr 56 Col 140 I. **MS** (MALDI-TOF): *m/z* calculated for C₇₆H₉₈N₂O₄:1103.60, found (M, 100 %): (1102.79). **IR** (thin film) ν 2924, 2853, 2228, 2210 cm⁻¹; **UV-Vis** (CH₂Cl₂) λ_{max} /nm (ϵ) 405(2.6×10⁴), 383(5.5×10⁴), 351(8×10⁴), 304(1.2×10⁵), 277(9.7×10⁴) nm.

¹H NMR (500 MHz, Chloroform-*d*) δ 8.72 (s, 2H), 7.87 (s, 2H), 7.77 (s, 2H), 7.75 (dt, *J* = 7.7, 1.0 Hz, 2H), 7.71 (ddd, *J* = 7.8, 1.3, 0.6 Hz, 2H), 7.59 (td, *J* = 7.7, 1.4 Hz, 2H), 7.42 (td, *J* = 7.7, 1.2 Hz, 2H), 4.31 (t, *J* = 6.5 Hz, 4H), 4.27 (t, *J* = 6.5 Hz, 4H), 2.02 (p, *J* = 6.6 Hz, 4H), 1.96 (p, *J* = 6.7 Hz, 4H) 1.70 – 1.59 (m, 8H), 1.46 (q, *J* = 7.0 Hz, 8H), 1.31 (m, 40H), 0.88 (m, 12H).

¹³C NMR (126 MHz, Chloroform-*d*) δ 158.27, 150.33, 132.91, 132.81, 132.40, 130.92, 129.15, 128.13, 127.88, 124.78, 122.43, 117.85, 115.08, 112.03, 107.73, 104.60, 93.28, 90.05, 69.80, 69.45, 32.09, 32.06, 29.85, 29.78, 29.76, 29.69, 29.67, 29.56, 29.54, 29.52, 29.43, 26.42, 26.36, 22.85, 22.84, 14.27.

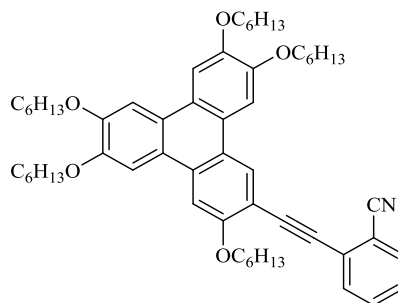
3.3.18. Bis-benzonitrile substituted diad 157A



The above compound was also isolated from the previous reaction as a minor product as a brown solid. Yield (0.004 g, 1 %). **Mp**. The quantity of pure compound is insufficient.

¹H NMR (400 MHz, Chloroform-*d*) δ 8.68 (d, $J = 5.4$ Hz, 2H), 7.84 (d, $J = 3.9$ Hz, 2H), 7.79 – 7.72 (m, 1H), 7.73 (d, $J = 2.9$ Hz, 2H), 7.69 (dt, $J = 7.2, 0.7$ Hz, 1H), 7.57 (td, $J = 7.7, 1.3$ Hz, 1H), 7.39 (td, $J = 7.7, 1.3$ Hz, 0H), 4.36 – 4.22 (m, 8H), 2.08 – 1.91 (m, 8H), 1.68 – 1.55 (m, 8H), 1.46 – 1.17 (m, 56H), 0.93 – 0.83 (m, 12H).

3.3.19. Synthesis of 3, 6, 7, 10, 11-pentakis (hexyloxy)-2- ethynyl - (2-benzonitrile) triphenylene 158



A mixture of 2-bromobenzonitrile (0.130g, 0.70 mmol, 1.5eq.), 2-ethynyl-3, 6, 7, 10, 11-tetrakis (hexyloxy) triphenylene (0.36 g, 0.5 mmol, 1 eq.), CuI (0.0032 g, 0.017 mmol, 0.035 eq.), PdCl₂ (PPh₃)₂ (0.007 g, 0.009 mmol, 0.02 eq.) in triethylamine (2 ml) was heated in a sealed tube at 120 °C overnight. The crude was cooled at room temperature then washed with NH₄Cl solution then extracted by EtOAc. The organic layer was collected then dried over anhydrous magnesium sulphate. The solvents were removed in *vacuo* and the crude product was purified by column chromatography (ethyl acetate/petroleum ether 1:30) to obtain the title compound (0.04 g, 10%) as a creamy yellow solid. **IR** (thin film) ν 2955-2870, 2207, 2228, 1132, 758cm⁻¹; **Rf** = 0.55 (1:5) EtOAc: Pet.ether. **UV-Vis** (CH₂Cl₂) λ_{max} /nm (ϵ) 369 (2×10⁴), 288 (7×10⁴), 261 (5×10⁴) nm; **MS** (MALDI-TOF): *m/z* calculated for C₅₇H₇₅NO₅:854.21, found (M, 100 %): (853). **Mp.** (The material is not solid; it was trying another crystallisation system). **¹H NMR** (500 MHz, Chloroform-*d*) δ 8.69 (s, 1H), 7.94 (s, 1H), 7.88 (s, 1H), 7.84 – 7.79 (m, 3H), 7.74 – 7.69 (m, 2H), 7.63 – 7.56 (m, 1H), 7.41 (dd, *J* = 7.8, 1.1 Hz, 1H), 4.31 (t, *J* = 6.5 Hz, 2H), 4.29 – 4.19 (m, 8H), 2.06 – 1.89 (m, 10H), 1.68 – 1.55 (m, 10H), 1.48 – 1.33 (m, 20H), 0.96 – 0.89 (m, 15H).

¹³C NMR (126 MHz, Chloroform-*d*) δ 157.77, 150.50, 149.71, 149.13, 148.96, 132.91, 132.41, 131.30, 129.50, 128.12, 127.92, 125.73, 123.08, 122.89, 115.30, 111.43, 108.26, 106.94, 104.74, 93.80, 70.05, 69.61, 69.41, 31.84, 31.82, 29.58, 29.49, 29.38, 26.03, 25.99, 22.81, 14.20.



4. References

- [1] C. Imrie, G. Luckhurst, D. Demus, J. Goodby, G. Gray, H. Spiess, V. Vill, Wiley-VCH, Weinheim, **1998**.
- [2] F. Reinitzer, *Liquid Crystals* **1989**, *5*, 7-18.
- [3] O. Lehmann, *Zeitschrift für physikalische Chemie* **1889**, *4*, 462-472.
- [4] S. Kumar, *Chemistry of discotic liquid crystals: from monomers to polymers*, CRC press, **2016**.
- [5] S. Chandrasekhar, B. Sadashiva, K. Suresh, *pramana* **1977**, *9*, 471-480.
- [6] M. Okazaki, Google Patents, **1998**.
- [7] X. Chen, L. Chen, Y. Chen, *RSC advances* **2014**, *4*, 3627-3632.
- [8] K.-Q. Zhao, J.-Q. Du, X.-H. Long, M. Jing, B.-Q. Wang, P. Hu, H. Monobe, B. Henrich, B. Donnio, *Dyes and Pigments* **2017**, *143*, 252-260.
- [9] C. Tschierske, *Current opinion in colloid & interface science* **2002**, *7*, 355-370.
- [10] G. W. Gray, *Thermotropic liquid crystals*, John Wiley & Sons Inc, **1987**.
- [11] S. Kumar, *Liq. Cryst.* **2004**, *31*, 1037-1059.
- [12] J. Luo, B. Zhao, H. S. O. Chan, C. Chi, *J. Mater. Chem.* **2010**, *20*, 1932-1941.
- [13] S. Kumar, *Chemical Society Reviews* **2006**, *35*, 83-109.
- [14] C. Destrade, P. Foucher, H. Gasparoux, N. H. Tinh, A. Levelut, J. Malthete, *Molecular crystals and liquid crystals* **1984**, *106*, 121-146.
- [15] F. Morale, R. W. Date, D. Guillon, D. W. Bruce, R. L. Finn, C. Wilson, A. J. Blake, M. Schröder, B. Donnio, *Chemistry—A European Journal* **2003**, *9*, 2484-2501.
- [16] S. Chen, H. Guo, X. Geng, F. Yang, *Journal of Molecular Liquids* **2018**, *252*, 145-150.
- [17] C. Vauchier, A. Zann, P. L. Barny, J. Dubois, J. Billard, *Molecular Crystals and Liquid Crystals* **1981**, *66*, 103-114.
- [18] A. Kotlewski, W. F. Jager, E. Mendes, S. J. Picken, *Liquid Crystals* **2010**, *37*, 579-586.
- [19] S. Kumar, S. K. Varshney, *Organic letters* **2002**, *4*, 157-159.
- [20] B. Alameddine, O. F. Aebischer, W. Amrein, B. Donnio, R. Deschenaux, D. Guillon, C. Savary, D. Scanu, O. Scheidegger, T. A. Jenny, *Chemistry of materials* **2005**, *17*, 4798-4807.
- [21] K. Hatsusaka, K. Ohta, I. Yamamoto, H. Shirai, *Journal of Materials Chemistry* **2001**, *11*, 423-433.
- [22] M. Ichihara, A. Suzuki, K. Hatsusaka, K. Ohta, *Liquid Crystals* **2007**, *34*, 555-567.
- [23] P. J. Collings, M. Hird, *Introduction to liquid crystals: chemistry and physics*, Crc Press, **2017**.
- [24] S. W. Lee, Y. J. Na, W. S. Choi, S. D. Lee, **1975**.
- [25] J. A. Dean, J. Dean, *Analytical chemistry handbook, Vol. 1*, McGraw-Hill New York, **1995**.
- [26] A. Zaki, *Phase Transitions* **2019**, *92*, 135-148.
- [27] B. Bahadur, *Liquid crystals: applications and uses, Vol. 1*, World scientific, **1990**.
- [28] M. H. Hoang, M. J. Cho, K. H. Kim, M. Y. Cho, J.-s. Joo, D. H. Choi, *Thin Solid Films* **2009**, *518*, 501-506.
- [29] C. J. Brabec, V. Dyakonov, J. Parisi, N. S. Sariciftci, *Organic photovoltaics: concepts and realization, Vol. 60*, Springer Science & Business Media, **2013**.
- [30] R. J. Bushby, O. R. Lozman, *Current Opinion in Solid State and Materials Science* **2002**, *6*, 569-578.

-
- [31] T. Kato, T. Yasuda, Y. Kamikawa, M. Yoshio, *Chemical communications* **2009**, 729-739.
- [32] P. J. Stackhouse, University of Hull **2008**.
- [33] J. W. Goodby, P. Raynes, The Royal Society, **2016**.
- [34] aB. R. Kaafarani, *Chemistry of Materials* **2011**, *23*, 378-396; bM. Okazaki, K. Kawata, H. Nishikawa, M. Negoro, *Polymers for Advanced Technologies* **2000**, *11*, 398-403.
- [35] M. Lu, K. Yang, *Japanese Journal of Applied Physics* **2000**, *39*, L412.
- [36] aB. Glösen, A. Kettner, J. Wendorff, *Molecular Crystals and Liquid Crystals Science and Technology. Section A. Molecular Crystals and Liquid Crystals* **1997**, *303*, 115-120; bT. Christ, B. Glösen, A. Greiner, A. Kettner, R. Sander, *Adv. Mater* **1997**, *9*, 48-52.
- [37] S. Laschat, A. Baro, N. Steinke, F. Giesselmann, C. Haegele, G. Scalia, R. Judele, E. Kapatsina, S. Sauer, A. Schreivogel, *Angewandte Chemie International Edition* **2007**, *46*, 4832-4887.
- [38] R. Freudenmann, B. Behnisch, M. Hanack, *Journal of Materials Chemistry* **2001**, *11*, 1618-1624.
- [39] B. Blanzat, C. Barthou, N. Tercier, J. J. Andre, J. Simon, *Journal of the American Chemical Society* **1987**, *109*, 6193-6194.
- [40] R. Bushby, *Journal of Materials Chemistry* **1999**, *9*, 2081-2086.
- [41] G. Horowitz, *Advanced materials* **1998**, *10*, 365-377.
- [42] A. Tsumura, H. Koezuka, T. Ando, *Synthetic metals* **1988**, *25*, 11-23.
- [43] R. Turner, University of East Anglia **2015**.
- [44] D. Pérez, E. Guitián, *Chemical Society Reviews* **2004**, *33*, 274-283.
- [45] R. J. Bushby, C. Hardy, *Journal of the Chemical Society, Perkin Transactions 1* **1986**, 721-723.
- [46] R. C. Borner, R. F. Jackson, *Journal of the Chemical Society, Chemical Communications* **1994**, 845-846.
- [47] A. N. Cammidge, H. Gopee, *Journal of Materials Chemistry* **2001**, *11*, 2773-2783.
- [48] H. Hart, C.-y. Lai, G. C. Nwokogu, S. Shamouilian, *Tetrahedron* **1987**, *43*, 5203-5224.
- [49] N. Boden, R. J. Bushby, A. N. Cammidge, *Journal of the Chemical Society, Chemical Communications* **1994**, 465-466.
- [50] N. Boden, R. J. Bushby, A. N. Cammidge, G. Headdock, *Synthesis* **1995**, *1995*, 31-32.
- [51] G. W. Gribble, R. B. Perni, K. D. Onan, *The Journal of Organic Chemistry* **1985**, *50*, 2934-2939.
- [52] F. M. Raymo, M. F. Parisi, F. H. Kohnke, *Tetrahedron letters* **1993**, *34*, 5331-5332.
- [53] A. U. Rahman, O. L. Tombesi, *Chemische Berichte* **1966**, *99*, 1805-1809.
- [54] Y.-H. Lai, Y.-L. Yong, S.-Y. Wong, *The Journal of organic chemistry* **1997**, *62*, 4500-4503.
- [55] D. Pena, A. Cobas, D. Pérez, E. Guitián, L. Castedo, *Organic letters* **2000**, *2*, 1629-1632.
- [56] N. Boden, R. Borner, R. Bushby, A. Cammidge, M. Jesudason, *Liquid Crystals* **1993**, *15*, 851-858.
- [57] H. Shirai, N. Amano, Y. Hashimoto, E. Fukui, Y. Ishii, M. Ogawa, *The Journal of Organic Chemistry* **1991**, *56*, 2253-2256.
- [58] J. T. Rademacher, K. Kanakarajan, A. W. Czarnik, *Synthesis (Stuttgart)* **1994**, 378-380.

-
- [59] P. CANONNE, A. REGNAULT, *TETRAHEDRON LETTERS* **1969**, 243-&.
- [60] A. N. Cammidge, C. Chausson, H. Gopee, J. Li, D. L. Hughes, *Chemical Communications* **2009**, 7375-7377.
- [61] X. Fang, H. Guo, J. Lin, F. Yang, *Tetrahedron Letters* **2016**, *57*, 4939-4943.
- [62] B. P. Mathew, H. J. Yang, J. Kim, J. B. Lee, Y. T. Kim, S. Lee, C. Y. Lee, W. Choe, K. Myung, J. U. Park, *Angewandte Chemie International Edition* **2017**, *56*, 5007-5011.
- [63] J. Bi, H. Wu, Z. Zhang, A. Zhang, H. Yang, Y. Feng, Y. Fang, L. Zhang, Z. Wang, W. Qu, *Journal of Materials Chemistry C* **2019**, *7*, 12463-12469.
- [64] E. J. Foster, R. B. Jones, C. Lavigueur, V. E. Williams, *Journal of the American Chemical Society* **2006**, *128*, 8569-8574.
- [65] aZ. Jia, Y. Li, H. Liu, Y. Li, *SCIENTIA SINICA Chimica* **2016**, *46*, 1050-1063; bX. Zhu, Y. Yang, G. Xiao, J. Song, Y. Liang, G. Deng, *Chemical Communications* **2017**, *53*, 11917-11920; cM. Gupta, S. P. Gupta, S. K. Pal, *The Journal of Physical Chemistry B* **2017**, *121*, 8593-8602.
- [66] S. Zhang, C. Zhang, J. Wang, F. Hong, X. Hao, A. Zhang, Y. Wang, H. Wu, W. Zhang, J. Pu, *Polymer Chemistry* **2016**, *7*, 3013-3025.
- [67] Y. Wu, W. Zhang, Q. Peng, C.-K. Ran, B.-Q. Wang, P. Hu, K.-Q. Zhao, C. Feng, S.-K. Xiang, *Organic letters* **2018**, *20*, 2278-2281.
- [68] N. Boden, R. Bushby, Z. Lu, A. Cammidge, *Liquid crystals* **1999**, *26*, 495-499.
- [69] R. Chico, C. Domínguez, B. Donnio, B. Heinrich, S. Coco, P. Espinet, *Crystal Growth & Design* **2016**, *16*, 6984-6991.
- [70] C. T. Imrie, P. A. Henderson, *Current opinion in colloid & interface science* **2002**, *7*, 298-311.
- [71] N. Boden, R. J. Bushby, A. N. Cammidge, P. S. Martin, *Journal of Materials Chemistry* **1995**, *5*, 1857-1860.
- [72] J. Li, Z. He, H. Gopee, A. N. Cammidge, *Organic letters* **2010**, *12*, 472-475.
- [73] J. L. Schulte, S. Laschat, V. Vill, E. Nishikawa, H. Finkelmann, M. Nimtz, *European journal of organic chemistry* **1998**, *1998*, 2499-2506.
- [74] N. Boden, R. J. Bushby, A. N. Cammidge, A. El-Mansoury, P. S. Martin, Z. Lu, *Journal of Materials Chemistry* **1999**, *9*, 1391-1402.
- [75] H. Mao, Z. He, J. Wang, C. Zhang, P. Xie, R. Zhang, *Journal of luminescence* **2007**, *122*, 942-945.
- [76] H. Ji, K. Zhao, W. Yu, B. Wang, P. Hu, *Science in China Series B: Chemistry* **2009**, *52*, 975-985.
- [77] L. Zhang, H. Gopee, D. L. Hughes, A. N. Cammidge, *Chemical Communications* **2010**, *46*, 4255-4257.
- [78] M. Gupta, S. P. Gupta, M. Rasna, D. Adhikari, S. Dhara, S. K. Pal, *Chemical Communications* **2017**, *53*, 3014-3017.
- [79] I. Bala, W.-Y. Yang, S. P. Gupta, J. De, R. A. K. Yadav, D. P. Singh, D. K. Dubey, J.-H. Jou, R. Douali, S. K. Pal, *Journal of Materials Chemistry C* **2019**, *7*, 5724-5738.
- [80] L. Zhang, D. L. Hughes, A. N. Cammidge, *The Journal of organic chemistry* **2012**, *77*, 4288-4297.
- [81] X. Kong, Z. He, H. Gopee, X. Jing, A. N. Cammidge, *Tetrahedron letters* **2011**, *52*, 77-79.
- [82] W. Xiao, Z. He, S. Remiro-Buenamañana, R. J. Turner, M. Xu, X. Yang, X. Jing, A. N. Cammidge, *Organic letters* **2015**, *17*, 3286-3289.
- [83] H. Dieck, F. Heck, *Journal of Organometallic Chemistry* **1975**, *93*, 259-263.
- [84] S. J. Blanksby, G. B. Ellison, *Accounts of chemical research* **2003**, *36*, 255-263.

-
- [85] aA. Loudet, K. Burgess, *Chemical reviews* **2007**, *107*, 4891-4932; bM. A. T. Rogers, *Journal of the Chemical Society (Resumed)* **1943**, 590-596.
- [86] R. Cantu, S. Seetharaman, E. M. Babin, P. A. Karr, F. D'Souza, *The Journal of Physical Chemistry A* **2018**, *122*, 3780-3786.
- [87] B. Hong, F. Yang, H. Guo, Z. Jiao, *Tetrahedron Letters* **2014**, *55*, 252-255.
- [88] S. Dalai, V. N. Belov, S. Nizamov, K. Rauch, D. Finsinger, A. de Meijere, *European journal of organic chemistry* **2006**, *2006*, 2753-2765.
- [89] R. Chinchilla, C. Nájera, *Chemical Society Reviews* **2011**, *40*, 5084-5121.
- [90] M. Hellal, G. D. Cuny, *Tetrahedron letters* **2011**, *52*, 5508-5511.
- [91] M. Cui, H. Wu, J. Jian, H. Wang, C. Liu, S. Daniel, Z. Zeng, *Chemical Communications* **2016**, *52*, 12076-12079.
- [92] A. Díaz-Moscoso, G. J. Tizzard, S. J. Coles, A. N. Cammidge, *Angewandte Chemie International Edition* **2013**, *52*, 10784-10787.
- [93] N. Alharbi, A. Díaz-Moscoso, G. J. Tizzard, S. J. Coles, M. J. Cook, A. N. Cammidge, *Tetrahedron* **2014**, *70*, 7370-7379.
- [94] J. H. Simpson, *Organic structure determination using 2-D NMR spectroscopy: a problem-based approach*, Academic Press, **2011**.
- [95] W. Xiao, Z. He, M. Xu, N. Wu, X. Kong, X. Jing, *Tetrahedron Letters* **2015**, *56*, 700-705.
- [96] S. K. Varshney, H. Takezoe, V. Prasad, D. S. Rao, *Molecular Crystals and Liquid Crystals* **2009**, *515*, 16-38.
- [97] K. Seto, H. Shimojitoshio, H. Imazaki, H. Matsubara, S. Takahashi, *Bulletin of the Chemical Society of Japan* **1990**, *63*, 1020-1025.
- [98] A. N. Cammidge, H. Gopee, *Journal of Porphyrins and Phthalocyanines* **2009**, *13*, 235-246.

